Computational Evaluation of Binding Properties for Covalent Ligands in Prolyl Oligopeptidase and Fibroblast Activation Protein

Jerry Kurian

Department of Chemistry

Faculty of Science

McGill University

Montreal, Quebec, Canada

December 2016

To my friends and family.

Acknowledgements

Firstly, I would like to thank Prof. Nicolas Moitessier for his patience and guidance throughout my studies. As someone who had zero background in computational chemistry, or computer programming, it was a relief to not be pressured for results as I learned about the field. Prof. Moitessier has allowed me to discover a new passion and has drastically shaped my future goals and plans and I cannot thank him enough.

The McGill chemistry department staff has also been a great help to me. I am very thankful for Chantal Marotte who has provided me with much administrative assistance over my time here.

I would also like to thank all the colleagues I have had over the past 2 and a half years. The group has been extremely resourceful and a joy to be around. I am glad to have met so many friends during my time at McGill. I would like to specifically thank Josh, Anna, Steph, and Leo for always being available to me whenever I had a question that needed answering. Thank you to Sylvain for always being ready to give advice on stressful situations and thank you to Paolo for always being entertaining.

Thank you!

Contribution of Co-Authors

This thesis includes work that was conducted by the author as well as a manuscript that contains work from other contributors.

Chapter 1: This chapter was work completed entirely by the author.

Chapter 2: This chapter was work completed entirely by the author.

Chapter 3: This chapter contains work completed by the author but also contains work completed my Stephane De Cesco (synthesis and evaluation of activity of a synthetic library of covalent ligands for POP) and Justin Di Trani (isothermal calorimetry to determine kinetic parameters of covalent ligands).

Chapter 4: This chapter was work completed entirely by the author.

Abstract

Over the past decade, an increasing interest for covalent inhibition – modulating enzyme activity through covalently binding to it – as a drug design strategy has been observed. To aid in the development of covalent inhibitors, techniques which allow for prediction and characterization of activity must be made available. Knowledge about covalent inhibitor strength, activation energies, residence times and mechanisms must be obtained to allow for successful covalent drug development methodologies. In this thesis, we assessed whether two serine proteases, prolyl oligopeptidase (POP) and fibroblast activation protein (FAP), react similarly with respect to kinetics and thermodynamics in relation to the electrophile on the covalent ligand. To streamline such investigations, we exploited computational techniques as a method for prediction of covalent druggability – the ability of an enzyme to be inhibited through covalent means. We investigated the influence of different electrophilic groups (aldehyde, boronic acid and nitrile) on potency and binding kinetics with a series of truncated analogous inhibitors of POP, using quantum mechanical (QM) methods, such as the quantum chemical cluster approach (QCCA). The direct correlation between inhibitor reactivity and residence time was demonstrated through the QCCA and was further supported by experimental studies in the Moitessier group. The validated computational method was then applied to FAP, which has previously been thought to be less reactive than POP. Computations in this work predicted that the truncated ligands binding to POP result in a larger energy lowering compared to FAP. Similar computational techniques were used to evaluate the atomic basis for this difference in reactivity through a detailed analysis of hydrogen bond lengths and angles in the active site of POP. This analysis was supplemented with calculations on the difference in basicity of the catalytic histidine in POP and FAP, responsible for removing the

proton off the catalytic serine. The stronger the base, the easier the catalytic serine residue can be deprotonated and hence more reactive and available for nucleophilic attack. The data suggests that the histidine in POP may be more basic than in FAP, supporting the claim that the serine in POP may be more reactive than in FAP.

Résumé

Au cours de la dernière décennie, l'intérêt pour les inhibiteurs covalents, en d'autres termes, la modulation de l'activité d'une enzyme par la liaison covalente d'un inhibiteur à celui-là, comme stratégie pour la conception de médicaments a été observée à la hausse. Dans le but d'assister le développement d'inhibiteurs covalents, des techniques permettant la prédiction et la caractérisation de l'activité doivent être accessibles. La puissance, l'énergie d'activation, le temps de résidence et le mécanisme d'inhibiteurs covalents doivent être déterminés afin de permettre des méthodologies de développement de médicaments covalents à succès. Dans cette thèse, nous avons évalué si les deux protéases à sérine, la protéine prolyl oligopeptidase (POP) et la protéine d'activation fibroblaste (FAP), réagissent similairement de manière cinétique et thermodynamique par rapport à leur réactivité avec les électrophiles du ligand covalent. Afin de rendre ces investigations davantage efficaces, nous avons utilisé des techniques computationnelles comme méthodes prédictives de thérapies covalentes, en d'autres mots, la capacité d'une enzyme à être inhibée de manière covalente. Nous avons étudié l'influence de différents groupes réactifs (aldéhyde, acide boronique et nitrile) sur la force ainsi que la cinétique de liaison du ligand avec une série d'analogues tronqués inhibiteurs de la prolyl oligopeptidase (POP), en utilisant des méthodes de mécanique quantique (QM), tel que l'approche par groupe chimique quantique (QCCA). La corrélation directe entre la réactivité des inhibiteurs et leur temps de résidence a été

démontrée par QCCA et a été soutenue par des études expérimentales du groupe Moitessier. Notre méthode computationnelle validée a ensuite été appliquée à FAP qui avait été prédite comme étant moins réactive. Nos calculs ont prédit que les ligands tronqués se liant à POP entraînent une baisse d'énergie plus importante par rapport à ceux se liant à FAP. D'autres techniques computationnelles similaires ont été utilisées afin d'évaluer les principes au niveau atomique qui expliquent cette différence à travers une analyse détaillée des angles et des distances de ponts hydrogène dans le site actif de POP. Cette analyse a été complétée par des calculs sur la différence de basicité de l'histidine catalytique dans POP et FAP, qui est responsable de la déprotonation de la sérine catalytique. Plus la base est forte, plus le résidu sérine catalytique est facilement déprotonné, ce qui le rend davantage réactif, permettant ainsi une attaque nucléophile. Les données suggèrent que l'histidine chez POP est plus basique que l'histidine chez FAP, soutenant l'affirmation selon laquelle la sérine chez POP est possiblement plus réactive que la sérine chez FAP.

Table of Contents

List of Figures

List of Tables

List of Equations

List of Symbols and Abbreviations

3D = 3 Dimensional

ε = Dielectric constant

BSSE = Basis set superposition error

CADD = Computer aided drug design

COSMO = Conductor like screening model

CPU = Central processing unit

DFT = Density functional theory

E_{off} = Dissociation energy

E_{on} = Activation energy

FAP = Fibroblast activation protein

HF = Hartree-Fock

H-bond = Hydrogen bond

IC_{50} = Half maximal inhibitory concentration

K_i = Inhibitor constant

K_{inact} = Inactivation rate constant

k_{off} = Off rate

k_{on} = On rate

LA = Lewis acid

LBHB = Low barrier hydrogen bond

LDF = London dispersion force

L-J = Leonard-Jones

MD = Molecular dynamics

MM = Molecular mechanics

MOE = Molecular operating environment

NMR = Nuclear magnetic resonance

PDB = Protein data bank

PES = Potential energy surface

POP = Prolyl oligopeptidase

t_r = Residence time

QCCA = Quantum chemical cluster approach

QM = Quantum mechanics

QM/MM = Quantum mechanics / molecular mechanics

QSAR = Quantitative structure activity relationship

RMSD = Root mean square deviation

TS = Transition state

VDW = van der Waals

vHTS = Virtual high throughput screen

VS = Virtual screen

ZPE = Zero point energy

Chapter 1

INTRODUCTION: COVALENT INHBITION DESIGN AND DEVELOPMENT THROUGH DOCKING AND QUANTUM MECHANICS

1.1   Summary

Fibroblast activating protein (FAP) and prolyl oligopeptidase (POP) are serine peptidases that cleave proteins after a proline residue. POP has been associated with neurodegenerative diseases such as Alzheimer's disease and bipolar disorder; the overexpression of POP and FAP has also been linked to tumour cell growth.[1,2] Inhibition of POP could reverse memory loss and other symptoms of Alzheimer's while inhibition of both POP/FAP could slow tumour cell growth.[2] These proteins cleave peptides through a nucleophilic serine in their active sites. This serine is a potential target for covalent drugs as binding this residue would block biological activity of the enzyme. In order to discover drugs for this purpose, computer aided drug design (CADD) has become a fundamental technique. One of the most widely used methods derived from computational chemistry is molecular docking, which attempts to predict the ability of a ligand to bind to an enzyme. The development of docking programs for covalent ligands has however been limited by potential off target binding (toxicity) of covalent binders.[3] This issue has recently been overcome due to their advantages over non-covalent ligands such as improved pharmacokinetics, stronger binding, lower dosing requirements, and higher selectivity.[4]

This thesis aims to study the mechanisms, kinetics, and binding modes of covalent ligands in POP/FAP through CADD in order to aid in the development of covalent ligands; this will provide insight into the improvement of covalent docking and scoring functions. The quantum chemical cluster approach (QCCA) is utilized in order to acquire highly accurate quantum mechanical (QM) data; this method is employed as enzymes are too large to be studied solely by QM. The QCCA exhibits reasonable calculation times by removing residues which are not directly involved in ligand binding and the stabilization of the transition state. This enables accurate QM methods to acquire information on proteins which were originally outside of the scope of QM modeling.

Chapter One will introduce POP and FAP as targets and the significance of modulating their activity with covalent inhibitors; it will also discuss current docking programs and scoring functions which can be used for inhibitor design, as well as the need to improve these programs for covalent ligands. Finally, the QCCA will be discussed along with density functional theory (DFT).

Chapter Two describes the active site model and the geometric constraints applied to the system. It will also discuss the selected QM parameters for minimizations, transition state (TS) searches, and potential energy surface scans (PES).

Chapter Three involves the analysis of kinetic and thermodynamic data obtained on POP/FAP ligand binding; it also explores the catalytic mechanisms, ligand activation, and proton transfers occurring as the ligand approaches the nucleophilic serine. The difference in reactivity between POP and FAP is also discussed with insight provided from atomistic movements and geometric orientations of residues in the active site.

The final chapter discusses the impact and overall implications of the research presented and future work to be completed.

1.2   Fibroblast Activation Protein and Prolyl Oligopeptidase

FAP and POP are of interest due to their implications in tumour cell growth.[1,2,5,6] FAP is an attractive target for cancer treatment as it is rarely found on normal tissues or benign tumours and is overexpressed on the stroma of over 90% of epithelial-derived cancers including breast, lung, and colon.[2] FAP accumulates on the stroma due to its resistance to the body's immune response and is thought to support angiogenesis in cancerous cells.[5–8] POP is overexpressed in cancerous tissues but is also expressed by many normal cell types.[1] POP has been shown to make secondary cleavages to degraded thymosin-B4 which yields acetyl-SDKP, a potent stimulator of angiogenesis.[1] It is unclear which enzyme, POP or FAP, is more important in tumour growth as uncoupling their proteolytic activities has proven difficult.[2] Prolyl specific endopeptidase activity was originally attributed solely to FAP, however, these activities were measured using non-specific substrates such as Z-Gly-Pro-AMC.[2] Since both enzymes are co-expressed by cells comprising cancerous tissues, measured activity should be attributed to both POP and FAP.[1,2]

These proteins elicit their peptidase activity via covalent bond formation between the substrate and a nucleophilic residue in the active site during catalysis. POP and FAP also possess the same catalytic triad, which consists of histidine, aspartic acid, and serine. The general peptide cleavage mechanism of these enzymes first involves nucleophilic attack of the serine oxygen onto the carbonyl of the amide bond. This is followed by the collapse of the tetrahedral intermediate with the loss of the primary amine. The remaining ester linkage to serine is hydrolyzed, releasing a carboxylic acid and restoring the protein to its original state (**Figure 1.1**). [9]
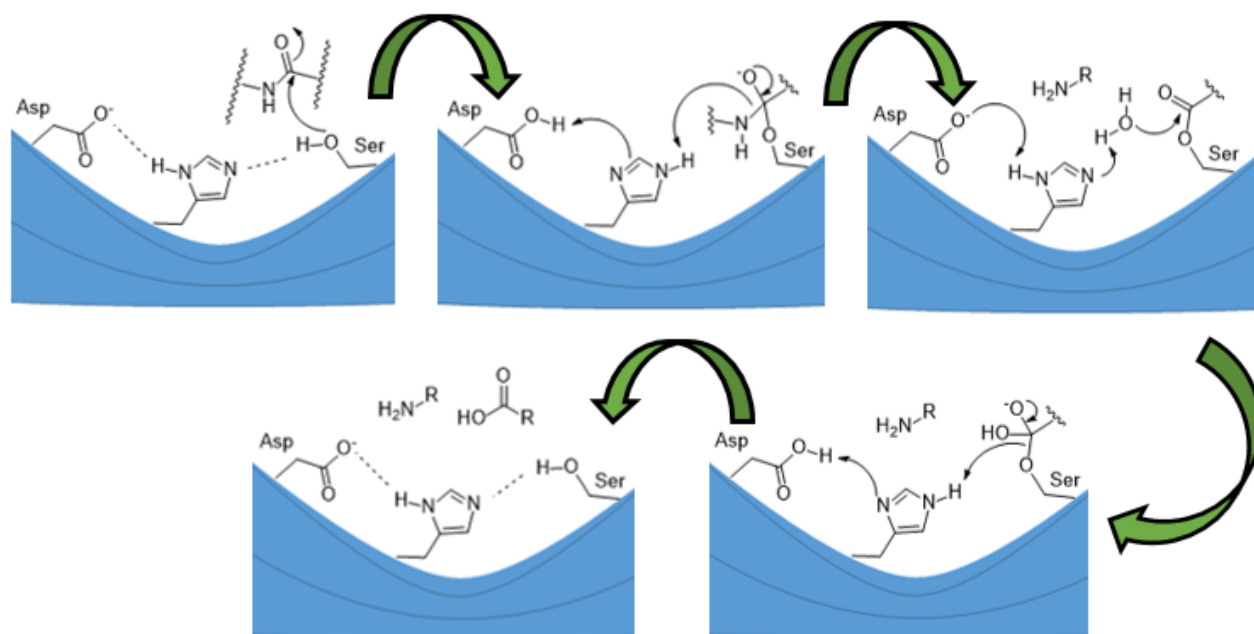
Figure 1.1: Catalytic mechanism in POP, similar to that of FAP.

The structure of POP has been studied in much more detail than FAP due to the availability of crystal structures. POP is known to possess two main conformations, open and closed, as shown in **Figure 1.2**.[10] The structure unbound by a ligand populates the open state, while the ligand co-crystalized structure populates the closed state.[10]
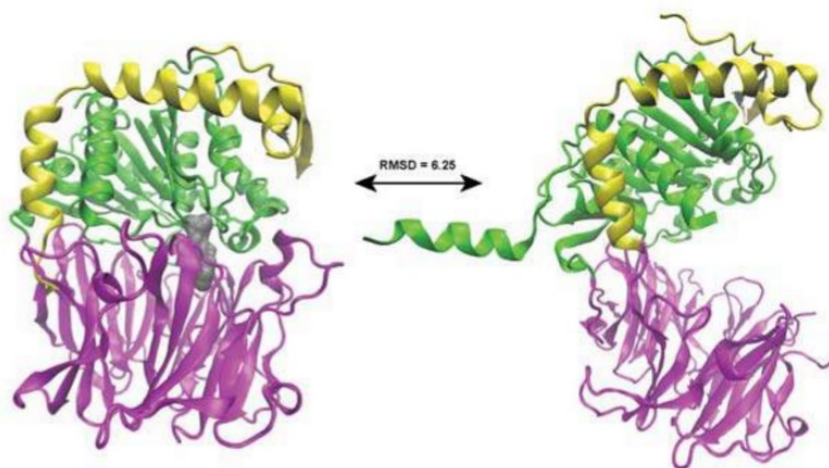
Figure 1.2: Closed and open structures of POP.[10]

POP contains a 7-bladed propeller domain that acts as a lid over the catalytic domain.[10] There is much less information available about the structure of bound FAP relative to unbound FAP as a crystal structure of FAP with a bound ligand co-crystalized has yet to be reported. In fact, the first endogenous FAP substrates have only recently been reported; they include many short peptides (< 35 amino acids) such as peptide YY and neuropeptide Y.[11] FAP is a homodimeric protein with an alpha/beta hydrolase domain and possesses an 8-bladed propeller domain;[12] the propeller domains of POP and FAP contain a pore which accommodates substrates. The pore in POP is smaller than in most proteases, which accounts for POP cleaving shorter polypeptides (<30 amino acids).[10] A unique property of POP and FAP is their ability to cleave after proline residues; most peptidases lack this ability as proline is an imino acid, protecting biologically active peptides from being degraded.

Studies have shown that the total rate enhancement observed from the catalysis of this triad is approximately 10^9 to 10^{10} times faster than without catalysis,[13] and that roughly 10^6 of this enhancement is attributed to the residues in the triad.[13] The remaining enhancement is attributed to the surrounding residues such as arginine, tyrosine, and backbone amides close to serine which interact strongly with the ligand through hydrogen bonding.[13] Studies have also shown that a low-barrier hydrogen bond (LBHB) may be present between the histidine and aspartic acid residues in the triad;[14,15] LBHBs are characterized by exceptionally short (< 2.29Å) and strong hydrogen bonds, which can result in a low barrier proton shuttle between histidine and aspartic acid (**Figure 1.3**).[16]
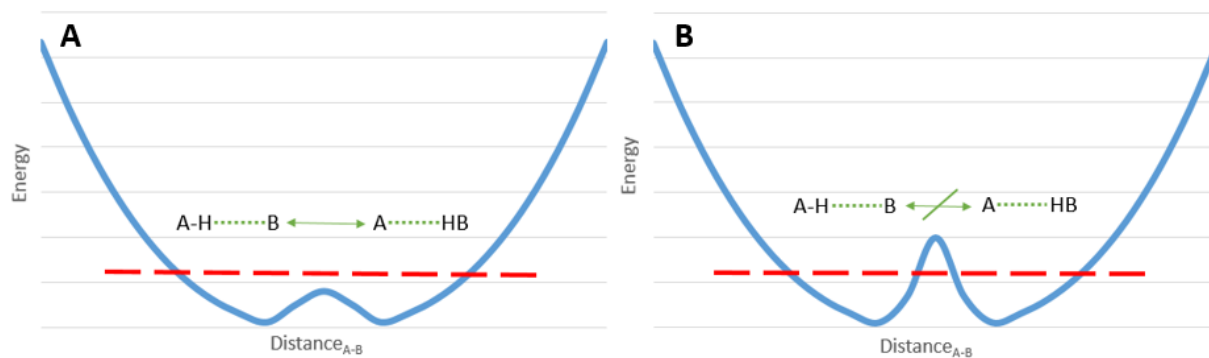
Figure 1.3: A- LBHB energy barrier (red line) for proton transfer at room temperature. B- Energy barrier (red line) associated with regular hydrogen bond proton transfer.

This could influence the basicity of the histidine and hence the nucleophilicity of serine. The reactivity of POP appears to be, in general, higher than that of FAP, although the reasons for this are unconfirmed. To find strong binders for both enzymes, ligands with tuned electrophilicity and non-covalent interactions have to be developed.

1.3   **Drug Discovery**

The identification, discovery, and optimization of drug candidates is an extremely lengthy and expensive process which proceeds through multiple stages. Following the identification and validation of a binding target, the next step is to identify promising scaffolds which can – once optimized – bind the target efficiently through covalent or non-covalent ligands. Binding this residue to POP and FAP would reduce the availability of their nucleophilic serines, which is crucial to their biological activity, thereby rendering them inactive. Covalent ligands are thus a promising class of potential POP/FAP inhibitors. Covalent ligands can be found by screening large libraries of compounds with high throughput methods such as in silico (virtual) or *in vitro* screening. Many drug discovery programs are moving towards in silico compound screening as the scope of

chemical space increases. Although *in vitro* high throughput screening still remains a very effective method to identify viable drugs, its associated cost, time, and chemical waste has led to the implementation of cheaper, quicker, and more effective in silico methods such as virtual high throughput screening (vHTS). The development of these in silico methods has historically focused on non-covalent ligands due to the concern of off target binding and the *in vivo* production of reactive metabolites, leading to toxic effects in the body. These concerns originally emerged from the identification of hepatotoxic compounds which bind covalently to liver proteins;[4] they were intermediates produced from metabolism of compounds such as bromobenzene and acetaminophen (**Figure 1.4**).[4]
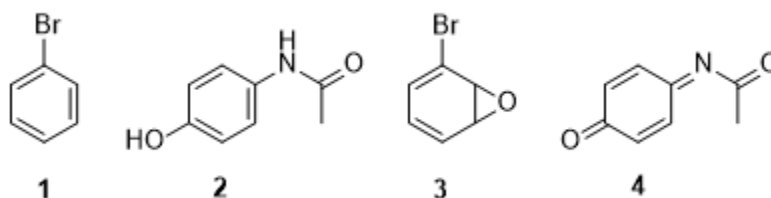
Figure 1.4: Compounds 1-2 are bromobenzene and acetaminophen while 3 and 4 are one of the possible toxic metabolites of these compounds which can covalently bind liver proteins.

These concerns have gradually diminished and covalent drugs have risen in interest (**Figure 1.5**). The commercialization of several highly successful covalent drugs has led to their acceptance and inclusion in drug discovery programs. Covalent drugs such as aspirin were commercialized despite being excluded from rational design; this was primarily due to serendipity.
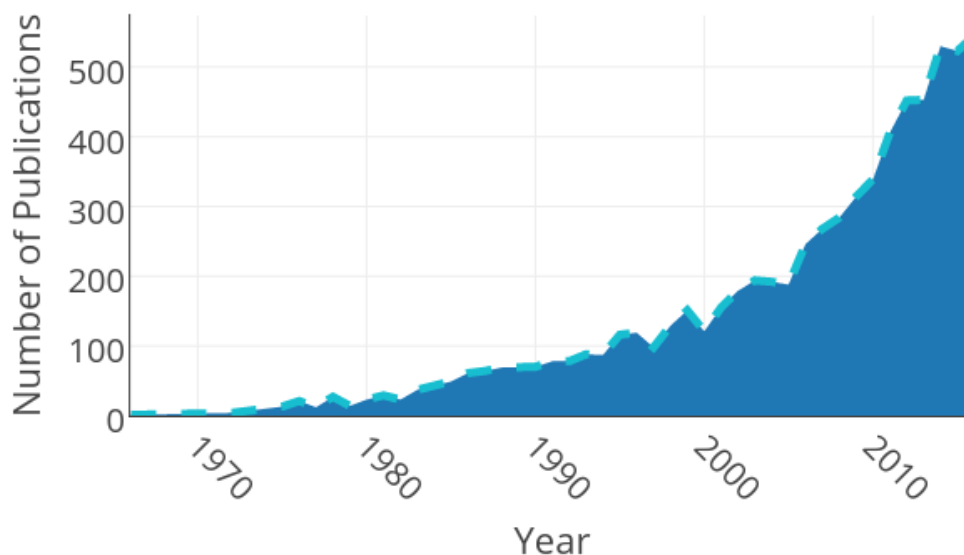
Figure 1.5: Scifinder search of the term "covalent drugs" sorted by year.

Aspirin elicits its biological activity through irreversibly acetylating cyclooxygenase.[17] In 2009, three of the top ten selling drugs on the US market acted through covalent modes (**Figure 1.6**) with 26 covalent drugs accounting for over \$33 billion in annual worldwide sales, illustrating the importance of this class of molecules.[4] Currently, more than 30% of drugs on the market act through covalent modes. [3,4]

Following these successes, further research into covalent drugs was performed and revealed several potential advantages over non-covalent drugs. These include – as previously mentioned – selectivity, improved pharmacodynamics, and less frequent dosing.[3] Additionally, through careful tuning of the reactivity of the covalent warhead during the drug discovery process, high target specificity can be achieved, greatly reducing the rate of off target binding.
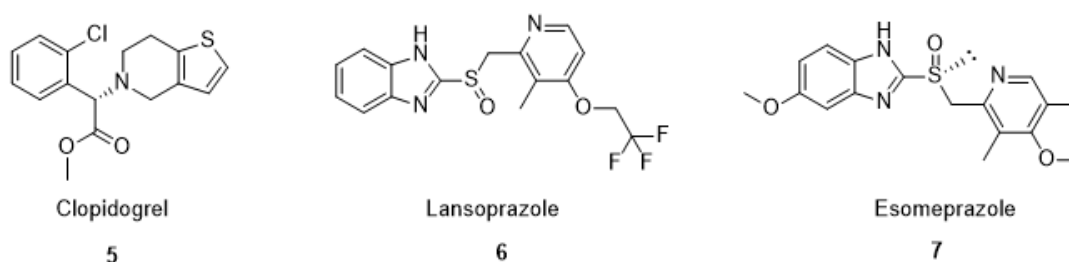
Figure 1.6: Three of the top 10 selling drugs which act through covalent mechanisms.

Due to the relative underdevelopment of covalent drugs, vHTS and docking methods that can efficiently identify covalent actives are not as accurate as those that can identify non-covalent ligands. The rising interest in covalent drugs has resulted in a surge in the development of docking methods to bolster their discovery and design.

1.4   Covalent Docking

Recently, several of the most popular docking programs have been modified to accommodate covalent docking; several new docking programs that focus on covalent docking have also emerged. Examples of these include DOCKovalent[18], DOCKTITE[19], CovDock[20], AutoDock[21], FlexX[22] and GOLD[23]. The process by which these programs predict binding poses and activity can be broken down into two fundamental steps: The first step involves sampling the conformational space in the active site with the ligand exhaustively; the second step involves ranking the sampled conformations with a scoring function to predict the best binding mode or, in the case of virtual screening, to distinguish actives from inactives. Sampling of conformational space can be completed by a variety of available algorithms such as matching algorithms, incremental construction algorithms[22], Monte-Carlo algorithms[24], and genetic algorithms[23], among others.[25] Once the conformational space has been sampled, each pose is scored to reveal the most

promising. Each docking program utilizes its own methodology in order to determine the most promising drug candidates; these will be discussed below.

One method to covalently dock ligands involves attempting to mimic the entire binding process; this typically involves twosteps: (1) the ligand binds non-covalently to the protein and (2) the covalent bond forms between the ligand and protein (**Equation 1.1**).

$$E + I \; \underset{K_{-1}}{\overset{K_1}{\rightleftharpoons}} \; E \cdots I \; \underset{K_{-2}}{\overset{K_2}{\rightleftharpoons}} \; E - I$$
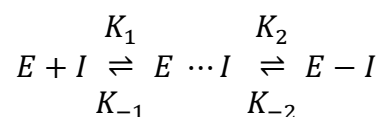
Equation 1.1

In CovDock, a program released by Schrödinger, the initial non-covalent binding pose is identified using classical non-covalent docking procedures with the exception that the nucleophilic residue is mutated to an alanine. [19] This ensures there is no steric clash between the ligand and nucleophilic residue and allows the reactive atoms to more closely approach each other in the pre-covalent state. Once the conformational space has been sampled adequately, the poses that yield distances greater than 8Å between the electrophilic atom in the ligand and the nucleophilic atom in the protein are filtered, as they are unlikely to form a covalent bond. The remaining poses are scored (GlideScore) and the best are re-docked with geometric constraints forcing a covalent bond between the ligand and protein. These bonded poses are then scored (AffinityScore) and combined with the pre-covalent scores to generate a total score, which is used to rank the ligands. CovDock has been tested on 38 complexes from the protein data bank (PDB) covering Michael additions and substitution reactions. The software exhibited a 76% success rate in correctly predicting the pose, measured by a root mean square deviation (RMSD) of <2Å from the crystal structure, and showed

an average RMSD of 1.52Å over the entire set (using only the best scored pose). This entire covalent docking procedure requires approximately 1-3 central processing unit (CPU) hours per molecule, which limits its throughputness for virtual screening. (VS). To allow for VS, this program has been modified to reduce the required CPU time by circumventing steps that are time consuming, and has been named CovDock-VS. For example, only poses within 5 Å are included and the AffinityScore algorithm has been replaced with the faster GlideScore algorithm. CovDock-VS was able to identify 71%, 72%, and 77% of known actives for Cathepsin K, HCV NS3 protease, and epidermal growth factor receptor within 5% of the decoy library. [19] The unmodified GlideScore scoring function does not account for differential ligand reactivity and covalent bond formation energy; if these parameters could be approximated, the accuracy of the program would be improved. The program supports only covalent ligands and thus non-covalent ligands must be screened separately using a different program.

Another popular method is the link atom (LA) approach; this involves manually defining the ligand atom that is bound to the protein atom. The protein and ligand files are set up with the link atom included in both. For example, the O in serine will be present in both the protein and ligand files. These atoms are forced to superimpose during the docking simulation, and the entire ligand is then treated as a flexible side chain of the bound residue. This constraint mimics a covalent bond by forcing the involved atoms to be within bond-length distance of each other.[26] The lack of automation of the LA approach prevents its use in virtual screening procedures. Instead, it is implemented in GOLD and FlexX docking programs, which have been validated on several test sets. The covalent mode was tested on a set of 76 complexes which contained 13 Michael acceptors, with the remaining belonging to the β-lactam family; the average RMSD was 3.69Å.[27] This method is rather simplistic, as the covalent bond formation simply involves a

geometric constraint while neglecting bond stretching, covalent bond energy and intrinsic reactivity.

An automated covalent docking workflow, DOCKTITE, has been implemented in the Molecular Operating Environment (MOE), which is a suite of programs released by the Chemical Computing Group. The focus of DOCKTITE during its development was on diversity with respect to the electrophilic warhead and receptor classes. DOCKTITE's workflow can be summarized into 4 steps: warhead screening, side chain attachment, pharmacophore guided docking, and side chain cleavage/pose rescoring. In the warhead screening step, the libraries of compounds are automatically scanned and tagged with atoms that are absent in the library. The default tags are Tantalum, Yttrium, and Germanium, but these can be customized to any other elements; these tags are used to label parts of the ligand that must be processed and reconfigured after ligand binding, such as electrophilic atoms, leaving groups, or tetravalent borons. The ligand is then transformed from the input ligand to the bound ligand; these transformations include leaving group deletion, addition of tetravalent boron if required, and nucleophilic bond formation to the electrophile. If the electrophile is prochiral, each stereoisomer is treated individually. Following bond formation, pharmacophore guided docking is completed, which involves conformer generation, scoring, pose refinement, and rescoring. DOCKTITE has two docking options, regular docking or VS; the difference lies in how the poses are refined. The regular docking method uses a forcefield approach (0.5-1 CPU hours per ligand), whereas the VS-docking applies a grid minimization (10-20s per ligand).[19] The final steps involve pose scoring and the estimation of binding free energy in order to rank the active ligands. This is done through a consensus scoring function which utilizes a function tailored towards pose prediction (DSX scoring function) followed by a function developed to predict binding affinities (Affinity dG or London dG); the combination of these two

provides an accurate overall score for the potential binders. DOCKTITE's pose prediction ability has been validated on 35 protein-ligand complexes, exhibiting a mean RMSD of 1.75A and a prediction rate of 71.4% with an RMSD < 2A. Additionally, a virtual screen with receiver operating characteristics yielded an under-curve-area of 0.81 and a significant correlation between predicted and experimental binding affinities ($R^2 = 0.649$). [19]

Autodock is another widely used docking program which has been modified to support covalent docking; the added methods include the two-point attractor method and the flexible side chain method (**Figure 1.7**).
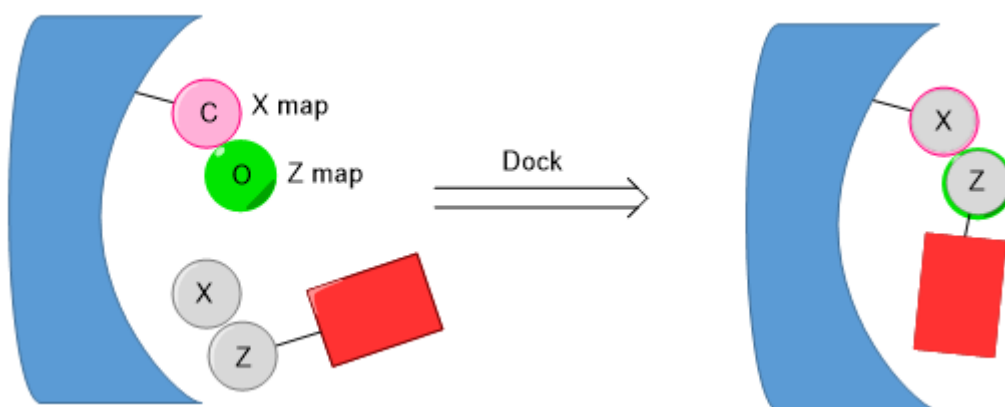
Figure 1.7: Autodock's two point attractor method to simulate covalent bond formation. X and Z are atoms cut from the nucleophilic residue.

The flexible side chain method is similar to the methods used in GOLD and FlexX, as previously described; after covalent attachment, the protein attachment residue and the ligand are treated as a flexible side chain of the receptor. Conversely, the two-point attractor method involves using an attractive Gaussian-based potential between two new atom types, X and Z. The Cα and Cβ atoms from the nucleophilic residue are removed to generate holes, which are used to create interaction

13

maps with a Gaussian potential centered on their locations; an energy gain is simulated as the X and Z atom types better occupy these holes. This enables modeling of flexibility of the bond, with a penalty that scales as the distance increases between X and Z and their respective holes. This method proved to be inferior to the flexible side chain method in most cases, although the application of both methods requires manual identification of the reactive atoms and reaction type; the ligand and protein files also have to be prepared manually, further limiting their use in virtual screening. [21]

DOCKovalent uses simple bond and angle constraints to force the covalent bond to the ligand, and a physics based scoring function to score each pose based on van der Waals (VDWs), electrostatics, and desolvation. Once the bond and angles are formed, all poses and ligand conformations with respect to these constraints are sampled; the nucleophile is also constrained, which requires different runs to be completed for different nucleophile rotamers. [18]

These docking methods have been modified or developed to support covalent docking, although several issues still remain. For example, they are unable to screen both covalent and non-covalent ligands in a single run, as both ligand types require different libraries and methodologies which have yet to be combined into a single workflow. Additionally, some of these methods are complicated: CovDock introduces mutations on the protein, whereas DOCKTITE disconnects the sidechain from the protein and adds additional constraints to the MOE protocol.[19,28] AutoDock and DOCKovalent require the complex modification of scoring functions to include covalent bonding energetics.[18,21] The complexity of these methods deters non-experts from using them. Since small changes in the chemical environment of a protein or ligand can cause large changes in its reactivity, the parameterization of bond formation has proven difficult and has resulted in the use of non-

simplistic models. This complexity is due to the inability to accurately model and score covalent parameters such as bond energy, electrophilicity, and activation energy.

1.5   Scoring Functions

Docking programs typically contain a function to score the generated poses for lead optimization and another function to differentiate between actives and inactives for virtual screening. A good scoring function is essential, as conclusions pertaining to binding effectiveness of drug scaffolds are drawn from them. Generally, as the hydrophobicity of the binding pocket increases, ligand scoring becomes easier and more accurate. This is due to the shape complementarity between the ligand and receptor accurately predicting drug effectiveness as hydrophobic effects are handled during shape complementarity optimization. More polar active sites or those involving strong electrostatic interactions are more difficult to score as functions must be developed to accurately model these interactions; simple shape complementarity does not take these effects into account.[29] The development of accurate scoring functions has led to fairly efficient and accurate functions that can be classified into three main categories: Force-field based, empirical based, and knowledge-based.

Classical molecular mechanics force-field based scoring functions derive their ranking from the summation of non-bonded terms – electrostatics, van der Walls, and steric strain. For example, one of the scoring functions implemented by DOCK to identify the best pose involves energy parameters taken from the AMBER forcefield in the form of **Equation 1.2**.

$$E = \sum_i \sum_j \left(\frac{A_{ij}}{r_{ij}^{12}} - \frac{B_{ij}}{r_{ij}^6} + \frac{q_i q_j}{\varepsilon(r_{ij}) r_{ij}} \right)$$

Equation 1.2

In the above expression, r_{ij} corresponds to the distance between protein atom i and ligand atom j, A_{ij} and B_{ij} correspond to the VDW parameters, and q_i and q_j are the atomic charges.[30–32] This scoring function implements a simple Coulombic interaction model with a distance-dependent dielectric constant to model the solvent implicitly and a Leonard-Jones (L-J) 12-6 potential to model the VDW forces, as shown in (**Equation 1.3**).[30]

$$V_{LJ} = \epsilon \left[\left(\frac{r_m}{r} \right)^{12} - 2 \left(\frac{r_m}{r} \right)^6 \right]$$

Equation 1.3

In **Equation 1.3**, ϵ corresponds to the depth of the potential well, r_m is the distance the potential reaches at its minimum, and r is the distance between the particles; these parameters can be varied in order to alter the strictness of the potential. For example, an 8-4 L-J potential (implemented in G-score)[33] enables more flexibility between the ligand and receptor relative to the 12-6 L-J potential (implemented in D-Score) (**Figure 1.8**).[34]

These force field based scoring functions can be modified to include hydrogen bonding, torsional entropy, among other terms.
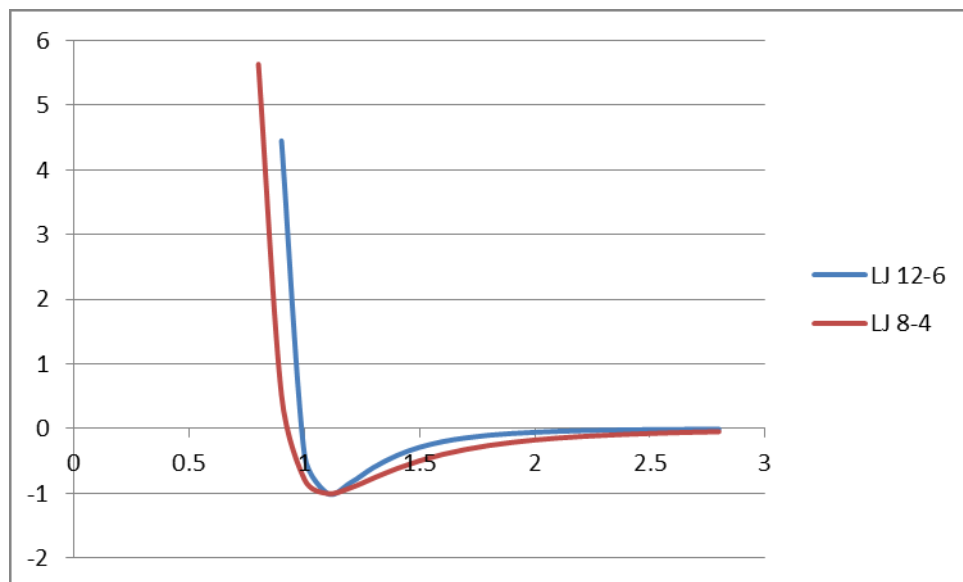
Figure 1.8: Illustrating the LJ 12-6 and the LJ 8-4 potential.

Another class of scoring functions are empirical scoring functions where the binding affinity is estimated by the Gibbs free energy (**Equation 1.4**).

$$\Delta G = \sum_i W_i \cdot \Delta G_i$$

Equation 1.4

ΔG_i represents energy terms such as VDW energy, hydrogen bonding, and entropy, whereas W_i is a coefficient that is determined by fitting the binding affinity data of a training set with known 3D structure complexes, usually from a crystal structure. A statistical analysis of ligand-protein complexes is used to determine which interactions are most frequent, with the rationale that the most favourable interactions will be the most frequent. Each interaction is then given a

corresponding energy contribution term based on its frequency. The benefit of empirical scoring functions stems from its computational simplicity.[30]

A third class consists of knowledge-based scoring functions, which include Potential Mean Force and DrugScore functions.[35–37] These functions aim to reproduce experimental structures, and are useful when a vast amount of ligand structural data is available for the target, which is encoded into a scoring function that rewards ligands that reproduce the observed data and penalize those that do not. The main advantage of this class of scoring functions is its low computational cost, allowing fast application to large libraries of compounds.[33]

Another strategy uses consensus scoring, which employs multiple scoring functions that each contribute to the final score; this technique can substantially improve enrichment in VS. However, the scoring functions must be chosen carefully in order to minimize function correlation and thus mitigate bias. Common consensus scoring functions include MultiScore, X-Cscore and GFscore.[30]

Despite this progress, covalent scoring remains under development; functions for active sites that possess covalent residues that bind ligands must be developed to accurately account for the stabilization provided by covalent bond formation, ligand electrophilicity, and residence time, among other effects. This task requires detailed QM studies pertaining to various electrophiles with various neighboring groups in various chemical environments, making parameterization an incredibly difficult task.[27] In order to improve docking, a method to broadly rank the relative electrophile reactivities could be developed. The effect of general peripheral groups – such as electron withdrawing or electron donating groups – can then be analyzed;   this study has been completed on glutathione using pseudo first order kinetics to rank the reactivities of various

electrophiles such acrylamides, nitriles, cyanamides and sulfone/sulfonamides.[37] Another factor that has yet to be computationally studied is the residence time of covalent ligands, which corresponds to the time the ligand remains bound to the catalytic nucleophile; electrophilic classes such as aldehydes, boronic acids, and nitriles can all be reversible depending on the target enzyme. The longer the residence time the longer the inhibitors will affect the activity of the protein. Thus, in a closed system, ligands with longer residence times should exhibit larger effective inhibitor constants ($K_i's$) relative to those that have lower residence times. A third factor that requires improvement is the enthalpic stabilization provided from the formation of covalent bonds. This should be parameterized based upon the electrophile and the nucleophile forming the bond. In order to improve current scoring functions for covalent inhibitors, the parameterization of the reactivity of the electrophilic warhead, residence times, and bond energies is crucial; this has been attempted in some covalent docking programs.

GOLD uses a modified version of its non-covalent scoring function to simulate covalent bonding; this function reduces the clash penalty associated with atoms in close proximity, but does not reward the actual bond formation. CovalentDock has implemented a modified scoring function from AutoDock that accounts for a covalent binding energy term; this function uses a Morse potential to describe the enthalpy change associated with bond formation and also estimates entropy change with simulated QM results (from the Gaussian electronic structure package), as shown in **Equation 1.5**.[27]

$$E \begin{cases} D\left(e^{-2\alpha(r-r_0)} - 2e^{-\alpha(r-r_0)}\right) - T\Delta S + C, \ r \leq r_m \\ 0, \ r > r_m \end{cases}$$

Equation 1.5

In the above expression, D corresponds to the dissociation energy, alpha is a factor controlling the Morse potential well width, r is the current bond length, r_0 is the equilibrium bond length, r_m is the maximum bond length prior to dissociation (where energy of the bond is zero), ΔS is the Gaussian estimated conformational entropy, and C is a correcting factor determined empirically.[27] The docking program DOCKTITE employs a physics-based scoring function that ignores the covalent bonding energy;[18] they argue that mixing covalent and non-covalent terms would cause optimization of the covalent terms while non-covalent interactions would be largely ignored.[18,38] This is because in general, the binding energy of a covalent bond is much larger than that of non-covalent interactions. This prevents any direct comparison and ranking of ligands with different electrophiles in the library when using DOCKTITE, requiring the user to separate their library according to different electrophiles in order to allow for direct ranking and comparison. This drawback could be overcome by scaling the covalent bonding energy with the aid of QM data.

Hence, most of the current scoring functions do not account for residence time or the intrinsic reactivities of the nucleophilic and electrophilic atoms. Scoring functions that implement the covalent enthalpy gain have been developed, but large-scale validation has yet to be completed. In order to improve these functions, the generation of accurate QM data or experimental data pertaining to different covalent ligands is required; this data would be used to parameterize terms that would improve these functions.

1.6   <u>Quantum Chemical Cluster Approach</u>

In order to investigate the kinetics and thermodynamics of the bond formation process in covalent inhibitors, QM studies can be completed to simulate ligand binding; methods to apply QM calculations to proteins have been developed, which were traditionally outside the scope of QM due to their sheer size (number of atoms). Two validated methods are the quantum mechanics/molecular mechanics (QM/MM) approach, and the quantum chemical cluster approach (QCCA). QM/MM treats the active site with QM, whereas the surrounding protein is treated with molecular mechanics (MM). This enables the entire protein to be treated, although it inaccurately treats the boundary between the QM and MM regions, particularly if bonds cross the QM and MM boundary.[39] The QCCA focuses on the residues that are involved in transition state stabilization and catalysis, and ignores the rest of the enzyme. This is done by clipping the residues at $C\alpha$ out of the active site and modelling them in the absence of the remaining protein. This enables the treatment of a small portion of the enzyme with highly accurate QM methods. However, two problems arise when the surrounding enzyme is removed: poor representation of long range interactions in the protein, and the unrealistic motion of residues that are naturally constrained by the protein backbone.[40] The former issue can be accounted for using polarizable continuum solvation techniques; these assume that the environment surrounding the active site can be approximated by a homogenous polarizable medium with a chosen dielectric constant. The choice of dielectric constant (ε) can be ambiguous depending on the model size, although typically $\varepsilon = 4$ is used to simulate the protein environment. For systems larger than 150 atoms, the choice of dielectric constant does not have a significant effect on the transition state and ground state energies;[40] as the system size increases, more residues are included and thus longer range effects are being accounted for inherently by the QM model. In order to prevent unrealistic residue motion,

their alpha carbons are constrained during the QM optimization process. This constrains the residues to the backbone positions, usually taken from a crystal structure, but enables side chain movement; large artificial movement is thus prevented during geometry optimizations. The application of these constraints to atoms that are close to the site of reaction, could result in large steric clash energies or poor modeling of natural orientations, thus resulting in large errors. As the system size increases and constraints are moved further from reaction sites, the accuracy of the approximation increases. Although this coordinate locking scheme minimizes unrealistic residue motion, there is still a concern regarding entropic effects within the protein: Often, after locking several coordinates in the model, several small imaginary frequencies appear ($<50i$ cm^{-1}).[40] It has been shown that these frequencies do not significantly contribute to the computed energies, but do affect harmonic entropy effects. Consequently, the computed energies correspond to enthalpy, not free energy. Despite this, the entropy effects are often quite small, and QM/MM studies have been conducted that show that the calculated free energy barriers differ from the potential energy barriers by only 1kcal/mol.[41,42]

1.7   Density Functional Theory

Once a model has been selected and constraints have been established, the selected atoms are treated with the most computationally affordable level. This typically corresponds to hybrid density functional theory (DFT), although semi- empirical methods and post Hartree Fock (HF) methods can also be effective. Most enzymatic studies rely on DFT methods, as HF methods are less accurate for larger systems: The HF method approximately determines the wave function and energy of a system, and depends on 3N spatial coordinates and N spin coordinates for an N electron system. HF methods can typically be applied to systems beneath 100 atoms. Consequently, in order to model larger systems, DFT method was developed which can handle well over 100 atoms. DFT

is briefly discussed below, and more information relating to it and other QM theories can be found in standard quantum mechanics textbooks.[43–45]

Although DFT has proven successful in computational chemistry on organic systems, large calculation errors can still arise. This includes delocalization error in many electron systems, which disperses the electron density artificially, resulting in unphysical electron delocalization. [46,47] Most approximate functions give convex deviations from the expected linear behavior (**Figure 1.9**), resulting in the underestimation of reaction barriers in most pre-DFT methods.[46]
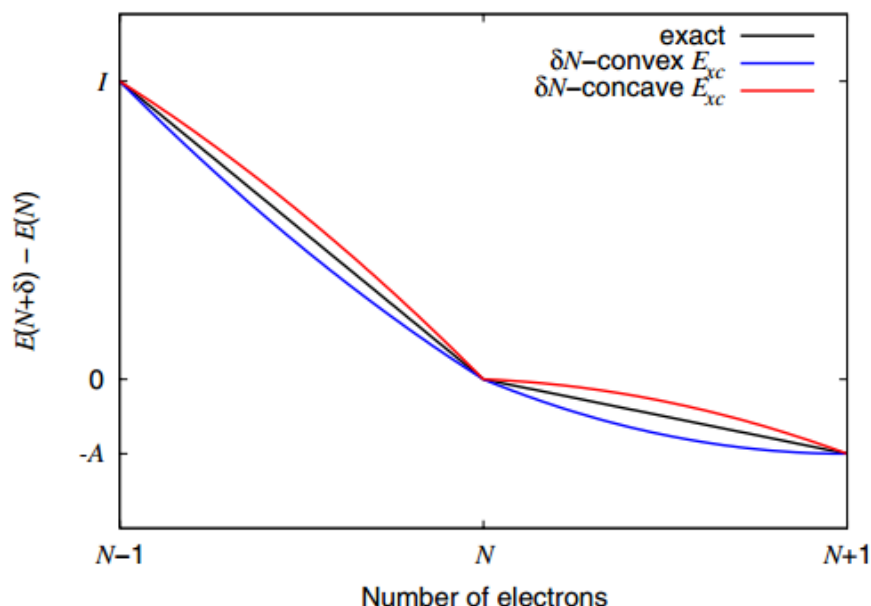
Figure 1.9: Illustrating the exact behavior of energy as a function of charge versus concave and convex behaviors.[46]

 Conversely, bond dissociation energies are typically overestimated by approximate functions, resulting from concave deviations; this arises since Kohn-Sham orbitals are produced from a single determinate. Neither approximate functions nor HF model constant energy as a function of fractional spins, resulting in overestimations. Hybrid functionals, such as B3LYP, are less affected

by these errors since they benefit from error cancellation. Another downside to the use of approximate functions is that they do not describe VDWs; this may result in an underestimation of ligand binding energy, since interactions such as π-stacking are not considered.[48,49]

The hybrid DFT method with the B3LYP functional – as shown in **Equation 1.6** – has been the most successful for treating large systems in the QCCA method.

$$F^{B3LYP} = (1 - A) \cdot F_x^{Slater} + A \cdot F_x^{HF} + B \cdot F_x^{Becke} + C \cdot F_C^{LYP} + (1 - C) \cdot F_C^{VWN}$$

Equation 1.6

F_x^{Becke} In the above expression, F_x^{Slater} corresponds to the Slater exchange, F_x^{HF} is the exact Hartree-Fock exchange, is the gradient part of the exchange functional, and F_C^{LYP} and F_C^{VWN} describe the electron correction. The constants A, B, and C are determined via curve fitting to experimental heats of formation; this is performed by electronic structure packages such as GAMESS and Orca.[43–45]

Depending on available computational resources, the 6-31G** basis set is the most commonly used for geometry optimizations. For accurate single point energy calculations, the basis set used is often expanded to, for example, 6-311+G**. To evaluate the effects of the protein environment, single point energy calculations are completed with polarizable continuum solvation models at the same basis set as the optimizations.

1.8   <u>Conclusions and perspectives</u>

In this chapter the importance of exploring covalent inhibition has been demonstrated. Covalent inhibitors account for over $33 billion in global annual sales and are thus a commercially important class of molecules. Additionally, many of the most widely used docking programs and their methodologies and scoring functions used for the discovery and design of covalent inhibitors were discussed. The drawbacks of these programs were also discussed, as well as improvements to better model covalent inhibition; these included QM methods to accurately model enzymatic binding in order to obtain information on entropic and enthalpic effects. Moreover, we also saw how binding kinetic parameters and binding thermodynamic parameters for different reactive groups can be extracted from this method. Lastly, the importance of POP/FAP was discussed, as well as the application of these methods to gain a better understanding of binding thermodynamics and kinetics. The results presented are expected to be applicable to other enzymatic models and could thus be utilized to improve current scoring functions in order to accelerate and improve the current covalent docking programs; this data could also be used to understand POP/FAP selectivity and drug design.

Chapter 2

<u>EXPERIMENTAL</u>

2.1 <u>Computational Resources</u>

Calculations were completed using several computational resources located in Montréal. Many calculations were performed using Forecaster, the cluster owned and operated by the Moitessier group. Other calculations were completed using resources provided under the Advanced Research Computing umbrella organization, Calcul Québec, which is comprised of several high-performance computing resources from universities around Montréal such as Guillimin (McGill High Performance Computing) and Mammouth (Centre for Scientific Computing at University de Sherbrooke).

2.2 <u>Computational Details</u>

All quantum mechanical calculations were completed using the electronic structure program package Orca (version 3.0.3). Unless otherwise specified, all structures were minimized with DFT and the hybrid B3LYP functional with dispersion correction. The basis set for all minimizations were 6-31G** with the alpha carbons of all residues frozen. The zero-point energy (ZPE) was computed by taking these structures, and computing a single point energy (SPE) calculation with a much larger basis set (QZVP/J). A larger basis set was not used in the optimization as computation times were exceedingly large. SPE calculations were also complete

with the QZVP/J basis set on the maximum and local minimum structures used to compute the activation energies, dissociation energies and binding energies. Several single point energies with QZVP/J were calculated with the counterpoise correction to account for basis set superposition error (BSSE), however little to no difference was observed and thus the BSSE was ignored. Solvent effects were accounted for where indicated with the conductor like screening model (COSMO) implemented in Orca. The dielectric constant chosen was 4, typical for modeling enzymatic environments, however, for large systems such as those studied here, the dielectric constant chosen should not have a large effect on the overall energies. PES scans were completed using DFT/B3LYP using the 6-31G** basis set on all atoms.

2.3   Selecting the Model

In order to begin quantum mechanical modeling of a protein, the active site residues to be included in the model must be chosen. This is typically done through careful manual analysis of a crystal structure of the enzyme, preferably with a ligand co-crystalized within the active site. To construct our model of POP, we looked at the crystal structure with Z-pro-prolinal co-crystalized in the active site (PDB code: 2XDW). The residues are all truncated at the alpha carbon, converting this to a CH_3 group. To illustrate this clearly, a truncated histidine is shown in **Figure 2.1**.
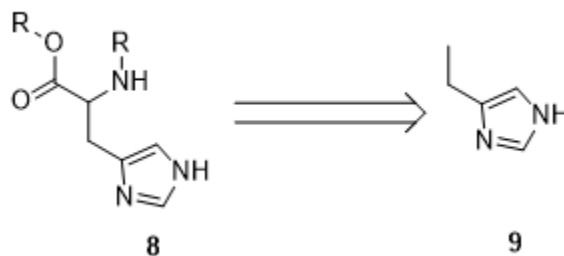
Figure 2.1: Truncation of a Histidine residue

The binding sites of both enzymes with relevant residues can be seen in **Figure 2.2** as obtained from docking. First, the catalytic triad must be included in the model. For POP, this triad consists of SER_{554}, HIS_{680}, and ASP_{641}.
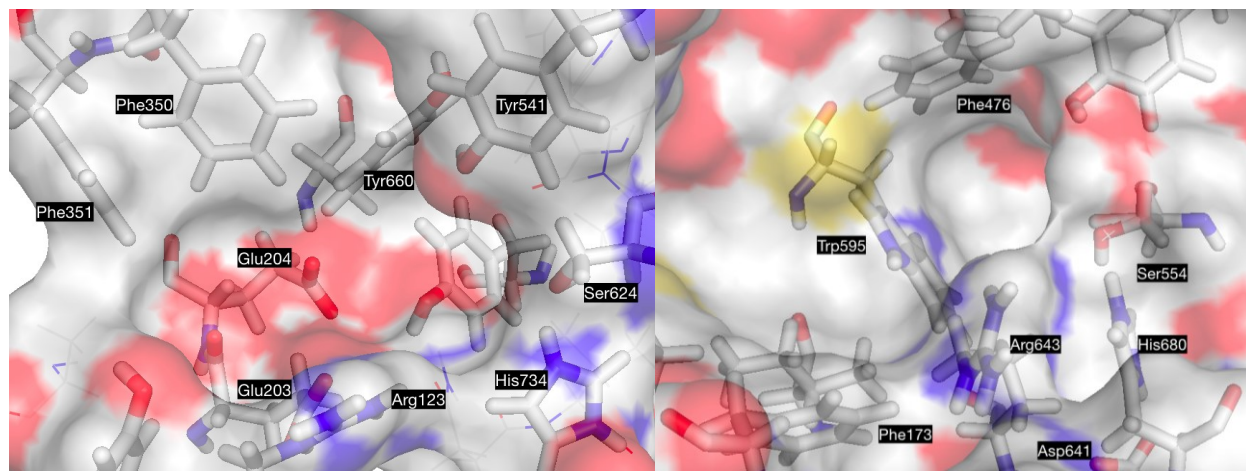
Figure 2.2: FAP active site (left) and POP active site (right).

Ligands bound to serine which form a sp^2 or sp^3 carbon are doubly stabilized by two hydrogen bonds, one from a backbone amide N-H and the other from the hydroxyl of tyrosine.[13] This correspond to TYR_{473} and the backbone N-H connecting SER_{554} to ASN_{555}. These residues are all known to be important in the binding process of the ligand and stabilization of the transition state and were thus included in the model. Other residues which interact with the ligand at locations distant to the electrophile should be included as these will influence the orientation of the ligand as it approaches the reactive residue. In order to get an accurate initial pose of the ligand in the active site of the protein, docking was completed. From the docking pose, it can be seen that ARG_{643} should also be included in the active site as there is a hydrogen bond with the ligand. To prevent unnatural motion of ARG_{643}, it is also important to include ASP_{149} which hydrogen bonds

to this arginine, constraining its geometry. One can also see Phe$_{476}$ and Phe$_{173}$ in the active site. These two residues were excluded as they are quite distal to the covalent binding site, and thus will not affect the transition state directly. Also, since arginine appears to interact strongly with the ligand electrophile, orienting it to the serine, Trp$_{595}$ was excluded as it was deemed unnecessary to modelling the covalent bond formation (**Figure 2.3**). For these reasons, the POP model consists of the above mentioned 6 residues.
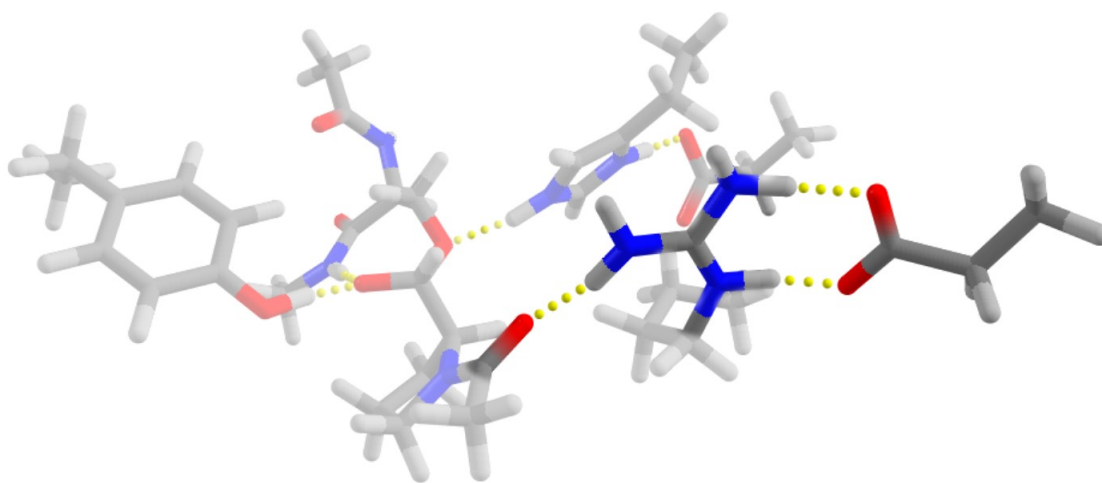
Figure 2.3: Interactions of the docked ligand and Arg$_{643}$ with Asp$_{149}$.

A similar approach was taken to choose the FAP model, with a very similar 6 residues chosen (excluding ASP$_{149}$ which is instead a glutamic acid – GLU$_{273}$).

2.4   Docking

As mentioned previously, in order to get a suitable pose for QM optimizations, the best scored pose from docking was taken as the starting geometry. Docking was completed using the

FITTED docking program. FITTED is broken down into a simple GUI comprised of workflows which visually illustrate the steps required to complete the docking process from start to finish. We used the "*docking 3D ligands to rigid protein*" workflow already defined in FITTED (**Figure 2.4**).
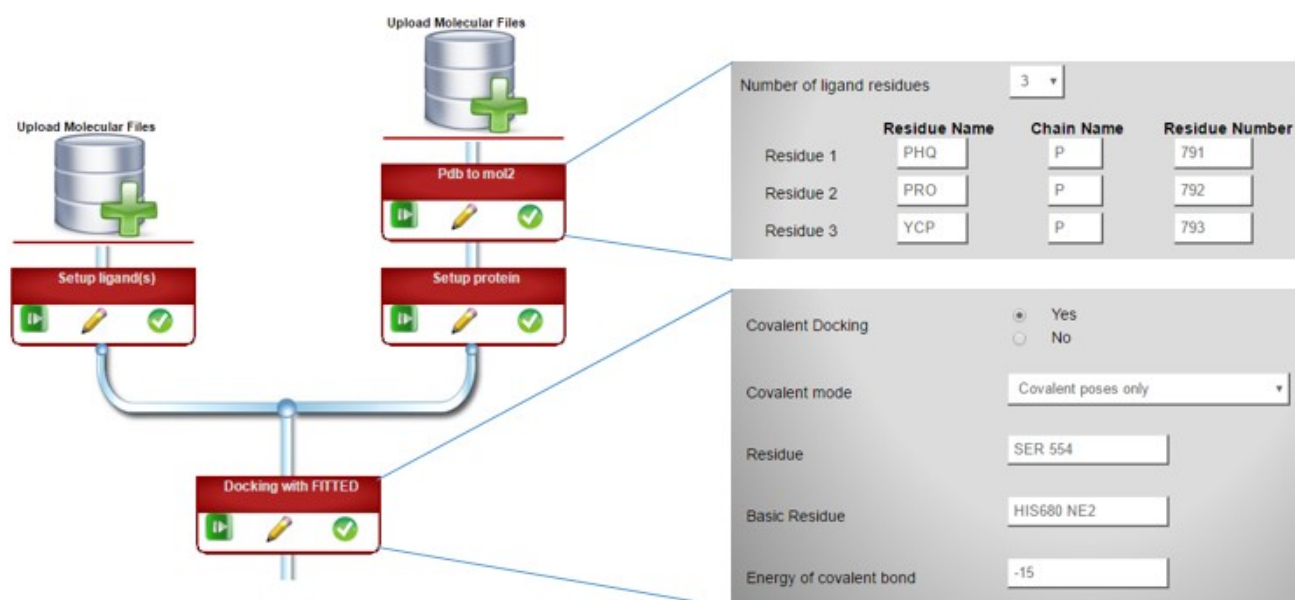
Figure 2.4: Docking workflow implemented into FITTED.

The ligands were drawn in Avogadro and saved in the mol2 format while the protein structure was downloaded from the PDB and converted to mol2 format using the *convert pdb to mol2* module (PREPARE program) in FORECASTER. Default parameters were used unless otherwise specified. Some input was required such as the co-cyrsalized ligand residue name, chain and residue number (PRO$_{791}$, YCP$_{792}$, PHQ$_{793}$) which is required to define the active site. Also, identification of the covalent residue (SER$_{554}$) and the basic residue which accepts the proton from serine (HIS$_{473}$) after bond formation was required as shown in **Figure 2.4**.
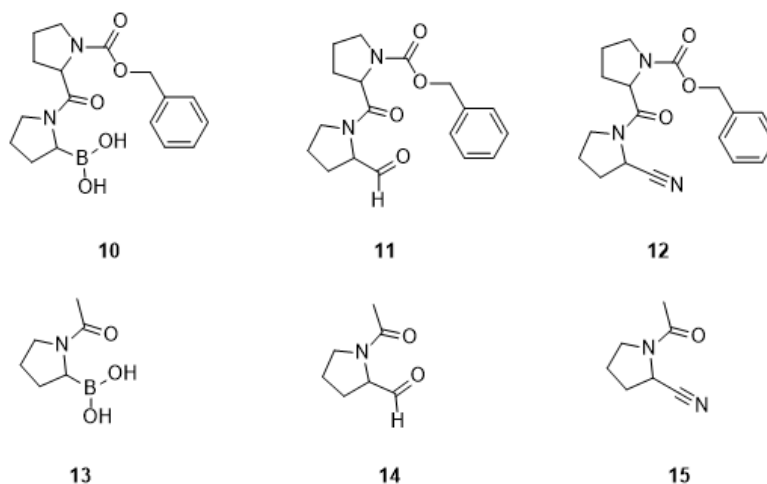
Figure 2.5: 10-12 are ligands reported to be binders to POP and 13-15 are the truncated ligands under study.

2.5   **Protonation States/Proton Transfer Barrier**

Ground state characterization of the active site was determined through single point energy calculations and geometry minimizations. First, from the active site model chosen previously, protons were added using the "add hydrogens" feature in Avogadro. Each atom was manually checked to ensure protons were added correctly. Aspartic and glutamic acid residues were unprotonated, histidine was neutral and arginine positively charged in the ground state. A forcefield minimization using the Universal force field in Avogadro was then complete on the entire active site with geometric constraints on all alpha carbons. From this, input files were generated for Orca. The energetics of each protonation state were calculated and analyzed. The states include His(+) – Asp(-) and His(neutral) – Asp (neutral). In cases where the proton spontaneously transferred to Histidine from aspartic acid or to aspartic acid from Histidine, the hydrogen was frozen at both distances of 1.09Å and 0.97Å (typical H-O length and H-N length).

2.6   Binding Energy/Residue Contribution

The Orca input files were generated using the same protocol as described previously. In order to obtain the overall binding energy, the active sites with the ligand bound were first minimized. A single point energy calculation on each optimized structure was complete using a larger basis set (QZVP/J). Since a relatively large basis set is being used, BSSE was not directly accounted for as this error should be small.[50] This was confirmed by completed a few calculations with counterpoise correction and observing little change in the overall energies obtained (<0.5kJ/mol). This energy was subtracted from the sum of the isolated ligand energy and the unbound active site energy. This provides the overall energy provided by all non-covalent and covalent interactions. Ligands were chosen from experimental results which showed them to be strong binders. These ligands were however truncated such that most non-covalent interactions were limited without affecting the electrophilicity of the ligand (**Figure 2.5**).

2.7   Potential Energy Scans

Starting at the minimized ground state structure of the active site with the ligand bound, the bond length between the serine nucleophilic oxygen and the electrophilic carbon (or boron) was increased (**Figure 2.6**). This distance was increased in the direction of the bond, pushing the ligand away from the serine residue. For most, the scanned range was between 1.4Å to 5Å in intervals of ~0.2Å with smaller intervals used for areas of interest (maxima or minima on the PES). At larger distances the intervals were also increased, as we are not particularly interested in these regions (>3.0Å). At each interval, the structure was minimized.
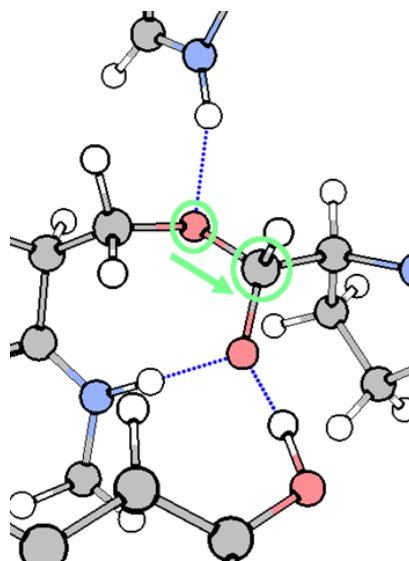
Figure 2.6: PES scan along the serine oxygen atom and electrophilic carbon of the electrophile.

Chapter 3

RESUTS/DISCUSSION: THERMODYNAMIC AND KINETIC INVESTIGATIONS INTO POP/FAP BINDING

3.1   Introduction

Due to a lack of predictive and accurate MM techniques available for discovery of covalent ligands, QM can be used to improve currently available tools through analysis of accurate simulations of covalent binding. The recent rise in interest of covalent inhibitors and the lack of accurate computational techniques available to investigate and/or design them has led to a surge in development. The QCCA allows for QM level treatment of large systems such as proteins which can be used to aid in the development of covalent inhibitors. It was used to assess the catalytic power of serine proteases, which can provide up to a 10^{26} fold rate enhancement, through a calculation of the energy barriers for proton transfers within the catalytic triad and the orientation of H-bonds present in the triad. Thermodynamic and kinetic data was also obtained for a series of covalent ligands with electrophilic warheads containing aldehyde, nitrile or boronic acid residues. The QCCA was also used to collect and analyze ligands binding to both POP and FAP to determine parameters such as activation binding energies as well as gain mechanistic insight. Detailed evaluation of processes such as the overall binding kinetics and binding thermodynamics for a ligand can help improve current molecular prediction tools such as docking and scoring functions.

Drug discovery programs have traditionally screened (scored) potential drug candidates based on predicted binding affinity, ranking activity by their inhibitory constant (K_i) and/or their half maximal inhibitory concentration (IC_{50}) values.[4] The binding affinity is composed of an enthalpic and entropic term. Since the activity of a covalent ligand is time dependent, the rate of inactivation (k_{inact}) must also be considered (**Figure 3.1**).[51]

$$E + S \rightleftharpoons ES \rightleftharpoons E + P$$

$$+ I \qquad + I$$

$$K_i \qquad K_i'$$

$$EI \qquad ESI$$

$$k_{inact}$$

$$EI^*$$
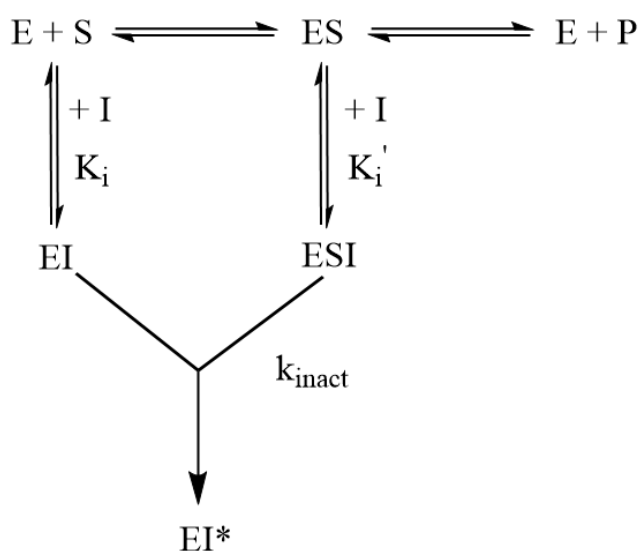
Figure 3.1: Kinetic scheme for a covalent (irreversible) inhibitor.

The importance of evaluation and optimization of binding kinetic parameters was demonstrated recently in a study by Guo *et. al.*[52] The authors claimed that in the case of covalent ligands, binding kinetics are a better predictor of the *in vivo* activity than thermodynamic parameters such as K_i, and IC_{50}.[53] The premise of this argument lies in binding affinity being determined in equilibrium conditions whereas most covalent inhibitors, which possess residence times too long to allow for equilibration, operate under non-equilibrium conditions. Therefore,

binding kinetics should be computed in parallel to assessment of binding affinity. The ratio of k_{inact}:K_i is normally reported in addition to K_i/IC$_{50}$ values in order to assess covalent ligand activity.[51] Optimization and analysis of both these properties are essential and can greatly improve success of lead compounds, propelling them further in pre-clinical and clinical stages.

Covalent binding is often presented as a two-step process: (1) Diffusion of the ligand into the active site to form a non-covalent complex and (2) covalent bond formation (**Figure 3.2**).[4]
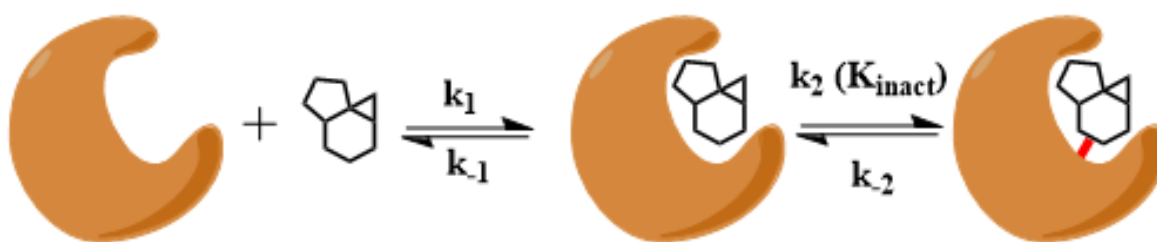
Figure 3.2 Step involved in covalent inhibitor binding.

Covalent bond forming step is often assumed to be the rate-limiting step. In contrast, the diffusion step is considered to be fast and is described by the forward association rate constant (k_1) and reverse dissociation rate constant (k_{-1}). In order to improve the activity of covalent drugs, synthetic strategies are required to lower k_{-1} which is inversely proportional to the time the ligand remains bound to the protein, referred to as the residence time ($t_r = 1/k_{-1}$).

Current computational methods used to predict covalent binding do not account for binding kinetics and often have an inaccurate representation of binding thermodynamics (bond energy). To improve current molecular prediction software, thermodynamics and kinetics must both be

considered. Classically, active compounds are first identified by having low K_i's however, for covalent ligands, it is imperative to include kinetics earlier in the drug discovery process. In this chapter we will discuss the fundamental differences in POP/FAP ligand binding, in terms of how various warheads affect the binding kinetics and thermodynamics, and how this data can be used to improve current docking/scoring functions, ultimately leading to better prediction of active covalent ligands.

3.2   **Docking**

The poses for ligands in POP generated by FITTED are shown in the figure below (**Figure 3.3**).
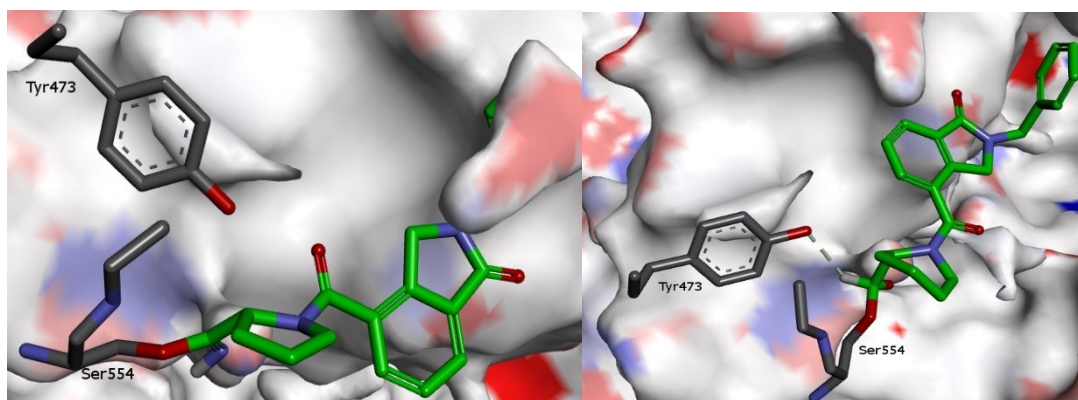
Figure 3.3: Top ranked pose of the nitrile **13** and aldehyde ligand **11** in POP.

Referring to the compounds in **Figure 3.3**, the left panel shows compound **13** (nitrile warhead) and the right panel shows compound **15** (aldehyde warhead). Focusing on the bond forming region, between the nucleophilic serine oxygen and electrophilic carbon, it can be seen that the anion generated is not positioned in the oxyanion hole. This hole is a network of hydrogen bonds which are known to stabilize the transition state of a covalent ligand binding to an enzyme.[54] For example,

in **Figure 3.3**, the oxyanion hole would be comprised of tyrosine 473 and the backbone N-H connected to serine 554 which point towards the same region of empty space. Although this inaccurate prediction may be a problem for identification of active compounds, the poses will only be used as a starting geometry for QM level calculations. The accuracy of the QM calculations will correct the position of this anion. Compound **15** appears to fit reasonably within the binding pocket, however compound **13** does not. The poses were still taken as is however since the region of compound **13** which appears to clash with the protein will be removed. As mentioned in section 2, the ligands will be truncated prior to QM calculations in order to focus on the interactions and properties of the warhead region of the ligands with the enzyme.

3.3 Energy barrier for proton shift between histidine and aspartic acid

As mentioned in section 1.1, differences in POP and FAP structure may explain and help predict the reactivity of these enzymes towards different substrates. One difference between the two enzymes is the orientation of the conserved catalytic triad residues (histidine, aspartic acid, and serine) and surrounding residues in the active site (tyrosine, arginine, glutamic acid, etc). This difference can affect properties such as relative basicity of the catalytic histidine, and by extension can influence the nucleophilicity of the catalytic serine residue. For example, consider the case in which the histidine residue becomes more electron rich, and hence more basic, caused by interaction with the aspartic acid in the catalytic triad. This would lead to a more nucleophilic serine as proton transfer onto the histidine would occur with a lower energy barrier, allowing for a lower activation energy for the nucleophilic attack by serine. The basicity of the histidine residues in POP and FAP can be studied through detailed analysis of the energy barrier associated with the proton shift between histidine and aspartic acid during a catalytic reaction.

The high reactivity of serine proteases can be partially explained in terms of the low barrier hydrogen bond (LBHB) theory.[16] Typically, hydrogens participating in weak hydrogen bonds fall within the NMR range of δ10-12ppm (or lower). However, NMR studies on serine proteases have revealed a low field proton at ~δ18ppm, indicating an abnormally strong hydrogen bond which is assigned to the histidine – aspartic acid hydrogen bond. In typical proteases, hydrogen bond donor and acceptor heteroatoms are separated by distances greater than 2.6Å. In the case of the serine protease it has also been shown that the distance between the two heteroatoms involved in hydrogen bonding, δ-nitrogen of histidine and oxygen of aspartic acid, is less than 2.6 Å. Based on the discussion above, the potential of this strong hydrogen bond has been estimated to be in the range of 14 kcal/mol to 40 kcal/mol.[16] In some cases, LBHBs are predicted to also form during catalysis with the formation of a TS, however this is often difficult to verify experimentally due to the lifetimes of TS species. The existence of LBHBs has been claimed to exist based in crystals and from NMR measurements of TS analogues.[16,55] Proponents of the LBHB theory argue that TS analogues have very different electronic structure than a true TS due to being located in an energy minimum as opposed to a saddle point (energy maximum). They furthermore argue that linking LBHB from crystals to enzymes is a stretch since a protein environment is much different from that of a crystal. Hydrogen bonds are typically attenuated/weaker due to competition with water in a protein.[55]

A literature survey on the published POP versus FAP inhibitors illustrates that FAP inhibitors generally possess more reactive electrophiles such as boronic acids while POP inhibitors contain less reactive electrophiles such as nitriles (**Figure 3.4**). As can be seen, many FAP inhibitors are boronic acids (compounds **21**, **24**).
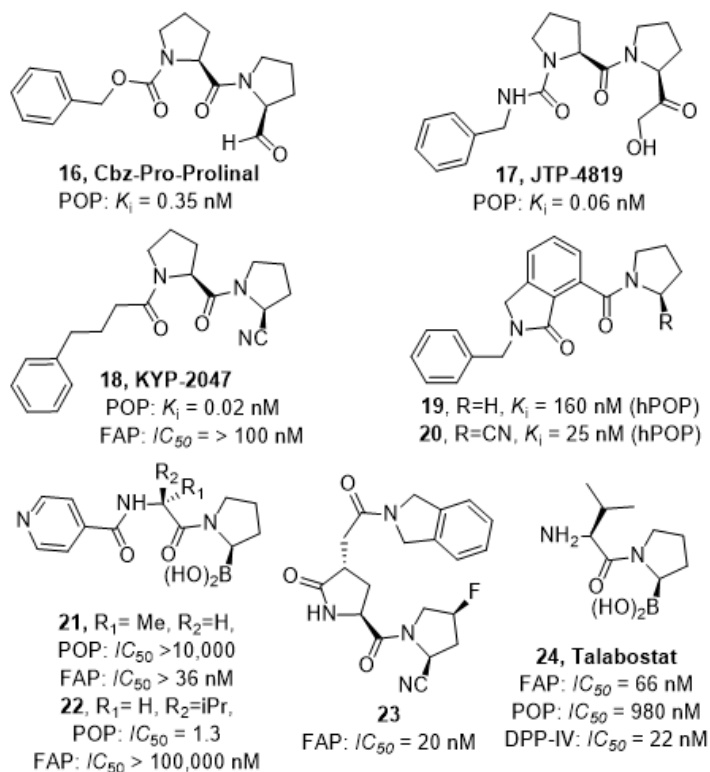
Figure 3.4: Survey of POP and FAP inhibitors reported in literature.[56]

Although nitrile ligands can be compatible with FAP (compound **23**), they are often shown to be too weak (compound **18**). This observation is also supported by results obtained from *in silico* docking studies of POP and FAP inhibitors.[57] Predicted affinities of nitrile ligands for FAP were inconsistent with *in vitro* measurements, overestimating their activity. One potential hypothesis that explains this discrepancy is the possibility of a lower reactivity of the nucleophilic serine in FAP, which is a detail that is not accounted for in covalent docking programs. To test this hypothesis, it is necessary to determine the energy difference for the various protonation states of the catalytic triad, which can give information on the basicity of histidine and nucleophilicity of serine in the active site.

In order to get an estimate of this energy barrier, various protonation states in the active site were analyzed for both POP and FAP (**Figure 3.5**). State A/B involves the unbound active site with the aspartic acid protonated and deprotonated. State C/D involves the bound active site with either the aspartic acid protonated or deprotonated.
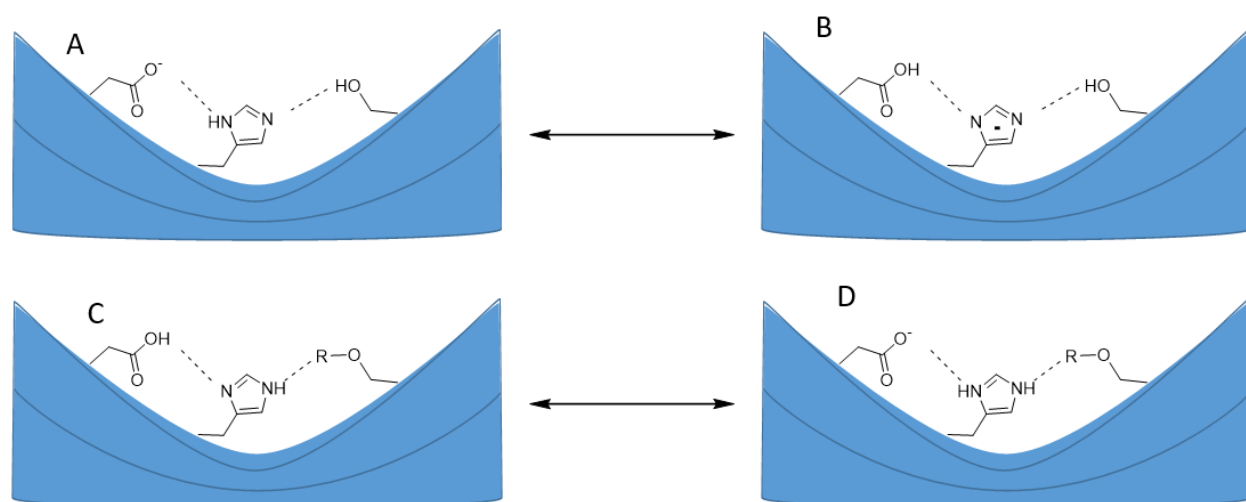
Figure 3.5: Protonation states of catalytic triad analyzed. The other residues in the QCCA model were also included (not shown here).

One could also envision analysis of a third state with the serine residue deprotonated, however during optimization of this state, both the proton on aspartic acid and histidine had to be constrained. This was required as proton shift from the histidine to serine and from aspartic acid to serine was occurring spontaneously. This led to energies that were biased and prone to large errors (>10kcal/mol), so this state was excluded.

Figure 3.6 illustrates the orientation of the residues in the lowest energy conformations of POP (top) and the lowest energy bound state of POP (bottom).
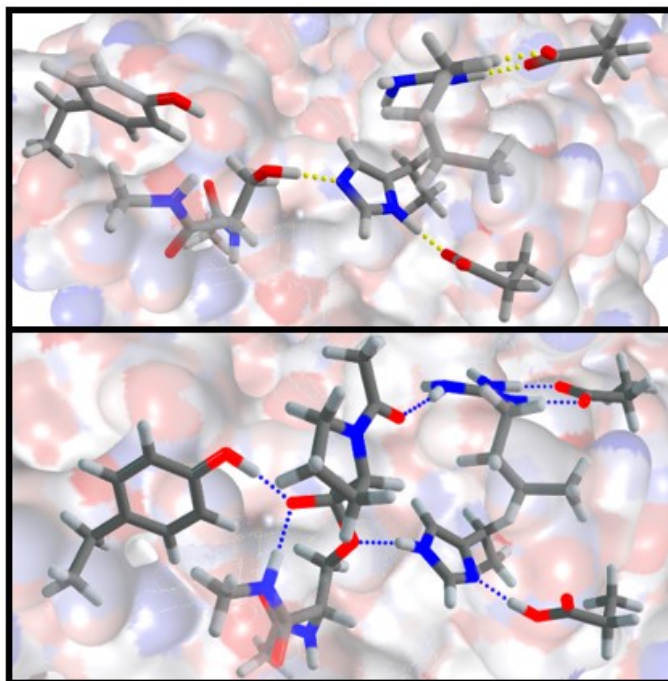
Figure 3.6: Ground state of unbound (top) and bound POP (bottom).

The catalytic triad appears to be linked together through a hydrogen bond network as expected and generally accepted.[58] Also it can be seen that the hemiacetal anion generated is stabilized in the oxyanion hole. This is a correction from the docking pose which could not identify this. Visual inspection of the generated orientation of the ligand/active site residues appears to correspond well with what is known about ligands binding to serine proteases.

As mentioned in Section 2.5, in order to determine the energy difference between different protonation states, the energy of one state (A) can be subtracted from the ground state (B).

Table 3.1 provides a summary of the data collected. 1.09A and 0.97A correspond to the distances between the δ-nitrogen proton on histidine and the aspartic acid oxygen closest to the histidine. The last entry is the energy difference between the ground state structure and the minimized structure of forcing histidine and aspartic acid away from each other by a distance of 3.0A. It can be seen that the energy difference for proton transfer in FAP is much larger than that in POP. This indicated that proton transfer from serine onto the histidine and from the histidine onto aspartic acid has a lower energy barrier in POP than in FAP. All of this information supports a more nucleophilic serine in POP. More convincing evidence could be provided from looking at the exact energy barrier for the proton transfer experimentally or through the use of other QM techniques such as QM/MM to account for the surrounding protein environment. Another interesting observation is the very small energy difference between the unprotonated histidine and ground states in POP. In this case, it is possible that the proton can rapidly transfer between the histidine and aspartic acid, or may be situated in between both residues as expected for a LBHB species. The data collected in this thesis supports the presence of a strong hydrogen bond in POP between the histidine and aspartic acid residues, in comparison with FAP.

Residue - Ligand	POP (kcal/mol)	FAP (kcal/mol)
His⁻ (1.09 Å) – No Ligand	-0.32	-11.6
HisH (0.97 Å) – No Ligand	-2.6	-7.4
$D_{HisH-Asp}$ = 3.0Å – No Ligand	-4.3	-18.5
HisH$_2^+$ (1.09 Å) - Aldehyde	-18.3	-14.2
HisH$_2^+$ (0.97 Å) - Aldehyde	-11.0	-7.1

Table 3.1 Energy barrier associated with proton transfer between histidine and aspartic acid.

3.4   Residue contribution to binding thermodynamics and overall binding energies

The QCCA model can also be used to collect other kinetic and thermodynamic parameters related to ligand binding such as total binding energies and activation energies. The total binding energy includes non-covalent interactions, such as H-bonding, VDWs, dipole-dipole, and solvent effects. It is obtained by taking the energy difference between the ligand bound within the active site and the free ligand plus free active site (unbound) energy (**Figure 3.7**).

Figure 3.7: Calculating the overall binding energy of a ligand with QM.

The general observation from this data is that the overall binding energy appears to be ~10kcal/mol. larger for electrophiles binding to POP than FAP (**Figure 3.8**).
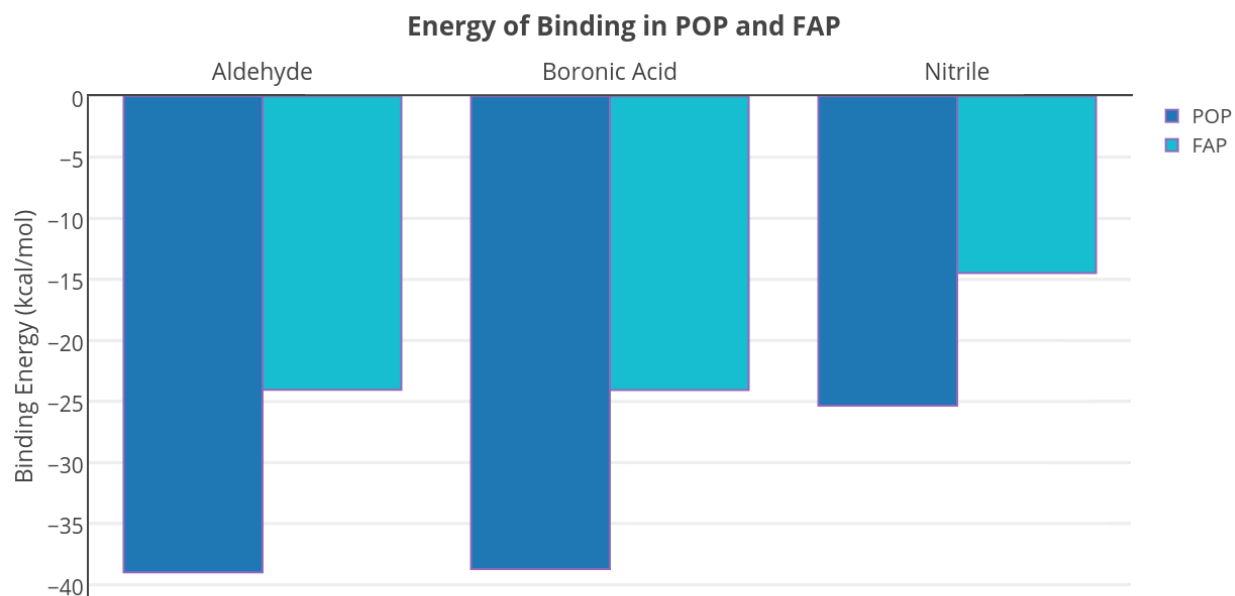
Figure 3.8: Binding energy of aldehyde, nitrile and boronic acid electrophiles in POP and FAP.

In order to rationalize this energy difference at an atomistic level, the bond distances and angles of the H-bonds formed between His – Ser and His – Asp were calculated in both the bound and unbound states (**Table 3.2**). No significant differences were observed in the unbound structure for the distance between the H-bonding atoms and heteroatoms. The bond angle between the Ser-His H-bond varies between FAP and POP by about 10 degrees. The H-bond angle in POP is closer to the optimal angle, 180 degrees. This may be part of the contribution to the lower activation energy for the proton shift from serine onto the histidine in this enzyme over FAP. In the bound structure the bond distances and angles were not significantly different and thus no conclusions were drawn from this data.

Residues	Protein	Distance (H-Bond)	Distance (Heteroatoms)	Angle
His - Ser	FAP	1.89	2.85	157.3
His - Asp	FAP	1.51	2.59	171.9
His – Ser	POP	1.81	2.79	167.0
His – Asp	POP	1.56	2.63	173.7

Table 3.2: Distances of H-bonds, heteroatoms participating in H-bonds and angles of H-bonds in both POP and FAP. Distances are all in angstroms (Å).

3.5   Potential energy scans

The effect of the electrophilic warhead on binding and covalent bond formation is further investigated by a calculation of the PES of the bond formation. The PES plots can provide insight into the activation barriers required for bond formation and release. (**Figure 3.9**).
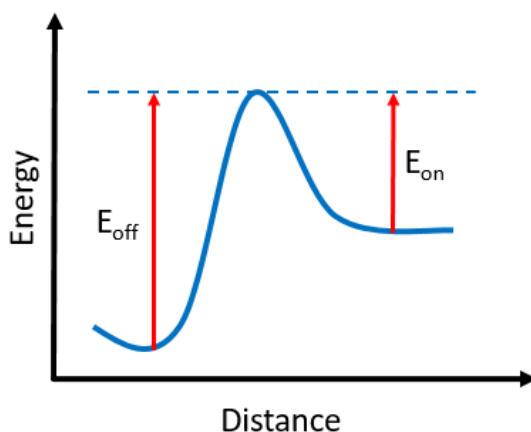
Figure 3.9: Graph illustrating the E_{off} and E_{on} parameters taken from the PES scans. The distance is measured between the serine oxygen and the electrophilic carbon of the ligand.

Experiments previously conducted illustrate several important observations about the difference in binding kinetics and thermodynamics for boronic acid, aldehyde and nitrile electrophilic

warheads. These three groups have previously been demonstrated to readily form covalent bonds in the active site of serine proteases. The boronic acid functional group has seen the most commercial success as it possesses an activity which is considered to be safe (not as reactive as an aldehyde), mitigating off-target problems. For example, Bortezomib, a boronic acid inhibitor of the 20S proteasome, has been approved in the treatment of multiple myeloma. The nitrile functional group is milder than both the aldehyde and boronic acid warheads. Nitrile containing electrophilic drugs have also seen success in many medicinal applications against serine proteases including Saxaglipitin, a covalent inhibitor of dipeptidyl peptidase IV.[59]

The Moitessier group has previously developed strong binding inhibitors of POP containing nitrile, aldehyde and boronic acid electrophiles (**Table 3.3**).[60] Out of the synthesized library, compound **25** elicits the greatest activity[57]. These results illustrate the electrophilic warhead on its own can have a large effect on binding affinity. It is believed that through careful analysis of the PES for these electrophiles, one could get a quantitative idea about how much energy is required to form and break the bonds between the electrophile of the ligand and nucleophile of the protein. One could also envision that through looking at the dynamics of ligand binding/unbinding, differences in the kinetic parameters can also be elucidated, if any, for different reactive warheads. This data could allow for development of parameters to improve scoring functions and docking results in the future which take into account the effect of electrophilic warheads on ligand binding.
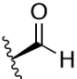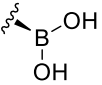
Compound	R₁	R₂	R₃	K$_i$ (nM)
19	H	H	H	160
20	H	H	CN	25
25	H	H	CH$_2$OH	4
26	H	H	(aldehyde group)	110
27	H	H	(boronic acid group)	22

Table 3.3 Potency of various covalent ligands developed previously by the Moitessier group.[60]

Initially during the PES scans, alpha carbons were the only frozen atoms in the model. However, it appeared that the residues were rotating and flipping unnaturally. This led to inaccurate simulation of ligand binding/unbinding. To circumvent this problem, all the hydrogens added to the alpha carbons were also frozen. This would prevent the entire truncated residue from flipping, and restrict the motion of the R groups in the model. The initial model also excluded glutamic acid, which interacts with arginine. This residue was deemed essential as the motion of arginine was drastic without glutamic acid. Although some backbone movement is present in an enzyme, it is difficult to consider them using the QCCA approach. The constraints applied only allow for R group motion of the residues.
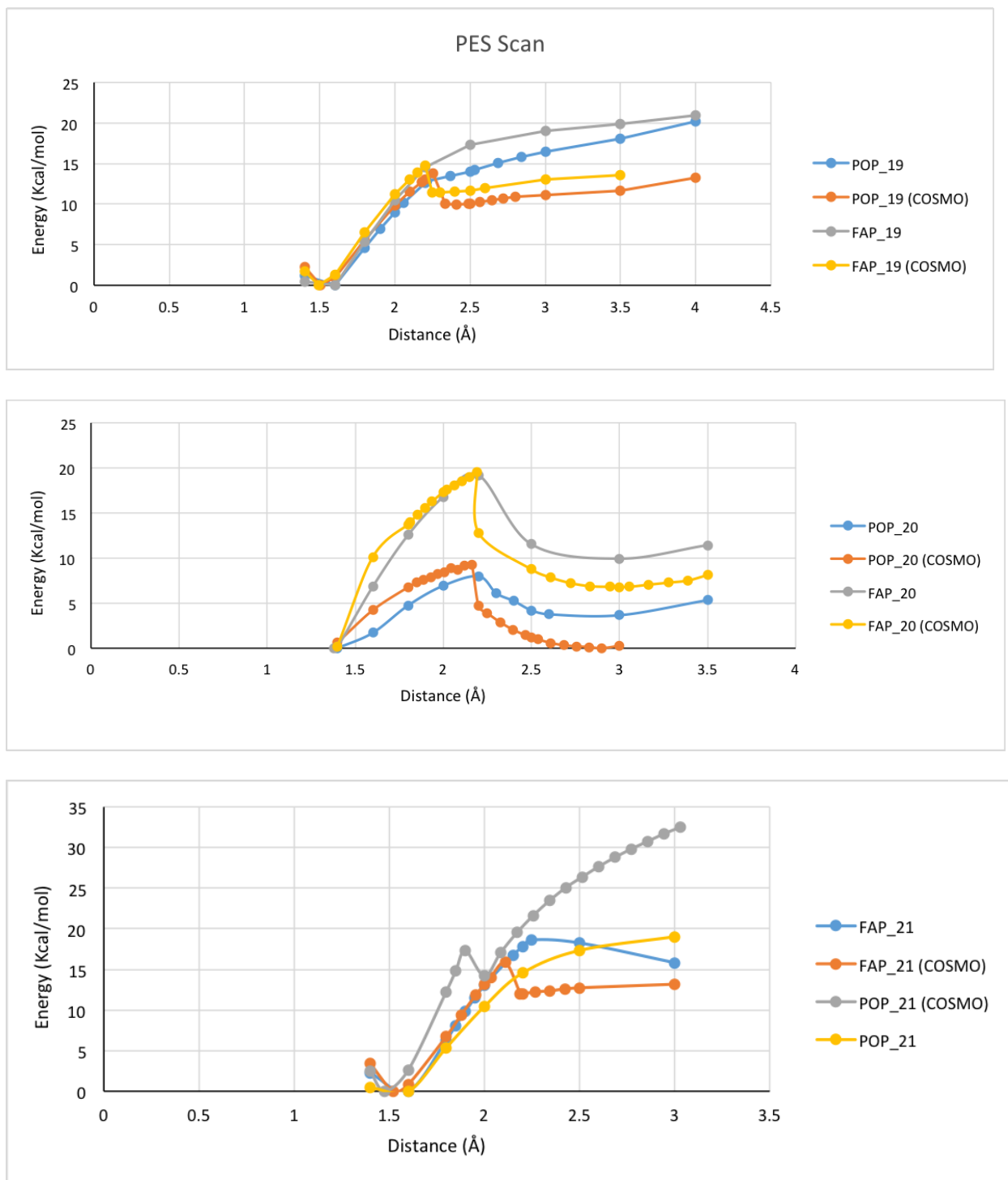
Figure 3.10: PES scans for three inhibitors – (A) Compound 19 (Aldeyde) (B) Compound 20 (Nitrile)

(C) Compound 21 (Boronic Acid)

The PES scans can be seen in **Figure 3.10** for the aldehyde, boronic acid and nitrile in POP and FAP. The data from the potential energy scans illustrated a few important findings. Firstly, the aldehyde and boronic acid appear to have a very small activation energy, if any, for bond formation. As mentioned previously, in enzymatic inhibition with covalent inhibitors, bond formation is believed to be the slow step while the ligand entering the active site and forming the covalent complex is the fast step. This data suggests that the covalent bond formation may be rapid depending on the warhead which is in contrast to what is commonly reported/assumed. A summary of the kinetic data obtained is illustrated in **Table 3.4**.

Compd.	Enz.	E_{off}	E_{off} (solv.)	E_{on}	E_{on} (solv.)	Binding Energy
14 (Aldehyde)	POP	17.2	17.3	~0	2.9	-39.0
15 (Nitrile)	POP	8.0	13.0	~0	4.5	-25.3
13 (Boronic Acid)	POP	20.8	>30.0	~0	3.1	-38.7
14 (Aldehyde)	FAP	17.3	16.8	~0	2.1	-24.0
15 (Nitrile)	FAP	19.0	25.4	9.3	8.7	-14.5
13 (Boronic Acid)	FAP	18.2	17.6	~0	2.6	-24.5

Table 3.4: Summary of parameters obtained computationally (all values are in kcal/mol).

Looking specifically at the E_{on} values taking into account solvation, it can be seen that the nitrile has a higher activation energy for bond formation than both the aldehyde and boronic acid in POP and FAP. In FAP, the nitrile activation energy appears to be quite large, indicating this electrophilic warhead may not be reactive enough for FAP. This is in accordance to what has been reported in the literature, as most high affinity covalent ligands for FAP are either boronic acids or aldehydes. In POP, the nitrile is still less reactive, however the activation energy is under 10 kcal/mol indicating it may be reactive enough for POP. The effects of quantum tunneling on lowering the

activation energy was not taken into account in this analysis. Enzymatic catalysis has been known to overcome significantly large energy barriers associated with deprotonation through quantum tunneling effects. These effects are typically significant when the activation energy associated with proton transfer/deprotonation is relatively high, making the reaction unlikely.[61] In our systems, the reaction is predicted to possess a very low activation barrier, and thus quantum tunneling effects are unlikely to have an impact on the reaction.

The correlation of the energy of bond breakage (E_{off}) with the residence times is another interesting result obtained. Kinetic parameters obtained from previous experimental work show the nitrile having a very short residence time (<1 min) while the boronic acid has the longest (73 +/- 10 min) and aldehyde is in between (20 +/- 0.8 min).[60] The computations predict the nitrile to also have a shorter residence time, while the boronic acid will have the longest and the aldehyde somewhere in between (with solvation effects taken into account). These correlations help to validate the predictability of the QCCA in regards to residence time and appropriate electrophilic class. This would allow one to determine whether a nucleophilic residue can be effectively targeted by an electrophilic warhead. This will identify if a nucleophilic reside in the protein can be targeted efficiently by a specific covalent warhead and whether this class of inhibitor is appropriate for the desired target.

The computational data illustrates that the electrophilic warhead has a direct influence on the kinetics and thus activity of the second step in ligand binding.[57] According to this data, the aldehyde and boronic acid are predicted to have longer residence times than the nitrile, represented by the significantly larger E_{off} value in POP. The data also shows that the aldehyde and boronic acid have a very low activation energy (E_{on}). This suggests that covalent bond formation is limited by diffusion of the ligand into the active site and reorientation of the electrophilic warhead to allow

51

covalent bond formation. This low energy barrier is attributed to two observations: (1) The ligands appear to be pre-activated by Tyr_{473} as they approach the nucleophilic serine and (2) the transition states of these reactions resemble the TS adopted by the natural substrates and are highly stabilized through hydrogen bonding. Although these predictions match the measured Ki's, the computed low energy barriers for the aldehyde and boronic acid are contrasting to the commonly reported slow covalent binding step.[57] This prompted us to look directly at the kinetics of ligand binding using isothermal calorimetry to extract out the association (k_{on}) and dissociation (k_{off}) rates. These experiments were completed by Justin Di Trani in the Mittermier lab on the aldehyde inhibitor 15.[60] The preliminary results indicate that the k_{on} is independent of the temperature, pointing towards a diffusion limited reaction (kinetic controlled, very low activation barrier) for ligand binding. The k_{off} is dependent on the temperature indicating thermodynamic control. This is in agreement with the computations, further supporting the prediction. Currently, experiments to acquire activation energies for the nitrile ligand **13** are also underway. This will provide more evidence on the ability of the QCCA to predict binding kinetics in covalent ligands.

Chapter 4

<u>CONCLUSIONS AND FUTURE WORK</u>

4.1   <u>Conclusion</u>

In summary, QM calculations completed in this thesis suggest the nucleophilic serine in POP may be more reactive than in FAP. This was supported by calculations which illustrate a lower energy barrier for proton movement to and from the catalytic histidine residue for POP. This, in turn, demonstrated that the histidine may be more basic and more readily accept the proton from serine, making the serine more nucleophilic. It was also shown that the overall binding energy was larger for ligands binding to POP over FAP. This again suggests, for our truncated systems, that ligands binding to POP is more energetically favorable than ligands binding to FAP. Atomistic level details were analyzed, such as bonding angles and lengths to understand a basis for this energy difference, however concrete evidence supporting this was not found. Lastly, PES scans were run for the three electrophilic ligand classes analyzed. Our data supports a fast covalent binding step for ligands bearing boronic acids and aldehyde electrophiles. This observation contradicts what is typically reported, with the covalent binding step being slower than the non-covalent binding. These results led to the experimental study of binding kinetics in POP with isothermal calorimetry completed by Justin Di Trani in the Mittermier lab. The experimental results confirmed the predicted diffusion limited reaction for an aldehyde inhibitor binding to POP.

This experimental data provided validation for the QCCA method, which allowed us to extend the technique to FAP, which is an extremely difficult protein to work with experimentally (poor stability). Similar trends were observed for the ligands, however a larger energy barrier was observed for the nitrile binding to FAP. This led us to believe that the nitrile ligand may not be reactive enough for FAP, which is supported by the very few reported nitrile inhibitors for FAP (most of which are more reactive ligands) compared to highly potent boronic acid-containing FAP inhibitors.

4.2   Future Work

Further experimental studies (isothermal calorimetry) should be completed in order to verify the prediction on the other electrophile classes which are predicted to have different kinetic properties than the aldehyde (nitrile has a larger activation energy). This will help verify the QCCA results obtained in this thesis. In order to acquire absolute activation energies, the true transition states could also be determined for the three inhibitors looked at (finding the saddle points on the PES). Further QM studies could also be complete to include other electrophiles. QM/MM simulations could also be run in parallel to check if they agree with the QCCA and experimental results. QM/MM could provide more accurate information as the entire protein environment will be taken into account and the catalytic site will be unconstrained. After the electrophile library has been expanded and data has been collected, trends and models can then be developed. This will address a limitation of current docking programs which are unable to rank covalent ligands which possess different electrophilic warheads alongside one another. By taking into consideration electrophile reactivity and bond energy, docking methodologies can be used to dock large libraries of different electrophiles in one run. Mathematical terms extracted from the QM data on the

electrophile reactivity and bond energy can be used when computing the scores of docked compounds. As the library of compounds evaluated increases, the terms can be further refined.

4.3 <u>References</u>

(1)   Jackson, K. W.; Christiansen, V. J.; Yadav, V. R.; Silasi-Mansat, R.; Lupu, F.; Awasthi, V.; Zhang, R. R.; McKee, P. A. *Neoplasia* **2015**, *17* (1), 43–54.

(2)   Christiansen, V. J.; Jackson, K. W.; Lee, K. N.; Downs, T. D.; McKee, P. A. *Neoplasia* **2013**, *15* (4), 348–358.

(3)   Johnson, D.; Weerapana, E.; Cravatt, B. *Future Med. Chem.* **2010**, *2* (6), 949–964.

(4)   Singh, J.; Petter, R. C.; Baillie, T. A.; Whitty, A. *Nat. Rev. Discov.* **2011**, *10* (4), 307–317.

(5)   Cheng, J. D.; Dunbrack, R. L.; Valianou, M.; Rogatko, A.; Alpaugh, R. K.; Weiner, L. M. *Cancer Res.* **2002**, *62* (16), 4767–4772.

(6)   Puré, E. *Expert Opin. Ther. Targets* **2009**, *13* (8), 967–973.

(7)   Garin-Chesa, P.; Oldt, L. J.; Rettigt, W. J. *Proc. Natl. Acad. Sci.* **1990**, *87*, 7235–7239.

(8)   Park, J. E.; Lenter, M. C.; Rainer, N.; Garin-chesa, P.; Old, L. J.; Rettig, W. J.; Zimmermann, R. N. *J. Biol. Chem.* **1999**, *274* (51), 36505–36512.

(9)   Hedstrom, L. *Chem. Rev.* **2002**, *102* (12), 4501–4523.

(10)   Kaushik, S.; Etchebest, C.; Sowdhamini, R. *Proteins Struct. Funct. Bioinforma.* **2014**, *82* (7), 1428–1443.

(11)   Wong, P. F.; Gall, M. G.; Bachovchin, W. W.; McCaughan, G. W.; Keane, F. M.; Gorrell,

M. D. *Peptides* **2016**, *75*, 80–95.

(12) Aertgeerts, K.; Levin, I.; Shi, L.; Snell, G. P.; Jennings, A.; Prasad, G. S.; Zhang, Y.; Kraus, M. L.; Salakian, S.; Sridhar, V.; Wijnands, R.; Tennant, M. G. *J. Biol. Chem.* **2005**, *280* (20), 19441–19444.

(13) Carter, P.; Wells, J. A. *Nature* **1988**, *332* (6164), 564–568.

(14) Kidd, R. D.; Sears, P.; Huang, D.-H.; Witte, K.; Wong, C.-H.; Farber, G. K. *Protein Sci.* **1999**, *8*, 410–417.

(15) Cleland, W. W.; Frey, P. A.; Gerlt, J. A. *Biochemistry* **1994**, *273* (40), 25529–25532.

(16) Frey, P. A.; Whitt, S. A.; Tobin, J. B. *Science (80-.).* **1994**, *264* (5167), 1927–1930.

(17) Baigent, C.; Patrono, C. *Arthritis Rheum.* **2003**, *48* (1), 12–20.

(18) London, N.; Miller, R.; Krishnan, S.; Uchida, K.; Irwin, J.; Eidam, O.; Gibold, L.; Cimerman, P.; Bonnet, R.; Shoichet, B.; Taunton, J. *Nat. Chem. Biol.* **2015**, *10* (12), 1066–1072.

(19) Scholz, C.; Knorr, S.; Hamacher, K.; Schmidt, B. *J. Chem. Inf. Model.* **2015**, *55* (2), 398–406.

(20) Toledo Warshaviak, D.; Golan, G.; Borelli, K. W.; Zhu, K.; Kalid, O. *J. Chem. Inf. Model.* **2014**, *65*, 1941–1950.

(21) Bianco, G.; Forli, S.; Goodsell, D. S.; Olson, A. J. *Protein Sci.* **2016**, *25* (1), 295–301.

(22) Kramer, B.; Rarey, M.; Lengauer, T. *Proteins Struct. Funct. Genet.* **1999**, *37* (2), 228–

241.

(23)   Jones, G.; Willett, P.; Glen, R. C.; Leach, A. R.; Taylor, R. *J. Mol. Biol.* **1997**, *267* (3), 727–748.

(24)   Hart, T. N.; Read, R. J. *Proteins Struct. Funct. Genet.* **1992**, *13* (3), 206–222.

(25)   Ferreira, L. G.; Dos Santos, R. N.; Oliva, G.; Andricopulo, A. D. *Molecules* **2015**, *20*, 13384–13421.

(26)   Kumalo, H. M.; Bhakat, S.; Soliman, M. E. S. *Molecules* **2015**, *20* (2), 1984–2000.

(27)   Ouyang, X.; Zhou, S.; Su, C. T. T.; Ge, Z.; Li, R.; Kwoh, C. K. *J. Comput. Chem.* **2013**, *34* (4), 326–336.

(28)   Ai, Y.; Yu, L.; Tan, X.; Chai, X.; Liu, S. *J. Chem. Inf. Model.* **2016**, *56* (8), 1563–1575.

(29)   Friesner, R. A.; Murphy, R. B.; Repasky, M. P.; Frye, L. L.; Greenwood, J. R.; Halgren, T. A.; Sanschagrin, P. C.; Mainz, D. T. *J. Med. Chem.* **2006**, *49* (21), 6177–6196.

(30)   Huang, S.-Y.; Grinter, S. Z.; Zou, X. *Phys. Chem. Chem. Phys.* **2010**, *12* (40), 12899–12908.

(31)   Meng, E.; Shoichet, B.; Kuntz, I. *J. Comput. Chem.* **1992**, *13* (4), 505–524.

(32)   Weiner, S. J.; Kollman, P. A.; Case, D. A.; Singh, U. C.; Ghio, C.; Alagona, G.; Profeta, S.; Weinerl, P. *J. Am. Chem. Soc.* **1984**, *106* (17), 765–784.

(33)   Kitchen, D. B.; Decornez, H.; Furr, J. R.; Bajorath, J. *Nat. Rev. Drug Disc.* **2004**, *3* (11), 935–949.

(34)   Wang, R.; Lu, Y.; Fang, X.; Wang, S. *J. Chem. Inf. Comput. Sci.* **2004**, *44* (6), 2114–2125.

(35)   Muegge, I. *Perspect. Drug Discov. Des.* **2000**, *20*, 99–114.

(36)   Gohlke, H.; Hendlich, M.; Klebe, G. *J. Mol. Biol.* **2000**, *295* (2), 337–356.

(37)   Flanagan, M. E.; Abramite, J. A.; Anderson, D. P.; Aulabaugh, A.; Dahal, U. P.; Gilbert, A. M.; Li, C.; Montgomery, J.; Oppenheimer, S. R.; Ryder, T.; Schuff, B. P.; Uccello, D. P.; Walker, G. S.; Wu, Y.; Brown, M. F.; Chen, J. M.; Hayward, M. M.; Noe, M. C.; Obach, R. S.; Philippe, L.; Shanmugasundaram, V.; Shapiro, M. J.; Starr, J.; Stroh, J.; Che, Y. *J. Med. Chem.* **2014**, *57* (23), 10072–10079.

(38)   Smith, A. J. T.; Zhang, X.; Leach, A. G.; Houk, K. N. *J. Med. Chem.* **2009**, *52* (2), 225–233.

(39)   Van Der Kamp, M. W.; Mulholland, A. J. *Biochemistry* **2013**, *52* (16), 2708–2728.

(40)   Siegbahn, P. E. M.; Himo, F. *Wiley Interdiscip. Rev. Comput. Mol. Sci.* **2011**, *1* (3), 323–336.

(41)   Hu, P.; Zhang, Y. *J. Am. Chem. Soc.* **2006**, *128* (4), 1272–1278.

(42)   Wang, S.; Hu, P.; Zhang, Y. *J. Phys. Chem.* **2007**, *111* (14), 3758–3764.

(43)   Szabo, A.; Ostlund, N. S. *Introduction to Advanced Electronic Structure Theory*. 1996, p 480.

(44)   Cramer, C. J. *Essentials of Computational Chemistry Theories and Models*; 2004; Vol. 42.

(45)   Jensen, F. *Introduction to Computational Chemistry*; 2007.

(46)   Zheng, X.; Liu, M.; Johnson, E. R.; Contreras-García, J.; Yang, W. *J. Chem. Phys.* **2012**, *137* (21), 214106.

(47)   Mori-Sánchez, P.; Cohen, A. J.; Yang, W. *Phys. Rev. Lett.* **2008**, *100* (14), 1–4.

(48)   Blomberg, L. M.; Blomberg, M. R. A.; Siegbahn, P. E. M. *J. Inorg. Biochem.* **2005**, *99* (4), 949–958.

(49)   Bassan, A.; Borowski, T.; Siegbahn, P. E. M. *Dalt. Trans.* **2004**, No. 20, 3153.

(50)   Kobko, N.; Dannenberg, J. J. *J. Phys. Chem.* **2001**, *105*, 1944–1950.

(51)   Miyahisa, I.; Sameshima, T.; Hixon, M. S. *Angew. Chemie - Int. Ed.* **2015**, *54* (47), 14099–14102.

(52)   Guo, D.; Heitman, L. H.; IJzerman, A. P. *ACS Med. Chem. Lett.* **2016**, *7*, 819–821.

(53)   Kuang, M.; Zhou, J.; Wang, L.; Liu, Z.; Guo, J.; Wu, R. *J. Chem. Inf. Model.* **2015**, *55* (9), 1926–1935.

(54)   Zhang, Y.; Kua, J.; McCammon, J. A. *J. Am. Chem. Soc.* **2002**, *124* (35), 10572–10577.

(55)   Graham, J. D.; Buytendyk, A. M.; Bowen, K. H.; Collins, K. D. *J. Am. Chem. Soc.* **2013**, *53*, 344–349.

(56)   Stephane De Cesco, Jerry Kurian, Justin Di Trani, Naela Janmamode, Anthony Mittermaier, N. M. *Manuscr. Prep.* **2016**.

(57)   Stephane De Cesco. Combining computational chemistry, synthesis and enzymology for the design of covalent inhibitors applied to prolyl oligopeptidase inhibition, McGill

University, 2016.

(58)   Fülöp, V.; Böcskei, Z.; Polgár, L.; Abrahams, J. .; Leslie, A. G. .; Atack, J. .; Suman-Chauhan, N.; Dawson, G.; Kulagowski, J. .; Baker, S. .; Saunders, N. F. .; Willis, A. .; Ferguson, S. .; Hajdu, J.; Fülöp, V.; Barton, G. .; Böcskei, Z.; Fuxreiter, M.; Náray-Szabó, G.; Szabó, E.; Polgár, L.; Brünger, A. .; Brünger, A. .; Camargo, A. C. .; Caldo, H.; Reis, M. .; Chevallier, S.; Goeltz, P.; Thibault, P.; Banville, D.; Gagnon, J.; Connolly, M.; Cygler, M.; Schrag, J. .; Sussman, J. .; Harel, M.; Silman, I.; Gentry, M. .; Doctor, B. .; Diefenthal, T.; Dargatz, H.; Witte, V.; Reipen, G.; Svendsen, I.; Esnouf, R. .; Faber, H. .; Groom, C. .; Baker, H. .; Morgan, W. .; Smith, A.; Baker, E. .; Fukunari, A.; Kato, A.; Sakai, Y.; Yoshimoto, T.; Ishiura, S.; Suzuki, K.; Nakajima, T.; Fülöp, V.; Moir, J. W. .; Ferguson, S. .; Hajdu, J.; Garavito, R. .; Rossmann, M. .; Argos, P.; Eventoff, W.; Goossens, F.; Meester, I. De; Vanhoof, G.; Hendricks, D.; Vriend, G.; Scharpé, S.; Ishiura, S.; Tsukahara, T.; Tabira, T.; Shimizu, T.; Arahata, K.; Sugita, H.; Jones, T. .; Zou, J. .; Cowan, S. .; Kjeldgaard, M.; Kabsch, W.; Sander, C.; Kraulis, P. .; Lambright, D. .; Sondek, J.; Bohm, A.; Skiba, N. .; Hamm, H. .; Sigler, P. .; Li, J.; Brick, P.; O'Hare, M. .; Skarzynski, T.; Lloyd, L. .; Curry, V. .; Clark, I. .; Bigg, H. .; Hazleman, B. .; Cawston, T. .; Al., E.; Maes, M.; Goossens, F.; Scharpé, S.; Meltzer, H. .; D'Hondt, P.; Cosyns, P.; Medrano, F. .; Alonso, J.; Garcia, J. .; Romero, A.; Bode, W.; Gomis-Ruth, F. .; Mentlein, R.; Merritt, E. .; Murphy, M. E. .; Miura, N.; Shibata, S.; Watanabe, S.; Moriyama, A.; Nakanishi, M.; Sasaki, M.; Neer, E. .; Smith, T. .; Ollis, D. .; Cheah, E.; Cygler, M.; Dijkstra, B.; Frolow, F.; Franken, S. .; Harel, M.; Remington, S. .; Silman, I.; Schrag, J.; Al., E.; Pathak, D.; Ollis, D.; Polgár, L.; Polgár, L.; Polgár, L.; Polgár, L.; Polgár, L.; Polgár, L.; Polgár, L.; Kollát, E.; Hollósi, M.; Portevin, B.; Benoist, A.;

Rémond, G.; Hervé, Y.; Vincent, M.; Lepagnol, J.; Nanteuil, G. De; Read, R. .; Rennex, D.; Hemmings, B. .; Hofsteenge, J.; Stone, S. .; Richardson, J. .; Russell, R. .; Barton, G. .; Scaloni, A.; Barra, D.; Jones, W. .; Manning, J. .; Shinoda, M.; Toide, K.; Ohsawa, I.; Kohsaka, S.; Smith, L. .; Faustinella, F.; Chan, L.; Sondek, J.; Bohm, A.; Lambright, D. .; Hamm, H. .; Sigler, P. .; Vanhoof, G.; Goossens, F.; Hendriks, L.; Meester, I. De; Hendriks, D.; Vriend, G.; Broeckhoven, C. Van; Scharpé, S.; Wall, M. .; Coleman, D. .; Lee, E.; Iniquez-Lluhi, J. .; Posner, B. .; Gilman, A. .; Sprang, S. .; Welches, W. .; Brosnihan, K. .; Ferrario, C. .; Wilk, S.; Yoshimoto, T.; Walter, R.; Tsuru, D.; Yoshimoto, T.; Kado, K.; Matsubara, F.; Koriyama, N.; Kaneto, H.; Tsuru, D.; Yoshimoto, T.; Kanatani, A.; Shimoda, T.; Inaoka, T.; Kobubo, T.; Tsuru, D. *Cell* **1998**, *94* (2), 161–170.

(59)   Metzler, W. J.; Yanchunas, J.; Weigelt, C.; Kish, K.; Klei, H. E.; Xie, D.; Zhang, Y.; Corbett, M.; Tamura, J. K.; He, B.; Hamann, L. G.; Kirby, M. S.; Marcinkeviciene, J. *Protein Sci.* **2008**, *17* (2), 240–250.

(60)   De Cesco, S.; Deslandes, S.; Therrien, E.; Levan, D.; Cueto, M.; Schmidt, R.; Cantin, L. D.; Mittermaier, A.; Juillerat-Jeanneret, L.; Moitessier, N. *J. Med. Chem.* **2012**, *55* (14), 6306–6315.

(61)   Sutcliffe, M. J.; Scrutton, N. S. *R. Soc.* **2010**, *358* (1766), 367–386.

Appendix 1: Cartesian Coordinates for QM calculations

Minimizations were completed using the hybrid DFT function B3LYP with the basis set 6-31G**.

Single point energies were computed on the optimized geometries with the QZVP/J basis set with

dispersion correction. The electronic structure package used was ORCA, with utilization of the

PES scan function implemented into the program. The following Cartesian coordinates are for the

energy maxima obtained from the PES scans and local/global minima (covalently bound and

unbound) obtained from geometry minimizations. The format of the reported data consists of the

atom symbol in column 1 followed by the X, Y and Z coordinates of each atom in columns 2, 3

and 4.

Compound 18

Minima

C	38.095900	-2.349920	58.441600
C	39.017110	-1.127970	58.410630
C	40.321380	-1.464920	57.647010
C	41.227760	-2.031880	58.754360
C	40.889130	-1.164420	59.979240
N	39.495390	-0.769810	59.739960
C	38.609390	-0.242350	60.642300
O	37.439920	-0.036370	60.328230
H	42.290010	-1.996970	58.497470
H	40.957990	-3.072490	58.958320
H	40.163130	-2.165670	56.821270
H	38.466500	-0.296460	57.958500
C	39.151300	0.065810	62.027660
H	39.347260	-0.863240	62.575690
H	40.992590	-1.720410	60.916380
H	41.542200	-0.281300	60.036030
H	40.743240	-0.545650	57.226390
O	38.145320	-3.214040	59.286600
H	38.396960	0.638310	62.567490
H	40.087130	0.633140	61.990590

H   37.396030   -2.422950   57.577950

Compound 19

Minima

C   38.374950   -2.610601   58.188217
C   38.891700   -1.300965   58.648094
C   40.350473   -1.072317   58.193138
C   41.163811   -1.742420   59.312394
C   40.376095   -1.394882   60.588174
N   38.992296   -1.246668   60.110186
C   37.883148   -0.914333   60.855205
O   36.798198   -0.721075   60.320717
H   42.199371   -1.395649   59.358025
H   41.177107   -2.827407   59.163938
H   40.550915   -1.481017   57.200501
H   38.196715   -0.530640   58.300951
C   38.092361   -0.812506   62.356263
H   38.401212   -1.776862   62.774923
H   40.456059   -2.176848   61.350874
H   40.734363   -0.455021   61.030847
H   40.539836   0.006306   58.168248
N   37.989659   -3.648552   57.839235
H   37.148055   -0.511105   62.809218
H   38.866596   -0.079642   62.609090

Compound 20

Minima

B   38.012331   -1.814679   58.896239
O   37.689357   -2.888317   58.109249
C   39.148870   -0.802263   58.385196
C   39.934533   -1.240735   57.133067
C   41.165679   -1.958747   57.707587
C   41.539201   -1.096100   58.918882
N   40.234618   -0.608468   59.403462
C   40.030997   0.050961   60.560166
O   38.890732   0.417545   60.920841
H   41.990757   -2.047080   56.995619

H	40.891671	-2.967015	58.038380
H	39.337585	-1.883648	56.482966
H	38.672352	0.175674	58.227325
C	41.240573	0.335913	61.429166
H	41.651341	-0.594826	61.836651
H	42.062069	-1.658411	59.697813
H	42.177877	-0.253045	58.620209
H	40.250433	-0.366135	56.551903
O	37.355097	-1.602041	60.066793
H	37.725328	-0.794984	60.498653
H	36.976291	-3.408344	58.506699
H	40.926439	0.973376	62.255830
H	42.038596	0.831459	60.866973

POP (no ligand)

Minima

C	28.381000	36.004000	82.438000
C	28.962200	36.520687	83.766291
C	30.468767	36.673669	83.727751
C	31.062113	37.766171	83.078614
C	31.317580	35.713322	84.297494
C	32.449780	37.897476	82.998632
C	32.707098	35.828001	84.226127
C	33.278133	36.923981	83.570750
O	34.651370	36.990503	83.518346
H	27.290251	35.910218	82.493375
H	28.794729	35.021097	82.186594
H	28.620890	36.685160	81.614473
H	28.499454	37.487260	84.004771
H	28.683146	35.834534	84.575381
H	30.433315	38.533215	82.620824
H	30.885542	34.856774	84.811331
H	32.863204	38.754790	82.477721
H	33.355441	35.080212	84.673813
H	34.912108	37.822675	83.098503
N	33.325052	41.283498	79.352987
C	34.370604	40.265885	79.418155
C	33.710768	38.903254	79.065634
O	32.721138	38.863896	78.330661

C	35.121962	40.347916	80.769631
O	36.420624	39.792996	80.707325
H	35.097496	40.499216	78.632410
N	34.242109	37.779958	79.597039
C	33.559000	36.502000	79.405000
H	35.097086	37.833436	80.134559
H	34.102140	35.729814	79.952535
H	32.535359	36.560618	79.785793
C	41.999945	47.588692	78.051878
C	41.648696	46.462499	77.072035
C	40.735963	45.383812	77.687853
O	41.051799	44.165258	77.534400
O	39.696209	45.825518	78.293329
H	42.616749	48.359556	77.574491
H	42.555391	47.202223	78.914316
H	41.086964	48.057673	78.429061
H	41.125512	46.896115	76.206139
H	42.551581	45.972547	76.693914
C	43.706694	42.544380	80.255017
C	42.200618	42.620925	80.539572
C	41.634982	41.423934	81.322696
C	42.214009	41.243525	82.740528
N	42.100209	42.432409	83.583480
C	41.057023	42.829259	84.303114
N	39.900084	42.099704	84.337098
N	41.159737	43.946444	85.051290
H	43.997925	43.340111	79.560820
H	43.978476	41.586947	79.791220
H	44.303396	42.669513	81.165012
H	41.989721	43.542372	81.096907
H	41.654144	42.722081	79.595715
H	40.542894	41.524739	81.380661
H	41.828004	40.491984	80.772291
H	41.752704	40.381000	83.237864
H	43.296490	41.046527	82.685285
H	42.950843	43.066386	83.545936
H	39.667717	41.486959	83.571490
H	39.103509	42.507235	84.802978
H	42.068481	44.474507	85.101003
H	40.343809	44.303720	85.522523

C	38.577297	46.938125	81.221988
C	38.926759	45.638411	81.966788
C	38.432073	44.378909	81.294982
N	38.599910	44.130601	79.939748
C	37.849885	43.231501	81.803531
C	38.150653	42.881135	79.703806
N	37.683257	42.289427	80.801569
H	38.948234	47.805670	81.779410
H	37.491995	47.045424	81.111887
H	39.027168	46.949638	80.225390
H	40.015558	45.579691	82.100000
H	38.488323	45.676586	82.974645
H	39.047854	44.814320	79.204209
H	37.531454	43.031421	82.823220
H	38.183711	42.431499	78.720462
H	37.026081	40.583293	80.726673
H	33.519052	36.231756	78.344844
C	32.228034	41.164866	80.156842
O	32.203634	40.437153	81.150274
C	31.036000	41.990000	79.756000
H	30.382560	41.399370	79.102940
H	31.325420	42.898800	79.219050
H	30.473080	42.255090	80.652180
H	34.522057	39.829645	81.519749
H	35.168125	41.407968	81.043658
H	33.176059	41.715191	78.451506
O	43.553025	45.271485	85.201522
C	45.858545	45.375206	84.506164
C	44.433290	44.832391	84.408129
H	45.436970	46.934170	85.985870
O	44.267643	43.922152	83.537055
C	45.955661	46.815920	85.027011
H	47.000612	47.119633	85.158776
H	46.327604	45.276485	83.522349
H	45.492706	47.516095	84.322074
H	46.407371	44.698382	85.177169

FAP (no ligand)

Minima

C	33.586000	7.906000	63.922000
C	34.175803	6.513025	63.670569
C	33.537761	5.844921	62.442764
C	34.009673	4.416688	62.147434
N	35.395488	4.385504	61.680936
C	35.947028	3.321771	61.102647
N	35.235539	2.169595	60.959955
N	37.196314	3.385794	60.637014
C	40.412000	6.546000	63.398000
C	39.483927	7.738144	63.135367
C	38.974602	7.798053	61.682215
C	38.092044	6.586879	61.360546
O	38.556319	5.705631	60.580315
O	36.963851	6.542890	61.940056
C	37.091000	-10.575000	59.530000
C	37.533746	-9.973812	60.880543
C	37.859913	-8.500316	60.717233
C	36.823417	-7.564863	60.576696
C	39.175462	-8.036429	60.584971
C	37.075457	-6.227611	60.273787
C	39.449474	-6.698974	60.289500
C	38.395651	-5.798052	60.106587
O	38.718384	-4.517187	59.718816
C	33.155000	-6.449000	56.011000
C	34.243813	-5.557141	56.589895
O	34.495889	-5.572107	57.795154
N	34.907022	-4.779353	55.679870
C	36.211000	-4.132000	55.939000
C	37.286409	-5.192156	55.674448
O	37.262120	-5.824463	54.611653
C	36.210504	-3.381691	57.289636
O	37.214594	-2.387211	57.341650
N	38.188353	-5.439160	56.641117
C	39.171000	-6.484000	56.454000
C	33.096000	5.670000	52.765000
C	33.517144	4.383353	52.049906
C	34.156125	3.392406	53.041272
O	33.735792	2.182865	52.986467
O	35.019017	3.837388	53.829661
C	31.864000	2.637000	56.109000

C	33.318278	2.788075	56.610134
C	34.174190	1.558736	56.459256
N	34.528486	1.047773	55.228317
C	34.819900	0.758257	57.381689
C	35.354488	0.002596	55.445246
N	35.564470	-0.216018	56.741103
H	34.033699	8.390435	64.796570
H	32.502283	7.852214	64.087489
H	33.759367	8.558540	63.058676
H	34.014167	5.876395	64.552265
H	35.256723	6.600584	63.522483
H	33.712448	6.462945	61.552426
H	32.449424	5.799576	62.581390
H	33.894977	3.798940	63.052368
H	33.361384	3.984014	61.373998
H	37.709967	4.311313	60.586648
H	37.563006	2.599786	60.121066
H	40.751674	6.524141	64.440429
H	41.299696	6.599304	62.756384
H	39.914503	5.596187	63.180013
H	38.613234	7.689704	63.800487
H	40.011938	8.671506	63.371047
H	39.817643	7.826817	60.983471
H	38.378702	8.708170	61.544716
H	36.615114	-11.560290	59.611689
H	37.934601	-10.659382	58.836258
H	36.367090	-9.886281	59.082598
H	38.399437	-10.515522	61.279453
H	36.722436	-10.092361	61.610100
H	35.790327	-7.890274	60.677552
H	40.003911	-8.732386	60.698620
H	36.249755	-5.536865	60.125019
H	40.471054	-6.347984	60.174931
H	37.929996	-3.954427	59.717590
H	32.784183	-6.121970	55.034750
H	32.324385	-6.520182	56.715326
H	33.591184	-7.448100	55.896931
H	34.756537	-5.011284	54.706871
H	36.331436	-3.370883	55.160339
H	36.344339	-4.091939	58.109335

H   35.215958   -2.938472   57.414845
H   38.267328   -4.842458   57.453291
H   38.697546   -7.408433   56.108817
H   39.676588   -6.669968   57.403908
H   39.916875   -6.196621   55.700684
H   32.701731   6.418046   52.068305
H   33.953790   6.095928   53.291384
H   32.317183   5.457518   53.505680
H   34.262262   4.618318   51.276520
H   32.668376   3.905750   51.549104
H   31.287536   3.559639   56.243720
H   31.354140   1.834743   56.654399
H   31.853537   2.381907   55.045765
H   33.317050   3.069562   57.670198
H   33.800813   3.602315   56.055731
H   35.792032   -0.571912   54.639410
H   34.794263   0.839079   58.460126
H   34.255154   1.477443   54.279245
H   36.004276   5.251130   61.760358
H   35.736922   1.336124   60.690621
H   34.438249   2.012116   61.557204
H   36.738975   -1.529507   57.168069

Compound 18 (in POP)

Maxima

C   28.381000   36.004000   82.438000
C   28.894034   36.549334   83.782537
C   30.404866   36.601025   83.887804
C   31.158134   37.498525   83.115356
C   31.103911   35.748978   84.754312
C   32.549581   37.544383   83.192845
C   32.495531   35.781209   84.847840
C   33.233015   36.678195   84.062306
O   34.585927   36.677415   84.194019
H   27.283843   35.992011   82.423430
H   28.736333   34.984810   82.249314
H   28.723677   36.629335   81.606869
H   28.478751   37.556021   83.929339
H   28.497155   35.932847   84.598595

H	30.661460	38.193945	82.441952
H	30.549312	35.044290	85.371502
H	33.091320	38.262267	82.584652
H	33.027294	35.115968	85.522651
H	35.006441	37.208641	83.476755
N	33.311080	41.226806	79.325244
C	34.424703	40.265451	79.392676
C	33.862540	38.892056	78.940435
O	33.156828	38.846423	77.925344
C	35.177948	40.381866	80.748623
O	36.530105	40.092307	80.633984
H	35.138498	40.572761	78.621747
N	34.158658	37.800628	79.679868
C	33.559000	36.502000	79.405000
H	34.742059	37.887764	80.506463
H	34.339157	35.753540	79.216119
H	32.953742	36.166500	80.254358
C	41.908000	47.615000	78.100000
C	41.633505	46.501964	77.076470
C	40.762849	45.388871	77.642634
O	41.068208	44.203516	77.574435
O	39.658497	45.846707	78.210946
H	42.629615	48.334463	77.698023
H	42.326360	47.199635	79.022431
H	40.990882	48.151634	78.355116
H	41.124162	46.923329	76.199545
H	42.563751	46.045213	76.727630
C	42.845000	42.788000	80.359000
C	41.484434	42.133523	80.619709
C	41.507517	40.928651	81.575240
C	42.350296	41.085505	82.856523
N	42.151680	42.324596	83.606145
C	41.182282	42.571133	84.478493
N	40.243640	41.653845	84.786835
N	41.147041	43.783218	85.072146
H	42.764059	43.518390	79.548874
H	43.617730	42.055845	80.087752
H	43.171565	43.300450	81.265956
H	40.808202	42.893433	81.024548
H	41.031815	41.813455	79.674195

H	40.479355	40.673681	81.851352
H	41.912992	40.046713	81.057494
H	42.177571	40.219353	83.507635
H	43.414115	41.079107	82.602064
H	42.926982	43.042097	83.543172
H	40.167223	40.752779	84.317228
H	39.461485	41.933686	85.357558
H	41.993709	44.392739	85.023151
H	40.562731	43.886371	85.888574
C	38.601000	46.945000	81.202000
C	38.955698	45.641373	81.943521
C	38.459381	44.397800	81.245514
N	38.537090	44.225533	79.874029
C	37.911465	43.251979	81.786697
C	38.056478	43.008622	79.627188
N	37.664921	42.377288	80.749531
H	38.855828	47.843637	81.774876
H	37.524603	46.959155	80.999628
H	39.129656	46.984026	80.248680
H	40.045875	45.582588	82.071118
H	38.537790	45.653745	82.957503
H	39.193748	45.122850	78.827495
H	37.693392	42.994561	82.813049
H	37.987756	42.563397	78.643956
C	40.682503	36.966642	84.154290
C	39.762302	37.876604	83.362313
O	39.622962	39.077606	83.652428
C	36.948432	38.481627	82.156562
N	39.091002	37.324643	82.325580
H	37.045288	39.252775	82.932781
C	38.244734	38.152611	81.422474
C	38.060764	37.252374	80.195445
C	39.199624	35.926711	81.867217
C	38.133315	35.824982	80.765231
H	38.759685	39.087918	81.204749
H	37.122044	37.474696	79.687029
H	38.881982	37.427372	79.491360
H	40.205352	35.737871	81.467451
H	39.025164	35.226348	82.689724
H	37.168875	35.559960	81.206631

H	38.394327	35.071151	80.017288
H	37.211994	41.348005	80.762464
H	32.930688	36.592752	78.517208
C	32.219762	41.115095	80.133474
O	32.172864	40.344366	81.095083
C	31.036000	41.990000	79.756000
H	30.382557	41.399372	79.102939
H	31.325424	42.898798	79.219052
H	30.473083	42.255091	80.652184
H	34.680729	39.739377	81.492335
H	35.007049	41.422051	81.087868
H	33.185444	41.715067	78.450213
H	41.437504	36.504600	83.509179
H	40.117185	36.158203	84.630517
H	41.177324	37.557765	84.925249
O	35.957645	37.730391	82.129301
O	43.502070	45.320805	85.092519
C	45.846145	45.380936	84.501496
C	44.406123	44.863614	84.339255
H	45.436975	46.934170	85.985866
O	44.264957	43.940695	83.477585
C	46.041000	46.782000	85.087000
H	47.099552	46.908026	85.344667
H	46.343861	45.291361	83.529869
H	45.771554	47.571879	84.376536
H	46.342809	44.647533	85.154336

Minima (unbound)

C	28.381000	36.004000	82.438000
C	28.891229	36.547444	83.784081
C	30.401463	36.573530	83.896637
C	31.170957	37.467762	83.137180
C	31.082677	35.694455	84.750260
C	32.563008	37.482940	83.215665
C	32.474459	35.696187	84.843792
C	33.227202	36.589513	84.070600
O	34.582580	36.558590	84.198298
H	27.283843	35.992011	82.423430
H	28.736333	34.984810	82.249314

H	28.723677	36.629335	81.606869
H	28.491743	37.561227	83.924039
H	28.479396	35.940202	84.599467
H	30.687680	38.181919	82.473906
H	30.513675	34.991948	85.356373
H	33.120425	38.198503	82.618796
H	32.993083	35.010185	85.507690
H	35.001642	37.095703	83.492415
N	33.326623	41.244140	79.335662
C	34.424703	40.265451	79.392676
C	33.844145	38.896134	78.948754
O	33.114615	38.859827	77.953431
C	35.164006	40.360155	80.745811
O	36.524553	39.985215	80.628174
H	35.140437	40.563708	78.620593
N	34.160318	37.800220	79.674089
C	33.559000	36.502000	79.405000
H	34.761903	37.877429	80.485125
H	34.339157	35.753540	79.216119
H	32.953742	36.166500	80.254358
C	41.908000	47.615000	78.100000
C	41.623029	46.492116	77.094202
C	40.664532	45.425005	77.656089
O	40.963641	44.218377	77.547371
O	39.599138	45.889838	78.203140
H	42.629615	48.334463	77.698023
H	42.326360	47.199635	79.022431
H	40.990882	48.151634	78.355116
H	41.167291	46.918852	76.189058
H	42.550172	45.996865	76.786883
C	42.845000	42.788000	80.359000
C	41.484768	42.134425	80.623632
C	41.501714	40.931218	81.581017
C	42.343796	41.088515	82.862892
N	42.152305	42.331892	83.607064
C	41.180787	42.592741	84.471649
N	40.237473	41.680710	84.789181
N	41.148796	43.808954	85.055210
H	42.753717	43.516103	79.547561
H	43.617730	42.055845	80.087752

H	43.171565	43.300450	81.265956
H	40.812799	42.896128	81.031141
H	41.028408	41.818626	79.678980
H	40.470398	40.684931	81.854808
H	41.904255	40.045485	81.066989
H	42.168641	40.226036	83.518619
H	43.407453	41.076158	82.608076
H	42.937664	43.040989	83.545419
H	40.152086	40.786668	84.310090
H	39.437069	41.982388	85.322538
H	41.997730	44.416401	85.001633
H	40.562797	43.921009	85.869239
C	38.601000	46.945000	81.202000
C	38.963836	45.656086	81.963022
C	38.495436	44.400763	81.277570
N	38.608110	44.196300	79.917506
C	37.942036	43.239939	81.778156
C	38.147471	42.958406	79.654533
N	37.728821	42.336355	80.754355
H	38.855828	47.843637	81.774876
H	37.524603	46.959155	80.999628
H	39.129656	46.984026	80.248680
H	40.052799	45.614041	82.105489
H	38.530686	45.670152	82.970352
H	39.030326	44.870808	79.178914
H	37.698411	43.001235	82.804806
H	38.141913	42.539765	78.657723
C	40.787182	37.041616	84.231959
C	39.819659	37.880776	83.421252
O	39.606155	39.076023	83.681400
C	37.012134	38.326613	82.195256
N	39.182904	37.269346	82.391857
H	37.076702	39.106098	82.967728
C	38.318817	38.040195	81.459954
C	38.172343	37.105047	80.253558
C	39.373251	35.873068	81.952941
C	38.314477	35.695434	80.854343
H	38.799741	38.990819	81.224803
H	37.222485	37.263603	79.740985
H	38.981142	37.305478	79.543003

H	40.387773	35.738829	81.554377
H	39.239251	35.176960	82.785981
H	37.364336	35.388409	81.300242
H	38.612738	34.941774	80.120930
H	37.063502	40.851396	80.716567
H	32.930688	36.592752	78.517208
C	32.223968	41.118502	80.131745
O	32.183368	40.335671	81.083407
C	31.036000	41.990000	79.756000
H	30.382557	41.399372	79.102939
H	31.325424	42.898798	79.219052
H	30.473083	42.255091	80.652184
H	34.669667	39.739208	81.499249
H	35.089808	41.401527	81.080646
H	33.213779	41.743169	78.464783
H	41.578423	36.626054	83.598720
H	40.271834	36.201296	84.709351
H	41.232958	37.671257	85.002167
O	36.023061	37.595958	82.111512
O	43.500306	45.335207	85.072897
C	45.849791	45.380970	84.501750
C	44.411928	44.859867	84.340340
H	45.436975	46.934170	85.985866
O	44.279901	43.916253	83.499878
C	46.041000	46.782000	85.087000
H	47.099552	46.908026	85.344667
H	46.346335	45.293018	83.529321
H	45.771554	47.571879	84.376536
H	46.349879	44.648243	85.152681

Minima (bound)

C	28.381000	36.004000	82.438000
C	28.928097	36.535818	83.776265
C	30.443743	36.579880	83.829766
C	31.168785	37.507183	83.064614
C	31.181103	35.686999	84.620769
C	32.561544	37.542177	83.073390
C	32.577308	35.708045	84.645890
C	33.292072	36.633328	83.864510

O	34.641508	36.623641	83.913921
H	27.283843	35.992011	82.423430
H	28.736333	34.984810	82.249314
H	28.723677	36.629335	81.606869
H	28.520674	37.542128	83.946723
H	28.553589	35.909954	84.596146
H	30.643746	38.233019	82.446091
H	30.653384	34.956599	85.232664
H	33.086014	38.270419	82.466223
H	33.133221	35.008341	85.264972
H	35.042188	37.244328	83.205243
N	33.313338	41.228423	79.322983
C	34.424703	40.265451	79.392676
C	33.878025	38.879620	78.936421
O	33.214394	38.852453	77.888143
C	35.107273	40.404860	80.766773
O	36.408860	39.824339	80.773261
H	35.143776	40.572727	78.625519
N	34.144451	37.804284	79.694990
C	33.559000	36.502000	79.405000
H	34.706092	37.889434	80.568681
H	34.339157	35.753540	79.216119
H	32.953742	36.166500	80.254358
C	41.908000	47.615000	78.100000
C	41.630668	46.504749	77.073857
C	40.740571	45.407183	77.633101
O	41.026956	44.218244	77.592393
O	39.625525	45.887579	78.175283
H	42.629615	48.334463	77.698023
H	42.326360	47.199635	79.022431
H	40.990882	48.151634	78.355116
H	41.134932	46.932107	76.192257
H	42.557700	46.034611	76.735198
C	42.845000	42.788000	80.359000
C	41.483442	42.135287	80.619650
C	41.479524	40.978738	81.633812
C	42.229369	41.219048	82.960379
N	41.990559	42.506962	83.611676
C	41.071787	42.775082	84.534558
N	40.137692	41.878576	84.907028

N	41.090439	43.996167	85.110559
H	42.764856	43.517928	79.548215
H	43.617730	42.055845	80.087752
H	43.171565	43.300450	81.265956
H	40.795866	42.911339	80.970953
H	41.057334	41.765650	79.679251
H	40.443348	40.705325	81.857647
H	41.941590	40.086573	81.185775
H	41.999834	40.400762	83.653637
H	43.309113	41.190096	82.783998
H	42.770937	43.211346	83.520907
H	39.949577	41.007603	84.400873
H	39.424595	42.176271	85.554985
H	41.969844	44.560892	85.055595
H	40.509033	44.138227	85.923142
C	38.601000	46.945000	81.202000
C	38.963217	45.651422	81.954398
C	38.490764	44.394480	81.265015
N	38.520793	44.235984	79.888044
C	38.031590	43.223108	81.826282
C	38.104508	43.003533	79.639594
N	37.797536	42.350359	80.782026
H	38.855828	47.843637	81.774876
H	37.524603	46.959155	80.999628
H	39.129656	46.984026	80.248680
H	40.052788	45.602805	82.088074
H	38.540729	45.665828	82.966010
H	39.164631	45.181156	78.774742
H	37.877078	42.934816	82.854600
H	38.022215	42.555540	78.659661
C	39.767928	37.526386	84.897479
C	39.162154	38.290764	83.734939
O	39.223197	39.535419	83.670946
C	36.608022	38.857729	81.908464
N	38.554586	37.573430	82.770084
H	36.736942	39.491608	82.809140
C	37.985582	38.223069	81.569028
C	37.891894	37.066020	80.562872
C	38.488280	36.101740	82.709137
C	37.663004	35.822383	81.441807

H	38.669577	39.011998	81.244958
H	37.082720	37.231044	79.848285
H	38.833012	36.980201	80.006576
H	39.500671	35.682183	82.633737
H	38.017224	35.691837	83.608361
H	36.606013	35.766204	81.706327
H	37.967525	34.888232	80.960318
H	37.437283	41.385569	80.837399
H	32.930688	36.592752	78.517208
C	32.221245	41.124993	80.140395
O	32.179884	40.381401	81.120851
C	31.036000	41.990000	79.756000
H	30.382557	41.399372	79.102939
H	31.325424	42.898798	79.219052
H	30.473083	42.255091	80.652184
H	34.489891	39.953532	81.540443
H	35.187764	41.481839	80.970873
H	33.164539	41.667780	78.425650
H	40.525662	36.814494	84.552244
H	39.002340	36.955607	85.433870
H	40.229046	38.238541	85.582540
O	35.593613	37.997157	82.001435
O	43.490843	45.402731	85.117397
C	45.821634	45.386929	84.499286
C	44.362059	44.932053	84.332248
H	45.436975	46.934170	85.985866
O	44.164303	44.053191	83.438182
C	46.041000	46.782000	85.087000
H	47.099552	46.908026	85.344667
H	46.321433	45.283386	83.530275
H	45.771554	47.571879	84.376536
H	46.289264	44.639156	85.157161

Compound 19 (in POP)

Maxima

C	28.381000	36.004000	82.437999
C	29.200106	35.132472	83.407081
C	30.706145	35.242134	83.258033
C	31.378004	36.463632	83.419714

C	31.485966	34.111906	82.973338
C	32.765031	36.561366	83.302712
C	32.873616	34.187366	82.854468
C	33.528318	35.416613	83.016999
O	34.882038	35.438435	82.897431
H	27.309620	35.811686	82.579680
H	28.630864	35.796168	81.391364
H	28.558175	37.071531	82.610545
H	28.912022	35.396611	84.434874
H	28.911044	34.082662	83.275141
H	30.811263	37.363873	83.648223
H	30.997954	33.147826	82.842945
H	33.261416	37.519107	83.430945
H	33.465503	33.303709	82.632643
H	35.219224	36.365868	82.882871
N	33.219369	41.150090	79.235659
C	34.392992	40.279288	79.387552
C	33.918934	38.882622	78.918213
O	33.427773	38.785235	77.783676
C	35.156387	40.429949	80.727008
O	36.486654	40.073199	80.572434
H	35.114176	40.589970	78.621381
N	33.996912	37.844077	79.774258
C	33.559000	36.502000	79.405000
H	34.473798	37.971673	80.660478
H	34.411503	35.898537	79.067514
H	33.108995	36.011072	80.271533
C	41.908000	47.615000	78.100000
C	41.596553	46.543321	77.043348
C	40.750903	45.413504	77.612060
O	41.112514	44.242168	77.611584
O	39.602447	45.844168	78.110751
H	42.548720	48.397376	77.678481
H	42.432820	47.179464	78.956882
H	40.989705	48.080311	78.465970
H	41.047916	46.999083	76.209093
H	42.514673	46.105148	76.642738
C	42.845000	42.788000	80.359000
C	41.478214	42.491676	80.981781
C	41.385047	41.164855	81.749423

C	42.423212	40.965456	82.868149
N	42.467648	42.036516	83.860285
C	41.668058	42.149652	84.916202
N	40.761029	41.198319	85.239326
N	41.787623	43.234730	85.700817
H	42.772611	43.619622	79.652041
H	43.230357	41.925387	79.798524
H	43.580089	43.052846	81.127357
H	41.206879	43.311977	81.656241
H	40.715270	42.487111	80.196951
H	40.379454	41.065300	82.173081
H	41.510578	40.324142	81.050868
H	42.249390	40.003041	83.364856
H	43.429425	40.917631	82.441294
H	43.233039	42.759687	83.756045
H	40.486865	40.456009	84.595155
H	40.063549	41.439935	85.927459
H	42.583222	43.903596	85.553138
H	41.331092	43.226982	86.600282
C	38.601000	46.945000	81.202000
C	39.013007	45.591737	81.811509
C	38.438707	44.378727	81.122459
N	38.470180	44.213420	79.749252
C	37.902776	43.233676	81.676441
C	37.975275	42.999869	79.511281
N	37.618749	42.364905	80.643415
H	39.044532	47.786764	81.744900
H	37.511632	47.060491	81.228932
H	38.920830	47.004481	80.159579
H	40.110378	45.522350	81.795807
H	38.725538	45.552895	82.869217
H	39.134795	45.114673	78.720842
H	37.713556	42.972926	82.707753
H	37.865492	42.561338	78.528721
C	40.632950	36.939893	84.026948
C	39.727334	37.916134	83.301865
O	39.542271	39.073558	83.711829
C	36.882854	38.380111	81.855742
N	39.121218	37.468705	82.174963
C	38.286273	38.363530	81.354694

C	38.350561	37.702361	79.963414
C	39.304255	36.142743	81.549888
C	38.404579	36.203532	80.301612
H	38.680102	39.376711	81.377163
H	37.501392	38.004144	79.351154
H	39.273314	38.021780	79.466807
H	40.357166	35.998613	81.276834
H	39.016787	35.338426	82.234255
H	37.402370	35.837726	80.549428
H	38.796994	35.590847	79.486311
H	37.173403	41.333373	80.669846
H	32.837894	36.568624	78.588260
C	32.410493	41.614715	80.226758
O	32.704577	41.678968	81.420439
C	31.022193	41.990771	79.754106
H	30.428764	41.104339	79.976692
H	30.935932	42.210206	78.688229
H	30.643208	42.824429	80.339599
H	34.661540	39.844802	81.524060
H	35.048279	41.480870	81.034979
H	32.786775	41.042856	78.326382
H	41.447178	36.598084	83.378764
H	40.075072	36.054104	84.348987
H	41.052500	37.436544	84.902116
N	35.948725	37.953278	82.427080
O	43.881641	44.977770	85.330759
C	45.807280	45.675562	84.057466
C	44.631410	44.725853	84.344669
H	46.221069	46.365787	86.083587
O	44.510367	43.746960	83.546584
C	46.041000	46.782000	85.087000
H	46.911814	47.385832	84.804452
H	45.631869	46.106788	83.062598
H	45.171384	47.440414	85.168749
H	46.703668	45.051981	83.946667

Minima (unbound)

C	28.381000	36.004000	82.438000
C	29.163163	35.106193	83.416235

C	30.661599	35.039648	83.204049
C	31.497280	36.135967	83.461672
C	31.267057	33.854041	82.761914
C	32.880811	36.057376	83.292742
C	32.645998	33.755054	82.586339
C	33.466146	34.858773	82.854401
O	34.808118	34.706391	82.683982
H	27.309620	35.811686	82.579680
H	28.630864	35.796168	81.391364
H	28.558175	37.071531	82.610545
H	28.950580	35.445517	84.439452
H	28.761485	34.087912	83.348332
H	31.065526	37.070831	83.813175
H	30.645824	32.984605	82.556215
H	33.508775	36.917151	83.511363
H	33.104517	32.830507	82.247331
H	35.265832	35.564870	82.783306
N	33.244257	41.181049	79.228075
C	34.392992	40.279288	79.387552
C	33.886926	38.891300	78.923752
O	33.338358	38.809610	77.817939
C	35.122359	40.392465	80.739357
O	36.450739	39.925396	80.597926
H	35.133118	40.574994	78.634450
N	34.007123	37.842488	79.765192
C	33.559000	36.502000	79.404999
H	34.557905	37.948854	80.606146
H	34.411503	35.898537	79.067514
H	33.108995	36.011072	80.271533
C	41.908000	47.615000	78.100000
C	41.587093	46.534937	77.058836
C	40.654007	45.449328	77.625666
O	41.018552	44.256219	77.604083
O	39.540877	45.890719	78.091596
H	42.548720	48.397376	77.678481
H	42.432820	47.179464	78.956882
H	40.989705	48.080311	78.465970
H	41.089292	46.999548	76.196276
H	42.504034	46.058823	76.695849
C	42.845000	42.788000	80.359000

C	41.480761	42.487124	80.982728
C	41.401948	41.163958	81.759314
C	42.459005	40.977385	82.862711
N	42.496283	42.040919	83.861799
C	41.684816	42.148988	84.907974
N	40.793284	41.184242	85.232665
N	41.769026	43.247354	85.679571
H	42.772611	43.619622	79.652041
H	43.230357	41.925387	79.798524
H	43.580089	43.052846	81.127357
H	41.202642	43.308548	81.652616
H	40.719237	42.471093	80.197389
H	40.400537	41.066439	82.195415
H	41.522895	40.320585	81.062622
H	42.317459	40.007554	83.355100
H	43.458950	40.954590	82.420089
H	43.268841	42.763010	83.768242
H	40.597765	40.386397	84.631953
H	40.073892	41.412552	85.901724
H	42.551552	43.929534	85.523147
H	41.340235	43.220091	86.592545
C	38.601000	46.945000	81.202000
C	39.024721	45.604960	81.828391
C	38.472419	44.383010	81.148756
N	38.525760	44.192175	79.784672
C	37.934605	43.219951	81.661788
C	38.048985	42.956474	79.531273
N	37.674533	42.325349	80.641179
H	39.044532	47.786764	81.744900
H	37.511632	47.060491	81.228932
H	38.920830	47.004481	80.159579
H	40.122938	45.550028	81.823028
H	38.726179	45.568742	82.882958
H	38.941835	44.867603	79.044984
H	37.730826	42.975078	82.695962
H	37.989450	42.549305	78.531089
C	41.547631	37.106814	83.649715
C	40.299678	37.836454	83.197980
O	39.821566	38.791961	83.826227
C	37.301662	37.576692	82.070854

N	39.712822	37.392117	82.053648
C	38.556868	38.099824	81.485340
C	38.653617	37.773912	79.980149
C	40.242788	36.358225	81.136981
C	39.235967	36.352042	79.972589
H	38.602548	39.166267	81.705831
H	37.691978	37.880896	79.479520
H	39.353280	38.485546	79.530332
H	41.245290	36.642294	80.796193
H	40.312410	35.387402	81.636545
H	38.445811	35.617446	80.162622
H	39.712853	36.093291	79.024520
H	37.011660	40.761937	80.614355
H	32.837894	36.568624	78.588260
C	32.413401	41.603754	80.223537
O	32.702439	41.617745	81.420032
C	31.025821	41.989886	79.754273
H	30.428764	41.104339	79.976692
H	30.935932	42.210206	78.688229
H	30.643208	42.824429	80.339599
H	34.600782	39.836251	81.527466
H	35.114935	41.441258	81.045257
H	32.825527	41.090872	78.310348
H	42.354011	37.216598	82.916152
H	41.355696	36.035721	83.769974
H	41.870469	37.524370	84.603486
N	36.344859	37.094959	82.516296
O	43.848764	45.007418	85.292102
C	45.808721	45.676791	84.056424
C	44.633641	44.727427	84.342062
H	46.221069	46.365787	86.083587
O	44.546837	43.719185	83.575492
C	46.041000	46.782000	85.087000
H	46.911814	47.385832	84.804452
H	45.630893	46.110802	83.063018
H	45.171384	47.440414	85.168749
H	46.705218	45.054388	83.942964

Minima (bound)

C	28.381000	36.004000	82.438000
C	29.224280	35.138581	83.399462
C	30.729113	35.336644	83.330590
C	31.357808	36.454349	83.911406
C	31.575370	34.393006	82.725036
C	32.739643	36.622244	83.898225
C	32.963016	34.541252	82.702590
C	33.622895	35.660305	83.305534
O	34.917135	35.783789	83.324130
H	27.309620	35.811686	82.579680
H	28.630864	35.796168	81.391364
H	28.558175	37.071531	82.610545
H	28.876123	35.336905	84.423934
H	28.995792	34.081812	83.206188
H	30.742196	37.211631	84.400128
H	31.133280	33.506788	82.266484
H	33.185560	37.499389	84.363167
H	33.587666	33.780243	82.237115
H	35.450546	37.370680	82.851970
N	33.185226	41.089551	79.209594
C	34.392992	40.279288	79.387552
C	34.005914	38.856185	78.901911
O	33.693940	38.740474	77.707988
C	35.011368	40.443343	80.781021
O	36.296809	39.772008	80.818559
H	35.137104	40.617484	78.654067
N	33.961061	37.850105	79.789576
C	33.559000	36.502000	79.405000
H	34.232733	38.006596	80.762977
H	34.411503	35.898537	79.067514
H	33.108995	36.011072	80.271533
C	41.908000	47.615000	78.100000
C	41.588315	46.540869	77.046947
C	40.741090	45.419030	77.623329
O	41.090220	44.247258	77.647061
O	39.583729	45.860954	78.112637
H	42.548720	48.397376	77.678481
H	42.432820	47.179464	78.956882
H	40.989705	48.080311	78.465970
H	41.038338	46.995218	76.213174

H	42.501582	46.094270	76.645584
C	42.845000	42.788000	80.359000
C	41.469217	42.487074	80.956555
C	41.353117	41.167791	81.732480
C	42.288306	41.023604	82.948130
N	42.297027	42.163847	83.861475
C	41.428759	42.386728	84.844441
N	40.360362	41.588042	85.058812
N	41.661331	43.410446	85.684265
H	42.772611	43.619622	79.652041
H	43.230357	41.925387	79.798524
H	43.580089	43.052846	81.127357
H	41.176039	43.311553	81.616098
H	40.731199	42.472613	80.147916
H	40.315843	41.034810	82.057891
H	41.571649	40.322209	81.063888
H	42.035772	40.108829	83.499397
H	43.323477	40.913145	82.611418
H	43.106813	42.837307	83.774957
H	40.005517	40.896090	84.395419
H	39.740478	41.819974	85.819628
H	42.466585	44.063358	85.513169
H	40.920498	43.709164	86.299759
C	38.601000	46.945000	81.202000
C	39.042362	45.620015	81.840634
C	38.487745	44.378289	81.198739
N	38.441385	44.196490	79.825548
C	38.058256	43.223932	81.810729
C	38.008934	42.962146	79.622856
N	37.765539	42.334178	80.797169
H	39.044532	47.786764	81.744900
H	37.511632	47.060491	81.228932
H	38.920830	47.004481	80.159579
H	40.140250	45.568570	81.810268
H	38.771469	45.606386	82.902961
H	39.128392	45.146140	78.692990
H	37.961085	42.954351	82.851054
H	37.864692	42.494245	78.659433
C	39.369257	37.741645	85.011751
C	38.829638	38.383982	83.749714

O	38.873307	39.616309	83.564570
C	36.404182	38.676670	81.667723
N	38.292519	37.558399	82.823090
C	37.810142	38.092227	81.545393
C	37.843830	36.854778	80.618466
C	38.244285	36.080943	82.888759
C	37.567277	35.674991	81.567303
H	38.481440	38.883009	81.204670
H	37.120483	36.932177	79.802463
H	38.843053	36.777213	80.175523
H	39.261836	35.679573	82.975308
H	37.655010	35.748803	83.748215
H	36.495990	35.552576	81.756600
H	37.965971	34.731490	81.183681
H	37.443450	41.372983	80.903768
H	32.837894	36.568624	78.588260
C	32.439277	41.695944	80.178365
O	32.837588	41.956099	81.313363
C	31.021506	41.994237	79.752133
H	30.428764	41.104339	79.976692
H	30.935932	42.210206	78.688229
H	30.643208	42.824429	80.339599
H	34.385073	40.058711	81.579909
H	35.199739	41.498444	80.971897
H	32.722666	40.888021	78.331337
H	40.142372	37.001109	84.780607
H	38.571233	37.223305	85.553923
H	39.793380	38.516526	85.650878
N	35.405949	38.269340	82.315692
O	43.770932	45.113131	85.256375
C	45.789376	45.674601	84.061570
C	44.567454	44.777650	84.333467
H	46.221069	46.365787	86.083587
O	44.453364	43.758864	83.585860
C	46.041000	46.782000	85.087000
H	46.911814	47.385832	84.804452
H	45.647953	46.105555	83.060739
H	45.171384	47.440414	85.168749
H	46.661959	45.015690	83.971708

Compound 20 (in POP)

Maxima

C	28.381000	36.004000	82.437999
C	29.200106	35.132472	83.407081
C	30.706145	35.242134	83.258033
C	31.378004	36.463632	83.419714
C	31.485966	34.111906	82.973338
C	32.765031	36.561366	83.302712
C	32.873616	34.187366	82.854468
C	33.528318	35.416613	83.016999
O	34.882038	35.438435	82.897431
H	27.309620	35.811686	82.579680
H	28.630864	35.796168	81.391364
H	28.558175	37.071531	82.610545
H	28.912022	35.396611	84.434874
H	28.911044	34.082662	83.275141
H	30.811263	37.363873	83.648223
H	30.997954	33.147826	82.842945
H	33.261416	37.519107	83.430945
H	33.465503	33.303709	82.632643
H	35.219224	36.365868	82.882871
N	33.219369	41.150090	79.235659
C	34.392992	40.279288	79.387552
C	33.918934	38.882622	78.918213
O	33.427773	38.785235	77.783676
C	35.156387	40.429949	80.727008
O	36.486654	40.073199	80.572434
H	35.114176	40.589970	78.621381
N	33.996912	37.844077	79.774258
C	33.559000	36.502000	79.405000
H	34.473798	37.971673	80.660478
H	34.411503	35.898537	79.067514
H	33.108995	36.011072	80.271533
C	41.908000	47.615000	78.100000
C	41.596553	46.543321	77.043348
C	40.750903	45.413504	77.612060
O	41.112514	44.242168	77.611584
O	39.602447	45.844168	78.110751
H	42.548720	48.397376	77.678481

H	42.432820	47.179464	78.956882
H	40.989705	48.080311	78.465970
H	41.047916	46.999083	76.209093
H	42.514673	46.105148	76.642738
C	42.845000	42.788000	80.359000
C	41.478214	42.491676	80.981781
C	41.385047	41.164855	81.749423
C	42.423212	40.965456	82.868149
N	42.467648	42.036516	83.860285
C	41.668058	42.149652	84.916202
N	40.761029	41.198319	85.239326
N	41.787623	43.234730	85.700817
H	42.772611	43.619622	79.652041
H	43.230357	41.925387	79.798524
H	43.580089	43.052846	81.127357
H	41.206879	43.311977	81.656241
H	40.715270	42.487111	80.196951
H	40.379454	41.065300	82.173081
H	41.510578	40.324142	81.050868
H	42.249390	40.003041	83.364856
H	43.429425	40.917631	82.441294
H	43.233039	42.759687	83.756045
H	40.486865	40.456009	84.595155
H	40.063549	41.439935	85.927459
H	42.583222	43.903596	85.553138
H	41.331092	43.226982	86.600282
C	38.601000	46.945000	81.202000
C	39.013007	45.591737	81.811509
C	38.438707	44.378727	81.122459
N	38.470180	44.213420	79.749252
C	37.902776	43.233676	81.676441
C	37.975275	42.999869	79.511281
N	37.618749	42.364905	80.643415
H	39.044532	47.786764	81.744900
H	37.511632	47.060491	81.228932
H	38.920830	47.004481	80.159579
H	40.110378	45.522350	81.795807
H	38.725538	45.552895	82.869217
H	39.134795	45.114673	78.720842
H	37.713556	42.972926	82.707753

H	37.865492	42.561338	78.528721
C	40.632950	36.939893	84.026948
C	39.727334	37.916134	83.301865
O	39.542271	39.073558	83.711829
C	36.882854	38.380111	81.855742
N	39.121218	37.468705	82.174963
C	38.286273	38.363530	81.354694
C	38.350561	37.702361	79.963414
C	39.304255	36.142743	81.549888
C	38.404579	36.203532	80.301612
H	38.680102	39.376711	81.377163
H	37.501392	38.004144	79.351154
H	39.273314	38.021780	79.466807
H	40.357166	35.998613	81.276834
H	39.016787	35.338426	82.234255
H	37.402370	35.837726	80.549428
H	38.796994	35.590847	79.486311
H	37.173403	41.333373	80.669846
H	32.837894	36.568624	78.588260
C	32.410493	41.614715	80.226758
O	32.704577	41.678968	81.420439
C	31.022193	41.990771	79.754106
H	30.428764	41.104339	79.976692
H	30.935932	42.210206	78.688229
H	30.643208	42.824429	80.339599
H	34.661540	39.844802	81.524060
H	35.048279	41.480870	81.034979
H	32.786775	41.042856	78.326382
H	41.447178	36.598084	83.378764
H	40.075072	36.054104	84.348987
H	41.052500	37.436544	84.902116
N	35.948725	37.953278	82.427080
O	43.881641	44.977770	85.330759
C	45.807280	45.675562	84.057466
C	44.631410	44.725853	84.344669
H	46.221069	46.365787	86.083587
O	44.510367	43.746960	83.546584
C	46.041000	46.782000	85.087000
H	46.911814	47.385832	84.804452
H	45.631869	46.106788	83.062598

H   45.171384   47.440414   85.168749
H   46.703668   45.051981   83.946667

Minima (bound)

C   28.381000   36.004000   82.438000
C   29.224280   35.138581   83.399462
C   30.729113   35.336644   83.330590
C   31.357808   36.454349   83.911406
C   31.575370   34.393006   82.725036
C   32.739643   36.622244   83.898225
C   32.963016   34.541252   82.702590
C   33.622895   35.660305   83.305534
O   34.917135   35.783789   83.324130
H   27.309620   35.811686   82.579680
H   28.630864   35.796168   81.391364
H   28.558175   37.071531   82.610545
H   28.876123   35.336905   84.423934
H   28.995792   34.081812   83.206188
H   30.742196   37.211631   84.400128
H   31.133280   33.506788   82.266484
H   33.185560   37.499389   84.363167
H   33.587666   33.780243   82.237115
H   35.450546   37.370680   82.851970
N   33.185226   41.089551   79.209594
C   34.392992   40.279288   79.387552
C   34.005914   38.856185   78.901911
O   33.693940   38.740474   77.707988
C   35.011368   40.443343   80.781021
O   36.296809   39.772008   80.818559
H   35.137104   40.617484   78.654067
N   33.961061   37.850105   79.789576
C   33.559000   36.502000   79.405000
H   34.232733   38.006596   80.762977
H   34.411503   35.898537   79.067514
H   33.108995   36.011072   80.271533
C   41.908000   47.615000   78.100000
C   41.588315   46.540869   77.046947
C   40.741090   45.419030   77.623329
O   41.090220   44.247258   77.647061

O	39.583729	45.860954	78.112637
H	42.548720	48.397376	77.678481
H	42.432820	47.179464	78.956882
H	40.989705	48.080311	78.465970
H	41.038338	46.995218	76.213174
H	42.501582	46.094270	76.645584
C	42.845000	42.788000	80.359000
C	41.469217	42.487074	80.956555
C	41.353117	41.167791	81.732480
C	42.288306	41.023604	82.948130
N	42.297027	42.163847	83.861475
C	41.428759	42.386728	84.844441
N	40.360362	41.588042	85.058812
N	41.661331	43.410446	85.684265
H	42.772611	43.619622	79.652041
H	43.230357	41.925387	79.798524
H	43.580089	43.052846	81.127357
H	41.176039	43.311553	81.616098
H	40.731199	42.472613	80.147916
H	40.315843	41.034810	82.057891
H	41.571649	40.322209	81.063888
H	42.035772	40.108829	83.499397
H	43.323477	40.913145	82.611418
H	43.106813	42.837307	83.774957
H	40.005517	40.896090	84.395419
H	39.740478	41.819974	85.819628
H	42.466585	44.063358	85.513169
H	40.920498	43.709164	86.299759
C	38.601000	46.945000	81.202000
C	39.042362	45.620015	81.840634
C	38.487745	44.378289	81.198739
N	38.441385	44.196490	79.825548
C	38.058256	43.223932	81.810729
C	38.008934	42.962146	79.622856
N	37.765539	42.334178	80.797169
H	39.044532	47.786764	81.744900
H	37.511632	47.060491	81.228932
H	38.920830	47.004481	80.159579
H	40.140250	45.568570	81.810268
H	38.771469	45.606386	82.902961

H	39.128392	45.146140	78.692990
H	37.961085	42.954351	82.851054
H	37.864692	42.494245	78.659433
C	39.369257	37.741645	85.011751
C	38.829638	38.383982	83.749714
O	38.873307	39.616309	83.564570
C	36.404182	38.676670	81.667723
N	38.292519	37.558399	82.823090
C	37.810142	38.092227	81.545393
C	37.843830	36.854778	80.618466
C	38.244285	36.080943	82.888759
C	37.567277	35.674991	81.567303
H	38.481440	38.883009	81.204670
H	37.120483	36.932177	79.802463
H	38.843053	36.777213	80.175523
H	39.261836	35.679573	82.975308
H	37.655010	35.748803	83.748215
H	36.495990	35.552576	81.756600
H	37.965971	34.731490	81.183681
H	37.443450	41.372983	80.903768
H	32.837894	36.568624	78.588260
C	32.439277	41.695944	80.178365
O	32.837588	41.956099	81.313363
C	31.021506	41.994237	79.752133
H	30.428764	41.104339	79.976692
H	30.935932	42.210206	78.688229
H	30.643208	42.824429	80.339599
H	34.385073	40.058711	81.579909
H	35.199739	41.498444	80.971897
H	32.722666	40.888021	78.331337
H	40.142372	37.001109	84.780607
H	38.571233	37.223305	85.553923
H	39.793380	38.516526	85.650878
N	35.405949	38.269340	82.315692
O	43.770932	45.113131	85.256375
C	45.789376	45.674601	84.061570
C	44.567454	44.777650	84.333467
H	46.221069	46.365787	86.083587
O	44.453364	43.758864	83.585860
C	46.041000	46.782000	85.087000

H	*46.911814*	*47.385832*	*84.804452*
H	*45.647953*	*46.105555*	*83.060739*
H	*45.171384*	*47.440414*	*85.168749*
H	*46.661959*	*45.015690*	*83.971708*

Minima (unbound)

C	*28.381000*	*36.004000*	*82.438000*
C	*29.163163*	*35.106193*	*83.416235*
C	*30.661599*	*35.039648*	*83.204049*
C	*31.497280*	*36.135967*	*83.461672*
C	*31.267057*	*33.854041*	*82.761914*
C	*32.880811*	*36.057376*	*83.292742*
C	*32.645998*	*33.755054*	*82.586339*
C	*33.466146*	*34.858773*	*82.854401*
O	*34.808118*	*34.706391*	*82.683982*
H	*27.309620*	*35.811686*	*82.579680*
H	*28.630864*	*35.796168*	*81.391364*
H	*28.558175*	*37.071531*	*82.610545*
H	*28.950580*	*35.445517*	*84.439452*
H	*28.761485*	*34.087912*	*83.348332*
H	*31.065526*	*37.070831*	*83.813175*
H	*30.645824*	*32.984605*	*82.556215*
H	*33.508775*	*36.917151*	*83.511363*
H	*33.104517*	*32.830507*	*82.247331*
H	*35.265832*	*35.564870*	*82.783306*
N	*33.244257*	*41.181049*	*79.228075*
C	*34.392992*	*40.279288*	*79.387552*
C	*33.886926*	*38.891300*	*78.923752*
O	*33.338358*	*38.809610*	*77.817939*
C	*35.122359*	*40.392465*	*80.739357*
O	*36.450739*	*39.925396*	*80.597926*
H	*35.133118*	*40.574994*	*78.634450*
N	*34.007123*	*37.842488*	*79.765192*
C	*33.559000*	*36.502000*	*79.404999*
H	*34.557905*	*37.948854*	*80.606146*
H	*34.411503*	*35.898537*	*79.067514*
H	*33.108995*	*36.011072*	*80.271533*
C	*41.908000*	*47.615000*	*78.100000*

C	41.587093	46.534937	77.058836
C	40.654007	45.449328	77.625666
O	41.018552	44.256219	77.604083
O	39.540877	45.890719	78.091596
H	42.548720	48.397376	77.678481
H	42.432820	47.179464	78.956882
H	40.989705	48.080311	78.465970
H	41.089292	46.999548	76.196276
H	42.504034	46.058823	76.695849
C	42.845000	42.788000	80.359000
C	41.480761	42.487124	80.982728
C	41.401948	41.163958	81.759314
C	42.459005	40.977385	82.862711
N	42.496283	42.040919	83.861799
C	41.684816	42.148988	84.907974
N	40.793284	41.184242	85.232665
N	41.769026	43.247354	85.679571
H	42.772611	43.619622	79.652041
H	43.230357	41.925387	79.798524
H	43.580089	43.052846	81.127357
H	41.202642	43.308548	81.652616
H	40.719237	42.471093	80.197389
H	40.400537	41.066439	82.195415
H	41.522895	40.320585	81.062622
H	42.317459	40.007554	83.355100
H	43.458950	40.954590	82.420089
H	43.268841	42.763010	83.768242
H	40.597765	40.386397	84.631953
H	40.073892	41.412552	85.901724
H	42.551552	43.929534	85.523147
H	41.340235	43.220091	86.592545
C	38.601000	46.945000	81.202000
C	39.024721	45.604960	81.828391
C	38.472419	44.383010	81.148756
N	38.525760	44.192175	79.784672
C	37.934605	43.219951	81.661788
C	38.048985	42.956474	79.531273
N	37.674533	42.325349	80.641179
H	39.044532	47.786764	81.744900
H	37.511632	47.060491	81.228932

H	38.920830	47.004481	80.159579
H	40.122938	45.550028	81.823028
H	38.726179	45.568742	82.882958
H	38.941835	44.867603	79.044984
H	37.730826	42.975078	82.695962
H	37.989450	42.549305	78.531089
C	41.547631	37.106814	83.649715
C	40.299678	37.836454	83.197980
O	39.821566	38.791961	83.826227
C	37.301662	37.576692	82.070854
N	39.712822	37.392117	82.053648
C	38.556868	38.099824	81.485340
C	38.653617	37.773912	79.980149
C	40.242788	36.358225	81.136981
C	39.235967	36.352042	79.972589
H	38.602548	39.166267	81.705831
H	37.691978	37.880896	79.479520
H	39.353280	38.485546	79.530332
H	41.245290	36.642294	80.796193
H	40.312410	35.387402	81.636545
H	38.445811	35.617446	80.162622
H	39.712853	36.093291	79.024520
H	37.011660	40.761937	80.614355
H	32.837894	36.568624	78.588260
C	32.413401	41.603754	80.223537
O	32.702439	41.617745	81.420032
C	31.025821	41.989886	79.754273
H	30.428764	41.104339	79.976692
H	30.935932	42.210206	78.688229
H	30.643208	42.824429	80.339599
H	34.600782	39.836251	81.527466
H	35.114935	41.441258	81.045257
H	32.825527	41.090872	78.310348
H	42.354011	37.216598	82.916152
H	41.355696	36.035721	83.769974
H	41.870469	37.524370	84.603486
N	36.344859	37.094959	82.516296
O	43.848764	45.007418	85.292102
C	45.808721	45.676791	84.056424
C	44.633641	44.727427	84.342062

H	*46.221069*	*46.365787*	*86.083587*
O	*44.546837*	*43.719185*	*83.575492*
C	*46.041000*	*46.782000*	*85.087000*
H	*46.911814*	*47.385832*	*84.804452*
H	*45.630893*	*46.110802*	*83.063018*
H	*45.171384*	*47.440414*	*85.168749*
H	*46.705218*	*45.054388*	*83.942964*

Compound 18 (in FAP)

Maxima

C	*33.586000*	*7.906000*	*63.922001*
C	*34.294266*	*6.572241*	*63.637767*
C	*33.671828*	*5.811751*	*62.455326*
C	*34.294600*	*4.439886*	*62.156055*
N	*35.637762*	*4.559409*	*61.591346*
C	*36.295264*	*3.545608*	*61.024584*
N	*35.761357*	*2.292160*	*60.989779*
N	*37.473563*	*3.746315*	*60.437658*
C	*40.412000*	*6.546000*	*63.398000*
C	*39.533900*	*7.798746*	*63.274545*
C	*39.075091*	*8.093275*	*61.833236*
C	*38.190964*	*6.957193*	*61.305124*
O	*38.691494*	*6.171978*	*60.450104*
O	*37.030527*	*6.865070*	*61.811161*
C	*37.091000*	*-10.575000*	*59.530000*
C	*37.054015*	*-9.933806*	*60.927701*
C	*37.672917*	*-8.551210*	*60.981000*
C	*37.167149*	*-7.498358*	*60.202405*
C	*38.774677*	*-8.277396*	*61.803307*
C	*37.740197*	*-6.229225*	*60.233183*
C	*39.360879*	*-7.011531*	*61.847791*
C	*38.850984*	*-5.975583*	*61.053962*
O	*39.448690*	*-4.755857*	*61.118648*
C	*33.155000*	*-6.449000*	*56.011000*
C	*34.340797*	*-5.653328*	*56.554826*

O	34.798703	-5.871031	57.677572
N	34.869189	-4.716116	55.710033
C	36.211000	-4.132000	55.939000
C	37.232659	-5.261789	55.736069
O	37.069512	-6.074319	54.817117
C	36.253219	-3.282588	57.238386
O	37.079257	-2.175168	57.093678
N	38.285085	-5.341083	56.572118
C	39.171000	-6.484000	56.454000
C	33.096000	5.670000	52.765000
C	33.383167	4.359996	52.019470
C	34.068821	3.369388	52.946714
O	33.467777	2.191639	53.013394
O	35.069501	3.675898	53.586393
C	31.864000	2.637000	56.109000
C	33.333114	2.745942	56.568500
C	34.153220	1.502328	56.350105
N	34.303888	0.931743	55.098131
C	34.908224	0.774724	57.246266
C	35.132221	-0.096888	55.260219
N	35.526536	-0.235837	56.539985
H	34.052560	8.421880	64.769880
H	32.522740	7.760100	64.158970
H	33.648890	8.572270	63.052350
H	34.250056	5.935695	64.533310
H	35.351698	6.768288	63.431013
H	33.724413	6.426949	61.547370
H	32.605247	5.642888	62.655062
H	34.314918	3.842302	63.081781
H	33.654063	3.905515	61.442023
H	37.910877	4.700154	60.390222
H	37.947787	2.925349	60.070926
H	40.735690	6.403980	64.437430
H	41.308880	6.637620	62.771860
H	39.883450	5.643780	63.073920
H	38.640781	7.688723	63.901795
H	40.086058	8.666243	63.660008
H	39.942877	8.212920	61.175247
H	38.498669	9.026028	61.822308
H	36.622950	-11.568530	59.551320

H	*38.117790*	*-10.686050*	*59.161150*
H	*36.545250*	*-9.956960*	*58.808070*
H	*37.568996*	*-10.586140*	*61.643681*
H	*36.006710*	*-9.885232*	*61.258754*
H	*36.308330*	*-7.655470*	*59.553264*
H	*39.188123*	*-9.072322*	*62.421528*
H	*37.327737*	*-5.434631*	*59.620235*
H	*40.218699*	*-6.813271*	*62.484598*
H	*39.121735*	*-4.188692*	*60.380388*
H	*32.596850*	*-5.927990*	*55.225660*
H	*32.477250*	*-6.715620*	*56.824020*
H	*33.564230*	*-7.374410*	*55.585780*
H	*34.586710*	*-4.784668*	*54.742085*
H	*36.367520*	*-3.422862*	*55.118987*
H	*36.562980*	*-3.919566*	*58.081290*
H	*35.205265*	*-2.994791*	*57.445198*
H	*38.414754*	*-4.674047*	*57.325520*
H	*38.598180*	*-7.417440*	*56.448720*
H	*39.858020*	*-6.489460*	*57.303030*
H	*39.744900*	*-6.443620*	*55.519870*
H	*32.682340*	*6.417890*	*52.077560*
H	*34.018580*	*6.062470*	*53.202680*
H	*32.373810*	*5.520230*	*53.576740*
H	*34.061589*	*4.558228*	*51.180043*
H	*32.468619*	*3.920036*	*51.612634*
H	*31.325350*	*3.576160*	*56.285810*
H	*31.349590*	*1.838450*	*56.657850*
H	*31.811950*	*2.406820*	*55.040460*
H	*33.370096*	*3.000943*	*57.634411*
H	*33.811427*	*3.576076*	*56.032052*
H	*35.466409*	*-0.751503*	*54.466449*
H	*35.063990*	*0.912793*	*58.306557*
H	*33.865812*	*1.630955*	*53.820218*
H	*36.148242*	*5.481971*	*61.630073*
H	*36.399083*	*1.552180*	*60.712389*
H	*35.071164*	*2.044426*	*61.682368*
C	*38.445092*	*-2.122718*	*58.817553*
O	*38.882009*	*-3.282225*	*58.935993*
C	*39.246237*	*-1.010046*	*58.142328*
C	*40.323150*	*-1.526075*	*57.184021*

C	41.531863	-1.793458	58.099569
C	41.467496	-0.662694	59.140785
N	40.033118	-0.312904	59.193742
C	39.488750	0.663149	59.952444
O	38.280919	0.964410	59.854736
H	42.487098	-1.795551	57.567399
H	41.404729	-2.760760	58.592109
H	39.977333	-2.414518	56.653773
H	38.549688	-0.301515	57.695826
C	40.412686	1.384330	60.915478
H	40.899341	0.681013	61.598943
H	41.835474	-0.973593	60.123659
H	42.051319	0.209864	58.820524
H	40.558277	-0.750577	56.446647
H	36.231734	-1.042914	56.870896
H	37.628946	-1.763276	59.462120
H	41.202247	1.918061	60.374856
H	39.829675	2.101507	61.493721

Minima (unbound)

C	33.586000	7.906000	63.922000
C	34.289100	6.570803	63.637307
C	33.654903	5.812509	62.460211
C	34.271864	4.439647	62.158743
N	35.614100	4.558019	61.592310
C	36.273222	3.539411	61.037301
N	35.741000	2.285909	61.016225
N	37.451528	3.737514	60.448832
C	40.412000	6.546000	63.398000
C	39.532061	7.797058	63.271674
C	39.067979	8.083030	61.830004
C	38.185883	6.941609	61.310289
O	38.693293	6.143182	60.471215
O	37.021031	6.857917	61.806918
C	37.091000	-10.575000	59.530000
C	37.060135	-9.937182	60.929500
C	37.732405	-8.580717	60.991701
C	37.245267	-7.493800	60.249439
C	38.872793	-8.370256	61.779537

C	37.873817	-6.250873	60.284534
C	39.515070	-7.132276	61.826139
C	39.021221	-6.062493	61.069933
O	39.674019	-4.868173	61.135268
C	33.155000	-6.449000	56.011000
C	34.341762	-5.651532	56.550532
O	34.814184	-5.871249	57.666669
N	34.863853	-4.701389	55.712003
C	36.211000	-4.132000	55.939000
C	37.227656	-5.267294	55.735446
O	37.055648	-6.082029	54.823378
C	36.258570	-3.319735	57.251471
O	37.163652	-2.236214	57.142953
N	38.282814	-5.343792	56.569110
C	39.171000	-6.484000	56.454000
C	33.096000	5.670000	52.765000
C	33.378210	4.350209	52.040896
C	34.038327	3.328796	52.983103
O	33.549419	2.142133	52.964886
O	34.983344	3.723180	53.699418
C	31.864000	2.637000	56.109000
C	33.330625	2.775754	56.570079
C	34.175074	1.547757	56.389119
N	34.430906	1.001801	55.148443
C	34.889583	0.780628	57.285428
C	35.271927	-0.034131	55.328027
N	35.578820	-0.210208	56.611824
H	34.052560	8.421880	64.769880
H	32.522740	7.760100	64.158970
H	33.648890	8.572270	63.052350
H	34.247525	5.935606	64.533991
H	35.345969	6.762573	63.424070
H	33.703341	6.426761	61.551432
H	32.589199	5.647829	62.667651
H	34.292774	3.841335	63.084089
H	33.629087	3.907457	61.445087
H	37.895363	4.690177	60.404576
H	37.928870	2.916218	60.091827
H	40.735690	6.403980	64.437430
H	41.308880	6.637620	62.771860

H   39.883450   5.643780   63.073920
H   38.641240   7.689196   63.902646
H   40.084253   8.667454   63.650395
H   39.933823   8.201613   61.169281
H   38.488897   9.013942   61.816160
H   36.622950   -11.568530   59.551320
H   38.117790   -10.686050   59.161150
H   36.545250   -9.956960   58.808070
H   37.543692   -10.610549   61.647665
H   36.012556   -9.849457   61.250197
H   36.359827   -7.604645   59.627003
H   39.271968   -9.193839   62.368527
H   37.475387   -5.424122   59.705280
H   40.401605   -6.982392   62.435944
H   39.325865   -4.272779   60.439074
H   32.596850   -5.927990   55.225660
H   32.477250   -6.715620   56.824020
H   33.564230   -7.374410   55.585780
H   34.573585   -4.749239   54.745046
H   36.371634   -3.415843   55.126577
H   36.541848   -3.958820   58.092897
H   35.245241   -2.950507   57.447645
H   38.427323   -4.669864   57.310054
H   38.598180   -7.417440   56.448720
H   39.858020   -6.489460   57.303030
H   39.744900   -6.443620   55.519870
H   32.682340   6.417890   52.077560
H   34.018580   6.062470   53.202680
H   32.373810   5.520230   53.576740
H   34.066108   4.533161   51.203088
H   32.462369   3.921790   51.620225
H   31.325350   3.576160   56.285810
H   31.349590   1.838450   56.657850
H   31.811950   2.406820   55.040460
H   33.360392   3.052927   57.630512
H   33.798853   3.592776   56.007092
H   35.649796   -0.634553   54.511319
H   34.964418   0.899056   58.358070
H   34.106673   1.428212   54.207082
H   36.126263   5.479485   61.628234

H	36.378687	1.541359	60.753244
H	35.038822	2.048497	61.700034
C	38.607334	-2.126146	58.930036
O	39.040154	-3.278681	58.976439
C	39.357713	-0.981450	58.250664
C	40.467099	-1.445299	57.302768
C	41.677664	-1.658279	58.230362
C	41.547220	-0.538031	59.275951
N	40.094868	-0.266286	59.322327
C	39.490101	0.681941	60.076975
O	38.272043	0.916368	59.958199
H	42.635466	-1.609493	57.705936
H	41.599498	-2.634781	58.715672
H	40.176361	-2.348563	56.763860
H	38.632952	-0.299631	57.803706
C	40.363302	1.442311	61.055109
H	40.868333	0.759237	61.745743
H	41.924940	-0.833072	60.259599
H	42.083282	0.366301	58.961818
H	40.670695	-0.656538	56.571092
H	36.593364	-1.396494	56.995650
H	37.765658	-1.810097	59.565962
H	41.137444	2.011013	60.528263
H	39.739034	2.131920	61.623408

Minima (bound)

C	33.586000	7.906000	63.922000
C	34.283505	6.567439	63.638129
C	33.643927	5.813436	62.461101
C	34.228010	4.422846	62.175416
N	35.579239	4.497413	61.623086
C	36.207817	3.454107	61.077378
N	35.631588	2.222339	61.040309
N	37.407616	3.607817	60.515594
C	40.412000	6.546000	63.398000
C	39.521623	7.786448	63.250191
C	39.043277	8.020860	61.802534
C	38.172344	6.852015	61.323575
O	38.698553	6.008841	60.541781

O	36.995215	6.795439	61.794839
C	37.091000	-10.575000	59.530000
C	37.068660	-9.916465	60.921567
C	37.654396	-8.517607	60.925921
C	37.096669	-7.504102	60.130304
C	38.778272	-8.184858	61.694673
C	37.642565	-6.226072	60.084973
C	39.337575	-6.904446	61.664648
C	38.784691	-5.906156	60.844554
O	39.350531	-4.679969	60.815392
C	33.155000	-6.449000	56.011000
C	34.322693	-5.635105	56.561887
O	34.738255	-5.809447	57.706824
N	34.869516	-4.713880	55.702651
C	36.211000	-4.132000	55.939000
C	37.245334	-5.259719	55.736553
O	37.069992	-6.050195	54.796055
C	36.209227	-3.333353	57.252271
O	37.232145	-2.338557	57.233451
N	38.281011	-5.343930	56.580388
C	39.171000	-6.484000	56.454000
C	33.096000	5.670000	52.765000
C	33.380116	4.360317	52.017117
C	34.052398	3.364720	52.945233
O	33.436240	2.188617	53.005174
O	35.049571	3.652808	53.595038
C	31.864000	2.637000	56.109000
C	33.329467	2.769877	56.571707
C	34.177969	1.544089	56.367745
N	34.301827	0.928804	55.131467
C	34.991427	0.890438	57.265708
C	35.170566	-0.058037	55.288629
N	35.615685	-0.120828	56.563131
H	34.052560	8.421880	64.769880
H	32.522740	7.760100	64.158970
H	33.648890	8.572270	63.052350
H	34.237045	5.933233	64.535233
H	35.341402	6.751620	63.424075
H	33.714637	6.419708	61.548378
H	32.572767	5.675139	62.660250

H   34.221610   3.830017   63.104332
H   33.577008   3.904713   61.458530
H   37.882267   4.543376   60.482144
H   37.845167   2.777223   60.132518
H   40.735690   6.403980   64.437430
H   41.308880   6.637620   62.771860
H   39.883450   5.643780   63.073920
H   38.637225   7.688602   63.892010
H   40.067359   8.674010   63.596943
H   39.904618   8.128112   61.133874
H   38.452730   8.943577   61.762192
H   36.622950   -11.568530   59.551320
H   38.117790   -10.686050   59.161150
H   36.545250   -9.956960   58.808070
H   37.617235   -10.544048   61.635083
H   36.028221   -9.888297   61.276813
H   36.217444   -7.705197   59.521316
H   39.234391   -8.944915   62.327625
H   37.206318   -5.469493   59.445328
H   40.215215   -6.666322   62.260421
H   38.993962   -4.150935   60.008937
H   32.596850   -5.927990   55.225660
H   32.477250   -6.715620   56.824020
H   33.564230   -7.374410   55.585780
H   34.641978   -4.846101   54.726363
H   36.369682   -3.415580   55.124328
H   36.336249   -3.994318   58.106712
H   35.228245   -2.846101   57.337827
H   38.421032   -4.664215   57.354244
H   38.598180   -7.417440   56.448720
H   39.858020   -6.489460   57.303030
H   39.744900   -6.443620   55.519870
H   32.682340   6.417890   52.077560
H   34.018580   6.062470   53.202680
H   32.373810   5.520230   53.576740
H   34.065363   4.555767   51.182843
H   32.465650   3.926838   51.603596
H   31.325350   3.576160   56.285810
H   31.349590   1.838450   56.657850
H   31.811950   2.406820   55.040460

H	33.359919	3.035115	57.634962
H	33.796152	3.602813	56.029676
H	35.502533	-0.733489	54.512596
H	35.191651	1.067556	58.311652
H	33.830429	1.635590	53.788937
H	36.110296	5.409104	61.648787
H	36.255751	1.455495	60.788154
H	34.897072	2.013828	61.698977
C	38.059950	-2.344282	58.476170
O	38.611521	-3.542658	58.679694
C	39.064362	-1.179286	58.231489
C	40.322267	-1.616579	57.469100
C	41.276459	-2.111524	58.573269
C	40.967986	-1.211063	59.784647
N	39.604482	-0.707812	59.523712
C	38.947680	0.189058	60.282056
O	37.835907	0.652246	59.933590
H	42.331349	-2.051119	58.289402
H	41.026951	-3.144842	58.816858
H	40.087603	-2.398128	56.743139
H	38.541632	-0.344667	57.757514
C	39.616561	0.630029	61.570652
H	39.804192	-0.224417	62.229305
H	41.007369	-1.764617	60.728613
H	41.667741	-0.368811	59.854213
H	40.751379	-0.760293	56.935754
H	36.293447	-0.817729	56.910715
H	37.374064	-2.025164	59.289746
H	40.581868	1.107999	61.370630
H	38.967583	1.342355	62.080557

Compound 19 (in FAP)

Maxima

C	33.586000	7.906000	63.922000
C	34.321727	6.557570	63.899061
C	33.609920	5.520805	63.013244
C	34.260303	4.129241	62.969011
N	35.511260	4.130577	62.214541
C	36.062217	3.042005	61.671762

N	35.506445	1.807043	61.848289
N	37.140804	3.149320	60.903693
C	40.412000	6.546000	63.398000
C	39.567266	7.714168	62.871061
C	39.064277	7.522112	61.434617
C	38.091813	6.341801	61.302020
O	38.273981	5.538489	60.344146
O	37.171931	6.263917	62.172989
C	37.091000	-10.575000	59.530000
C	38.099965	-10.293764	60.657239
C	38.688604	-8.897498	60.609146
C	37.867320	-7.760850	60.652060
C	40.070733	-8.692235	60.498494
C	38.393064	-6.472881	60.575164
C	40.618258	-7.410495	60.422209
C	39.780689	-6.286832	60.450622
O	40.347413	-5.053379	60.369473
C	33.155000	-6.449000	56.011000
C	34.118422	-5.424215	56.580040
O	34.133699	-5.198905	57.790180
N	34.959664	-4.867243	55.664150
C	36.211000	-4.132000	55.939000
C	37.342779	-5.123412	55.667125
O	37.448970	-5.614101	54.533420
C	36.155432	-3.300115	57.258993
O	36.935866	-2.160981	57.193772
N	38.141159	-5.489980	56.684330
C	39.171000	-6.484000	56.454000
C	33.096000	5.670000	52.765000
C	33.989037	4.494040	52.365582
C	34.449233	3.702498	53.570433
O	34.245465	2.405941	53.450002
O	34.937150	4.251220	54.556040
C	31.864000	2.637000	56.109000
C	33.105362	2.829227	57.018332
C	34.046481	1.642723	56.908043
N	34.551120	1.261969	55.675494
C	34.568173	0.779001	57.853977
C	35.341566	0.218994	55.888380
N	35.388921	-0.116655	57.187830

H   34.096088   8.631965   64.564095
H   32.557665   7.797116   64.289425
H   33.534668   8.334654   62.914342
H   34.394499   6.160786   64.921953
H   35.346381   6.711874   63.543864
H   33.527156   5.900058   61.986089
H   32.582805   5.384600   63.377862
H   34.423061   3.770499   63.998367
H   33.565383   3.429530   62.489185
H   37.537777   4.087534   60.643613
H   37.579214   2.286406   60.589873
H   40.810379   6.798157   64.388005
H   41.262810   6.343999   62.736002
H   39.838099   5.618647   63.494991
H   38.697495   7.859201   63.521398
H   40.163442   8.635275   62.922651
H   39.898868   7.369159   60.741563
H   38.534337   8.429087   61.111921
H   36.773128   -11.625817   59.548078
H   37.529190   -10.366502   58.547533
H   36.197948   -9.948020   59.628616
H   38.915666   -11.025125   60.605202
H   37.603387   -10.460927   61.623936
H   36.789735   -7.877821   60.744807
H   40.736011   -9.553039   60.464041
H   37.737781   -5.607985   60.599600
H   41.690893   -7.264054   60.329864
H   39.648619   -4.389681   60.151567
H   33.072800   -6.469652   54.919724
H   32.161253   -6.349731   56.451421
H   33.577055   -7.404904   56.341425
H   34.925135   -5.256131   54.730876
H   36.300122   -3.381470   55.144473
H   36.424578   -3.940728   58.121189
H   35.092618   -3.054520   57.413548
H   38.075566   -5.018892   57.578741
H   38.752338   -7.360425   55.949921
H   39.596232   -6.784225   57.414406
H   39.967098   -6.085083   55.812339
H   32.823409   6.184233   51.837140

H	33.620262	6.371333	53.418603
H	32.171081	5.371131	53.269948
H	34.880252	4.881054	51.854425
H	33.474155	3.828953	51.666776
H	31.165367	3.472345	55.985160
H	31.303041	1.779952	56.499090
H	32.246752	2.363888	55.122211
H	32.812296	2.962429	58.065996
H	33.650925	3.728547	56.709716
H	35.895948	-0.316205	55.130564
H	34.434245	0.744784	58.925381
H	34.417325	1.924555	54.402958
H	36.100153	5.003134	62.160112
H	36.074108	1.025471	61.540691
H	34.976882	1.642269	62.691587
C	38.469097	-2.303713	58.750991
N	38.468017	-3.300665	59.371303
C	39.006090	-0.993940	58.290540
C	39.967702	-1.191902	57.102721
C	41.299135	-1.532198	57.793423
C	41.313000	-0.614408	59.029905
N	39.880093	-0.410469	59.323074
C	39.355392	0.316141	60.336174
O	38.122832	0.452566	60.451758
H	42.170587	-1.368409	57.154780
H	41.301129	-2.580972	58.109132
H	39.597362	-1.959980	56.423684
H	38.178903	-0.322312	58.076349
C	40.330408	0.956349	61.303477
H	40.900382	0.191353	61.842041
H	41.831617	-1.064674	59.881900
H	41.790972	0.347998	58.808072
H	40.044610	-0.247321	56.553764
H	36.023204	-0.982446	57.439700
H	41.048336	1.596196	60.779733
H	39.769458	1.555560	62.020866

Minima (unbound)

C	33.586000	7.906000	63.922000

C	*34.284365*	*6.541693*	*63.901319*
C	*33.548825*	*5.557088*	*62.977331*
C	*34.051029*	*4.110721*	*63.020321*
N	*35.400498*	*3.983892*	*62.478468*
C	*35.951133*	*2.817846*	*62.134276*
N	*35.275408*	*1.653203*	*62.343879*
N	*37.138809*	*2.790388*	*61.543279*
C	*40.412000*	*6.546000*	*63.398000*
C	*39.532643*	*7.655968*	*62.812084*
C	*38.998666*	*7.293507*	*61.414296*
C	*38.111019*	*6.041057*	*61.459821*
O	*38.468823*	*5.031060*	*60.785975*
O	*37.080305*	*6.109118*	*62.195548*
C	*37.091000*	*-10.575000*	*59.530000*
C	*38.108429*	*-10.298146*	*60.653757*
C	*38.844094*	*-8.976308*	*60.528421*
C	*38.177801*	*-7.742708*	*60.580363*
C	*40.236016*	*-8.949235*	*60.354331*
C	*38.864979*	*-6.531491*	*60.465966*
C	*40.940175*	*-7.752027*	*60.238556*
C	*40.259181*	*-6.527949*	*60.293920*
O	*40.997405*	*-5.390648*	*60.190700*
C	*33.155000*	*-6.449000*	*56.011000*
C	*34.120559*	*-5.421245*	*56.572006*
O	*34.156115*	*-5.193085*	*57.781453*
N	*34.953376*	*-4.850956*	*55.653482*
C	*36.211000*	*-4.132000*	*55.939000*
C	*37.336071*	*-5.130630*	*55.663491*
O	*37.426387*	*-5.628181*	*54.535019*
C	*36.160676*	*-3.351613*	*57.270642*
O	*37.049188*	*-2.248207*	*57.219987*
N	*38.139976*	*-5.492201*	*56.679005*
C	*39.171000*	*-6.484000*	*56.454000*
C	*33.096000*	*5.670000*	*52.765000*
C	*33.979022*	*4.474689*	*52.407744*
C	*34.458545*	*3.698526*	*53.638817*
O	*34.411245*	*2.420981*	*53.534301*
O	*34.851247*	*4.346947*	*54.632257*
C	*31.864000*	*2.637000*	*56.109000*
C	*33.076388*	*2.906985*	*57.034200*

C	34.063125	1.761963	57.038896
N	34.718134	1.377927	55.886517
C	34.537795	0.911583	58.022285
C	35.530315	0.352104	56.201211
N	35.462676	0.025660	57.490185
H	34.096088	8.631965	64.564095
H	32.557665	7.797116	64.289425
H	33.534668	8.334654	62.914342
H	34.312005	6.128144	64.919839
H	35.321753	6.659778	63.572409
H	33.593153	5.917606	61.941205
H	32.485843	5.532142	63.252400
H	34.017083	3.748283	64.060786
H	33.371170	3.477862	62.435408
H	37.608954	3.681224	61.240832
H	37.628074	1.906313	61.403731
H	40.810379	6.798157	64.388005
H	41.262810	6.343999	62.736002
H	39.838099	5.618647	63.494991
H	38.675682	7.840091	63.470297
H	40.101669	8.593156	62.753912
H	39.827022	7.118683	60.719357
H	38.398489	8.125855	61.025157
H	36.773128	-11.625817	59.548078
H	37.529190	-10.366502	58.547533
H	36.197948	-9.948020	59.628616
H	38.851518	-11.104421	60.667784
H	37.589433	-10.348771	61.621136
H	37.099184	-7.718185	60.720508
H	40.784290	-9.888169	60.309687
H	38.325995	-5.589176	60.529137
H	42.018267	-7.745822	60.105824
H	40.425297	-4.601842	60.095517
H	33.072800	-6.469652	54.919724
H	32.161253	-6.349731	56.451421
H	33.577055	-7.404904	56.341425
H	34.919948	-5.226722	54.714791
H	36.309589	-3.366000	55.161575
H	36.381532	-4.002428	58.126869
H	35.134386	-3.005606	57.413346

H	38.099317	-5.004502	57.561480
H	38.752338	-7.360425	55.949921
H	39.596232	-6.784225	57.414406
H	39.967098	-6.085083	55.812339
H	32.823409	6.184233	51.837140
H	33.620262	6.371333	53.418603
H	32.171081	5.371131	53.269948
H	34.867815	4.834378	51.869093
H	33.456146	3.788538	51.733064
H	31.165367	3.472345	55.985160
H	31.303041	1.779952	56.499090
H	32.246752	2.363888	55.122211
H	32.746121	3.092214	58.063038
H	33.598718	3.802277	56.677837
H	36.157207	-0.144957	55.472794
H	34.280599	0.896103	59.073794
H	34.626833	1.834928	54.907464
H	36.013138	4.829974	62.357381
H	35.763457	0.789647	62.154944
H	34.593448	1.611252	63.085811
C	39.455618	-1.925004	59.074995
N	39.649734	-2.968387	59.541845
C	39.245388	-0.590636	58.468749
C	39.653376	-0.551644	56.979216
C	41.139902	-0.171224	57.030142
C	41.217331	0.839276	58.184844
N	40.129248	0.409182	59.090668
C	39.772613	0.963882	60.278311
O	38.786833	0.524143	60.895390
H	41.501697	0.254348	56.091151
H	41.749882	-1.051927	57.260193
H	39.437266	-1.492500	56.474642
H	38.197961	-0.323905	58.628543
C	40.580297	2.130603	60.803667
H	41.588253	2.187301	60.390242
H	42.183209	0.816269	58.696466
H	41.032397	1.861558	57.834835
H	39.065113	0.235081	56.496955
H	36.514377	-1.454469	57.482922
H	40.057396	3.069663	60.578261

H   40.638155   2.041623   61.890659

Minima (bound)

C   33.586000   7.906000   63.922000
C   34.321867   6.555673   63.913356
C   33.605865   5.500507   63.052558
C   34.215220   4.087686   63.079362
N   35.473654   4.002929   62.339017
C   35.928166   2.894363   61.752916
N   35.274219   1.703577   61.872796
N   37.025037   2.943505   60.995522
C   40.412000   6.546000   63.398000
C   39.538644   7.673489   62.835038
C   39.005751   7.367662   61.427435
C   38.081659   6.140821   61.393883
O   38.255968   5.298338   60.467696
O   37.201815   6.067041   62.305849
C   37.091000 -10.575000   59.530000
C   38.102344 -10.273996   60.656329
C   38.594207   -8.839110   60.700826
C   37.815835   -7.810704   61.263625
C   39.842962   -8.464586   60.178752
C   38.247290   -6.488731   61.297809
C   40.293879   -7.144006   60.205217
C   39.514198   -6.083180   60.766601
O   39.918751   -4.847584   60.789715
C   33.155000   -6.449000   56.011000
C   34.061776   -5.358073   56.549817
O   33.975112   -4.994040   57.722281
N   34.958801   -4.859874   55.646318
C   36.211000   -4.132000   55.939000
C   37.342744   -5.135480   55.680733
O   37.433546   -5.597694   54.531762
C   36.113392   -3.348227   57.255915
O   37.217279   -2.422378   57.404478
N   38.130265   -5.505941   56.692892
C   39.171000   -6.484000   56.454000
C   33.096000   5.670000   52.765000
C   33.986463   4.454410   52.475923

C	34.502580	3.828789	53.762936
O	34.461235	2.498790	53.759158
O	34.905520	4.500437	54.703517
C	31.864000	2.637000	56.109000
C	33.010865	3.038761	57.055215
C	34.064741	1.985546	57.250036
N	34.818459	1.480333	56.199882
C	34.490233	1.401167	58.418791
C	35.670569	0.615466	56.731602
N	35.506818	0.533407	58.073679
H	34.096088	8.631965	64.564095
H	32.557665	7.797116	64.289425
H	33.534668	8.334654	62.914342
H	34.398281	6.178191	64.943337
H	35.345803	6.699707	63.551677
H	33.551632	5.839322	62.009534
H	32.568647	5.403073	63.401277
H	34.356560	3.770769	64.124574
H	33.499149	3.393480	62.624613
H	37.477367	3.864061	60.752114
H	37.338958	2.082577	60.566448
H	40.810379	6.798157	64.388005
H	41.262810	6.343999	62.736002
H	39.838099	5.618647	63.494991
H	38.682070	7.840903	63.497232
H	40.114896	8.607989	62.809285
H	39.828069	7.204711	60.722125
H	38.428024	8.227305	61.060459
H	36.773128	-11.625817	59.548078
H	37.529190	-10.366502	58.547533
H	36.197948	-9.948020	59.628616
H	38.962395	-10.948040	60.544144
H	37.635537	-10.536908	61.616807
H	36.841799	-8.058934	61.689003
H	40.483087	-9.232530	59.741041
H	37.617851	-5.718074	61.739443
H	41.271071	-6.888756	59.797719
H	38.791558	-3.979668	59.782117
H	33.072800	-6.469652	54.919724
H	32.161253	-6.349731	56.451421

H	*33.577055*	*-7.404904*	*56.341425*
H	*35.007217*	*-5.330798*	*54.751042*
H	*36.327166*	*-3.388855*	*55.139322*
H	*36.064984*	*-3.991914*	*58.127418*
H	*35.212855*	*-2.732385*	*57.217780*
H	*38.041747*	*-5.071939*	*57.622235*
H	*38.752338*	*-7.360425*	*55.949921*
H	*39.596232*	*-6.784225*	*57.414406*
H	*39.967098*	*-6.085083*	*55.812339*
H	*32.823409*	*6.184233*	*51.837140*
H	*33.620262*	*6.371333*	*53.418603*
H	*32.171081*	*5.371131*	*53.269948*
H	*34.863635*	*4.767136*	*51.893853*
H	*33.462135*	*3.697631*	*51.886042*
H	*31.165367*	*3.472345*	*55.985160*
H	*31.303041*	*1.779952*	*56.499090*
H	*32.246752*	*2.363888*	*55.122211*
H	*32.603220*	*3.303262*	*58.037967*
H	*33.494453*	*3.938148*	*56.656292*
H	*36.406697*	*0.033917*	*56.195467*
H	*34.176026*	*1.530631*	*59.443109*
H	*34.697639*	*2.124287*	*54.687020*
H	*36.120241*	*4.839116*	*62.300304*
H	*35.760543*	*0.888295*	*61.500981*
H	*34.706769*	*1.547312*	*62.692283*
C	*38.085274*	*-2.681100*	*58.438857*
N	*38.101577*	*-3.801983*	*59.016753*
C	*38.974138*	*-1.460101*	*58.687204*
C	*40.414705*	*-1.657336*	*58.167186*
C	*41.145370*	*-2.330694*	*59.342197*
C	*40.497036*	*-1.727074*	*60.601161*
N	*39.175927*	*-1.241988*	*60.128447*
C	*38.266504*	*-0.602602*	*60.883186*
O	*37.192109*	*-0.159147*	*60.402570*
H	*42.223304*	*-2.147996*	*59.318343*
H	*40.974084*	*-3.410692*	*59.360356*
H	*40.441068*	*-2.247578*	*57.247467*
H	*38.495138*	*-0.582991*	*58.248565*
C	*38.594149*	*-0.423671*	*62.350081*
H	*38.744078*	*-1.394383*	*62.833591*

H   40.369720   -2.492734   61.370633
H   41.070407   -0.884463   61.004798
H   40.845246   -0.673663   57.949355
H   36.087759   0.009380   58.728169
H   39.515854   0.153428   62.479030
H   37.773663   0.099525   62.840901

Compound 20 (in FAP)

Maxima

C   33.586000   7.906000   63.922000
C   34.074580   6.466258   63.729603
C   33.413812   5.774367   62.528540
C   33.920785   4.353351   62.257043
N   35.297642   4.371543   61.769501
C   35.943077   3.288281   61.336281
N   35.362961   2.057563   61.376355
N   37.161441   3.401352   60.810443
C   40.412000   6.546000   63.398000
C   39.403626   7.692529   63.238367
C   38.848971   7.846677   61.807627
C   37.979068   6.644040   61.422395
O   38.509885   5.741727   60.711603
O   36.799323   6.625823   61.889310
C   37.091000 -10.575000   59.530000
C   37.155992   -9.807927   60.864225
C   37.953648   -8.522449   60.784590
C   37.382251   -7.341714   60.288397
C   39.299429   -8.476884   61.178101
C   38.118954   -6.161941   60.185194
C   40.056676   -7.310663   61.065770
C   39.472659   -6.142082   60.557059
O   40.246830   -5.026093   60.454731
C   33.155000   -6.449000   56.011000
C   34.366055   -5.697046   56.551078
O   34.831375   -5.939358   57.665446
N   34.897079   -4.765078   55.708146
C   36.211000   -4.132000   55.939000
C   37.287641   -5.191306   55.659972
O   37.251095   -5.841184   54.608193

116

C	36.237185	-3.310869	57.255585
O	37.107771	-2.222473	57.161092
N	38.241652	-5.381158	56.589469
C	39.171000	-6.484000	56.454000
C	33.096000	5.670000	52.765000
C	33.501846	4.364048	52.070923
C	34.136460	3.409367	53.069900
O	33.597502	2.200684	53.071028
O	35.046069	3.766830	53.811201
C	31.864000	2.637000	56.109000
C	33.303150	2.677103	56.673293
C	34.133828	1.438625	56.441857
N	34.352748	0.924865	55.175485
C	34.867303	0.686258	57.338506
C	35.197288	-0.092425	55.330441
N	35.541134	-0.280696	56.618490
H	34.061249	8.362016	64.799103
H	32.497268	7.957537	64.064548
H	33.842832	8.519142	63.049382
H	33.871754	5.878930	64.636642
H	35.159877	6.485218	63.588108
H	33.563334	6.378045	61.623663
H	32.329441	5.714836	62.688832
H	33.844608	3.758151	63.181322
H	33.276642	3.871709	61.508900
H	37.653081	4.329641	60.730757
H	37.615522	2.542662	60.528412
H	40.768114	6.493691	64.435250
H	41.282255	6.706054	62.748064
H	39.978750	5.578881	63.124684
H	38.556279	7.543128	63.919626
H	39.882649	8.634227	63.538073
H	39.674455	7.942655	61.093225
H	38.234978	8.752995	61.756617
H	36.527927	-11.510075	59.651239
H	38.096797	-10.823486	59.169589
H	36.599240	-9.974620	58.755622
H	37.594409	-10.460072	61.630273
H	36.132707	-9.587043	61.194589
H	36.342196	-7.332712	59.968771

H	39.768861	-9.374482	61.577075
H	37.646290	-5.250598	59.832500
H	41.101119	-7.289303	61.364640
H	39.793372	-4.358278	59.890781
H	32.592285	-5.894790	55.252113
H	32.490056	-6.709060	56.836998
H	33.516632	-7.381287	55.558611
H	34.581557	-4.788330	54.748834
H	36.318949	-3.393439	55.136924
H	36.469636	-3.962462	58.108943
H	35.192869	-2.983530	57.414319
H	38.195901	-4.880247	57.467813
H	38.637716	-7.435938	56.357565
H	39.798310	-6.517732	57.347144
H	39.804636	-6.371057	55.565136
H	32.725159	6.394118	52.029230
H	33.955476	6.101740	53.286153
H	32.303385	5.502313	53.504300
H	34.247244	4.578243	51.294313
H	32.647484	3.882986	51.586962
H	31.346075	3.586198	56.292643
H	31.286603	1.833506	56.583196
H	31.878632	2.455428	55.029979
H	33.269484	2.870433	57.752327
H	33.829274	3.527416	56.219633
H	35.578743	-0.704434	54.523937
H	34.972052	0.777947	58.410451
H	33.956460	1.643393	53.900377
H	35.846581	5.271521	61.758881
H	36.001146	1.274706	61.260917
H	34.597068	1.912577	62.016725
B	38.361221	-2.139239	58.857772
O	39.107237	-3.334938	58.626355
C	38.995993	-0.702123	58.468389
C	40.097749	-0.710306	57.393277
C	41.392353	-0.944835	58.193663
C	41.181212	-0.111930	59.467668
N	39.717086	-0.114242	59.645290
C	39.061820	0.444556	60.667370
O	37.801333	0.459563	60.704885

H   42.297170   -0.645826   57.657574
H   41.491127   -2.002337   58.459745
H   39.914305   -1.467761   56.625221
H   38.185396   -0.015950   58.206658
C   39.877825   1.080743   61.775341
H   40.467245   0.323266   62.303805
H   41.687621   -0.535789   60.340351
H   41.541337   0.916445   59.332262
H   40.147766   0.258898   56.882524
H   36.263621   -1.090619   56.939414
H   40.575919   1.828274   61.384255
H   39.198169   1.557661   62.481631
H   39.607057   -3.275924   57.803369
O   37.542631   -2.248382   59.962940
H   37.284834   -1.356682   60.252117

Minima (unbound)

C   33.586000   7.906000   63.922000
C   34.069288   6.464309   63.729832
C   33.400767   5.774788   62.531523
C   33.890126   4.346683   62.264659
N   35.269151   4.346436   61.781739
C   35.897865   3.258181   61.339503
N   35.297104   2.035975   61.368184
N   37.118277   3.354182   60.815025
C   40.412000   6.546000   63.398000
C   39.398749   7.685803   63.226337
C   38.837439   7.806782   61.794440
C   37.975617   6.589600   61.437238
O   38.519592   5.662779   60.768601
O   36.788364   6.585663   61.884411
C   37.091000 -10.575000   59.530000
C   37.154517   -9.814989   60.868073
C   37.973795   -8.543237   60.802693
C   37.422822   -7.347616   60.320440
C   39.320511   -8.527362   61.195364
C   38.181402   -6.180678   60.229826
C   40.098833   -7.374234   61.096489

C	39.534228	-6.190882	60.602355
O	40.328543	-5.085600	60.514013
C	33.155000	-6.449000	56.011000
C	34.366847	-5.690456	56.543536
O	34.858781	-5.943561	57.643614
N	34.878229	-4.727960	55.716212
C	36.211000	-4.132000	55.939000
C	37.260709	-5.225177	55.680636
O	37.175944	-5.925221	54.666743
C	36.257922	-3.343962	57.263472
O	37.208633	-2.286502	57.187932
N	38.244152	-5.379609	56.585132
C	39.171000	-6.484000	56.454000
C	33.096000	5.670000	52.765000
C	33.497263	4.356800	52.088294
C	34.110039	3.371733	53.097942
O	33.682835	2.163048	53.037840
O	34.960878	3.812084	53.900479
C	31.864000	2.637000	56.109000
C	33.299425	2.716956	56.675500
C	34.155563	1.495787	56.487613
N	34.482719	1.006194	55.240197
C	34.847648	0.707813	57.385446
C	35.340199	-0.016675	55.418595
N	35.593439	-0.239099	56.706917
H	34.061249	8.362016	64.799103
H	32.497268	7.957537	64.064548
H	33.842832	8.519142	63.049382
H	33.866191	5.879059	64.638208
H	35.154215	6.478025	63.585238
H	33.556740	6.373146	61.624286
H	32.315868	5.728256	62.692446
H	33.803726	3.753975	63.189602
H	33.242609	3.872501	61.514831
H	37.635374	4.271914	60.759475
H	37.556900	2.487408	60.534906
H	40.768114	6.493691	64.435250
H	41.282255	6.706054	62.748064
H	39.978750	5.578881	63.124684
H	38.555466	7.544860	63.914513

H   *39.873873   8.635805   63.505055*
H   *39.660378   7.893527   61.075876*
H   *38.216456   8.706921   61.726078*
H   *36.527927   -11.510075   59.651239*
H   *38.096797   -10.823486   59.169589*
H   *36.599240   -9.974620   58.755622*
H   *37.575237   -10.477962   61.634616*
H   *36.131926   -9.579362   61.189841*
H   *36.382610   -7.317762   60.002904*
H   *39.773483   -9.437979   61.583308*
H   *37.724933   -5.256712   59.888543*
H   *41.143456   -7.374736   61.395033*
H   *39.881961   -4.408324   59.963065*
H   *32.592285   -5.894790   55.252113*
H   *32.490056   -6.709060   56.836998*
H   *33.516632   -7.381287   55.558611*
H   *34.554715   -4.729726   54.759101*
H   *36.339458   -3.396215   55.138267*
H   *36.488430   -3.992456   58.111232*
H   *35.257966   -2.930864   57.434737*
H   *38.266942   -4.820668   57.428015*
H   *38.637716   -7.435938   56.357565*
H   *39.798310   -6.517732   57.347144*
H   *39.804636   -6.371057   55.565136*
H   *32.725159   6.394118   52.029230*
H   *33.955476   6.101740   53.286153*
H   *32.303385   5.502313   53.504300*
H   *34.250560   4.560040   51.313734*
H   *32.642543   3.885819   51.591381*
H   *31.346075   3.586198   56.292643*
H   *31.286603   1.833506   56.583196*
H   *31.878632   2.455428   55.029979*
H   *33.260076   2.938132   57.748792*
H   *33.811196   3.556262   56.188015*
H   *35.769001   -0.574195   54.596467*
H   *34.868007   0.781672   58.464778*
H   *34.192402   1.458516   54.298702*
H   *35.827677   5.241349   61.772680*
H   *35.918372   1.242565   61.244596*
H   *34.530235   1.896326   62.008625*

B	38.516091	-2.158796	58.938784
O	39.223865	-3.348977	58.655139
C	39.099219	-0.715303	58.514463
C	40.216221	-0.704638	57.453451
C	41.509425	-0.856330	58.275343
C	41.242756	0.003349	59.519379
N	39.779569	-0.081705	59.691399
C	39.084842	0.467402	60.695974
O	37.826722	0.407925	60.726649
H	42.404745	-0.531435	57.739148
H	41.658203	-1.900038	58.574096
H	40.084091	-1.488219	56.700386
H	38.267023	-0.064739	58.226647
C	39.857111	1.180873	61.786679
H	40.523300	0.485248	62.308310
H	41.766955	-0.361083	60.407749
H	41.541057	1.046104	59.350558
H	40.225751	0.251306	56.917804
H	36.659611	-1.435262	57.057837
H	40.475417	1.986664	61.376891
H	39.148742	1.599843	62.501068
H	39.830448	-3.240925	57.912640
O	37.646635	-2.278479	59.987303
H	37.376506	-1.388961	60.282010

Minima (bound)

C	33.586000	7.906000	63.922000
C	34.067028	6.465387	63.724989
C	33.384354	5.783400	62.530939
C	33.882355	4.364307	62.238876
N	35.243351	4.381601	61.709657
C	35.844687	3.306604	61.198311
N	35.231568	2.091687	61.190168
N	37.049896	3.414856	60.640098
C	40.412000	6.546000	63.398000
C	39.398751	7.686676	63.229151
C	38.845804	7.820166	61.795963
C	37.967026	6.619008	61.420466
O	38.468783	5.735615	60.667172

O	36.805448	6.589588	61.931082
C	37.091000	-10.575000	59.530000
C	37.148106	-9.812718	60.867837
C	37.895356	-8.496287	60.797812
C	37.286430	-7.343554	60.278508
C	39.223022	-8.385625	61.235891
C	37.968736	-6.130950	60.195545
C	39.927479	-7.184184	61.144318
C	39.308302	-6.043251	60.611947
O	40.023972	-4.891277	60.533006
C	33.155000	-6.449000	56.011000
C	34.359960	-5.686038	56.549491
O	34.830072	-5.932604	57.659460
N	34.876449	-4.727818	55.717371
C	36.211000	-4.132000	55.939000
C	37.257650	-5.231013	55.675936
O	37.159983	-5.932278	54.660207
C	36.253100	-3.369402	57.279358
O	37.236079	-2.344248	57.256302
N	38.233228	-5.390021	56.582375
C	39.171000	-6.484000	56.454000
C	33.096000	5.670000	52.765000
C	33.496184	4.366633	52.062279
C	34.105748	3.395357	53.057162
O	33.539345	2.194686	53.044627
O	35.014388	3.723177	53.810650
C	31.864000	2.637000	56.109000
C	33.301367	2.693092	56.670386
C	34.139509	1.462602	56.437186
N	34.299774	0.904983	55.178400
C	34.926923	0.762684	57.325572
C	35.163673	-0.090940	55.315460
N	35.572042	-0.216730	56.596104
H	34.061249	8.362016	64.799103
H	32.497268	7.957537	64.064548
H	33.842832	8.519142	63.049382
H	33.870182	5.877490	64.632948
H	35.150578	6.478326	63.571302
H	33.518332	6.393398	61.627791
H	32.302919	5.725859	62.711230

H   33.829966   3.762865   63.160965
H   33.217269   3.888937   61.505496
H   37.570749   4.327607   60.613812
H   37.462714   2.558885   60.290425
H   40.768114   6.493691   64.435250
H   41.282255   6.706054   62.748064
H   39.978750   5.578881   63.124684
H   38.550991   7.539502   63.910093
H   39.872783   8.633902   63.519240
H   39.671194   7.904300   61.080033
H   38.234939   8.728078   61.731198
H   36.527927   -11.510075   59.651239
H   38.096797   -10.823486   59.169589
H   36.599240   -9.974620   58.755622
H   37.615867   -10.455625   61.624387
H   36.120485   -9.632234   61.210365
H   36.257566   -7.383658   59.926144
H   39.720647   -9.258888   61.654799
H   37.468969   -5.242251   59.824422
H   40.959362   -7.113648   61.478026
H   39.582012   -4.264535   59.898990
H   32.592285   -5.894790   55.252113
H   32.490056   -6.709060   56.836998
H   33.516632   -7.381287   55.558611
H   34.580032   -4.770724   54.752212
H   36.340317   -3.390641   55.142284
H   36.407909   -4.057335   58.110928
H   35.254001   -2.931723   57.420945
H   38.295695   -4.786396   57.401743
H   38.637716   -7.435938   56.357565
H   39.798310   -6.517732   57.347144
H   39.804636   -6.371057   55.565136
H   32.725159   6.394118   52.029230
H   33.955476   6.101740   53.286153
H   32.303385   5.502313   53.504300
H   34.253184   4.580182   51.297078
H   32.641839   3.901090   51.563607
H   31.346075   3.586198   56.292643
H   31.286603   1.833506   56.583196
H   31.878632   2.455428   55.029979

H	33.272035	2.888621	57.748796
H	33.819469	3.545386	56.211738
H	35.516688	-0.728717	54.517037
H	35.098976	0.890894	58.383731
H	33.884313	1.638012	53.855806
H	35.820488	5.263134	61.743248
H	35.852960	1.301388	61.014276
H	34.483321	1.934882	61.848339
B	38.099692	-2.239663	58.504622
O	39.016520	-3.440648	58.538386
C	38.935024	-0.813614	58.323728
C	40.213572	-0.862737	57.460248
C	41.335733	-1.198939	58.462500
C	40.933856	-0.432593	59.732513
N	39.470329	-0.303320	59.622392
C	38.694959	0.297373	60.524807
O	37.460220	0.471260	60.315975
H	42.330406	-0.908875	58.112018
H	41.354637	-2.271009	58.677472
H	40.139125	-1.591627	56.645590
H	38.247605	-0.046917	57.947996
C	39.341030	0.792973	61.804790
H	39.767265	-0.040730	62.373407
H	41.219330	-0.960477	60.648243
H	41.396544	0.562851	59.759263
H	40.415351	0.111623	56.996856
H	36.258601	-0.929151	56.925582
H	40.152370	1.499582	61.598853
H	38.584378	1.288515	62.413106
H	39.688070	-3.360878	57.850891
O	37.333813	-2.334555	59.720578
H	37.002715	-1.453541	59.943288